SOME FUNDAMENTAL ASPECTS OF EARTHQUAKE ENGINEERING

by MIHAIL IFRIM, Professor, Ph.D., Civ.Eng.,
Head of Department of Theoretical and Applied Mechanics
Faculty of Civil Engineering
Bucharest, Romania

SUMMARY

The work includes a series of observations on the effects of recent strong earthquakes and on some measures which become essential in earthquake engineering, and includes aspects related to: concept and design, seismic code of regulations, soil influence, numerical analysis, construction, research and professional education.

QUELQUES ASPECTS FONDAMENTAUX DU GENIE PARASEISMIQUE

RESUME

Le travail contient quelques observations sur les effets des recents et forts tremblements de terre et sur quelques mesures qui s'imposent dans le génie paraséismique, portant aussi sur des aspects concernant la conception et le projet, le code des normatifs paraséismiques, l'influence du sol, l'analyse numérique, la construction, la recherche et l'enseignement professionel.

EINIGE GRUNDANSICHTEN ÜBER DAS ERDBEBEN-ENGINEERING

Die Arbeit enthält eine Reihe von Beobachtungen über die Wirkungen des schweren Erdbebens, das vor einiger Zeit statt fand; sie enthält weiter die notwendigen zutreffenden Massnahmen und verschiedene Aspekte und Ansichten, betreffs: Auffassung und Projektieren, Normierung bei dem Erdbebenschutzbauen, Einfluss des Bodens, Numerische Untersuchung, Bauwesen, Forschung und Fachschulung.

From the theoretical, experimental and practical point of view as well as from that of the researchers and professionals, earthquake engineering has made during the last twenty years a great progress. This was directly reflected by the concept and design of structures of all kinds in seismic areas.

In spite of these, the strong earthquakes which have shaken such urban centres as Mexico-City (1957), Agadir (1960), Skopje (1963), Anchorage (1964), Niigata (1964), Caracas (1967), Tokachi-Oki (1968), San Fernando (1971) and recently Bucharest (March 4, 1977), had most destructive effects.

The analysis of structures behavior at strong seismic motions, regardless of the fact that they were or not build on a lateral actions safe concept and design basis, provides particularly important qualitative and quantitative informations which may help in the elucidation of some fundamental scientific aspects and in the improvement of the design process.

The examination and interpretation of effects produced by earthquakes upon structural and nonstructural elements as well as upon the extrapolation of these, should be done with utmost discernment and precaution since each building represents a particular case having a specific dynamic behavior.

The identification of these effects within certain "degrees of damage" in order to define a local scale of seismic intensity of risk represents a most difficult task, sometimes with misleading results.

The age of the buildings is of ultimate importance in the estimation of the degree of damage because of the phenomena to which they were subjected in time. For instance: the alteration or the degradation of physico-mechanical properties of materials used in the initial construction; the creep of concrete;soil layers settlement of the foundation; vibrations due to intense and steady traffic; accidental shocks such as moderate earthquakes, blast effects, strong winds a.s.o.; periodical changes of the buildings functions or destination; defficient maintenance of the resistant structure, etc.

The generally satisfactory behavior of structures built closer to the date of a strong earthquake has been clearly demonstrated even when the seismic motion exceeded the seismic design intensity. This was also valid for the event of March 4, 1977 (a Richter magnitude of 7.2).

The process of structural decay is permanent and unavoidable because Nature can not preserve in time all that man and technology was able to achieve at a certain stage of civilization.

The behavior of different types of structures to violent earthquakes recently produced in the world - including that of March 4, 1977 in Romania - was affected by the following main factors: concept and design, the seismic code of regulations, the soil influence, the numerical analysis, the construction, the research and the professional education.

1. CONCEPT AND DESIGN

The concept of structural dynamics of the three dimensional member and ensemble in relation to the seismic motion is larger and could therefore not be defined, as it is sometimes claimed, only by sort of an "engineer's commonsense". This simplistic way of belittling a most complex dynamical concept has often led to confusions. The dynamic concept of structural members taking also into account the share of nonbearing structures, assumes a thorough study of each individual detail and structural element, up to the entire structural ensemble. The effects of earthquakes produced during the last years have shown how the breach of the dynamical concept of design and construction of a building may lead to local partial or total damages of some urban blocks of flats.

The survey of the damaged buildings revealed the following deficiencies related to the dynamical concept of structures as a whole:
- remarkable geometric dissymmetries and geometrical discrepancies in the distribution of structural and rigid elements as well as in the arrangement of partition walls, both vertically and horizontally, due to a dynamically inadequate architectural design (spaces placed at nonuniform depths and having different destinations and functions, disproportionate compartments, heavy cantilevers, eccentrically placed stairwells, juts and recesses, accidental configuration within the project of the buildings, heavy finishings, a.s.o.);
- dynamically unreasonable disproportions in the distribution of structural and non-structural masses (dead overloads of upper floors; overloadings due to the turning of apartment blocks into office buildings; penthouses; heavy roofs; a.s.o.);
- marked discontinuities in the distribution and variation of stiffness in structural members in both horizontal and vertical planes, not ensuring the general three dimansional interactions (the discontinuity of structural elements; the undersized beams and columns; the absence of horizontal disc effect, high ground floors; columns with different axial forces; stair and elevator wells superficially designed within the structure as a whole, a.s.o.).

The presence of such errors of concept and design of a structure to lateral forces may lead, from the dynamical point of view, to the appearance of some inertial, elastic, energetic and tensional concentrators, all of which constitute a vulnerable and unsatisfactory behavior, which may result in disastrous effects during strong seismic motions.

In fact, the above-mentioned errors may lead to direct detrimental implications, mostly in the buildings whose design was based upon a gravitational concept. One may thus mention: the eccentricity between the mass center and the rigidity center, resulting in a tortional effect; the great lateral drifts of flexible framed structures which as found out, have evidently acted upon the vertical structural elements and upon the nonstructural partition walls; the concentration of strong motions at the ground floor level and at that of the lower stories; the nonuniform stresses in resistant vertical elements (columns and wall piers); the tendency to dislodging of members or even of units which, as compared to the whole structure, were greatly flexible or stiff; the different degrees of stress upon the structure, leading to failures in places of high seismic vulnerability.

Besides these global findings resulting from errors existing within the general dynamics concept, the survey of earthquake effects revealed also the serious errors of the conception and the superficial study of some details of structural composition, such as: the narrow spaces of separation between buildings, the high percentage of openings at the first floor stories, particularly in the bearing masonry, with floors of different types of structures and differently loaded (made of timber, metalic girders with small arches, reinforced concrete) with no boundary wall bonds; indirect transmissions of overloads to vertical resistant elements; local disproportions between the stiffness of columns and that of beams lacking the plane or space frame effect, eccentric beam-column connections; the undersize of corner or marginal columns; the presence of a single longitudinal diaphragm in linear structures; the eccentric position of free masonry walls within the openings of frames; the superficial design of the beam-column connections in order to ensure the deformation energy transfer between horizontal and vertical resistant elements; an inadequate longitudinal and transversal reinforcement of columns, beams, shear walls, lintels and joints with random ductility factors that may lead to postelastic deformations and to the appearance of plastic hinges; minimum safety coefficients to shear forces in resistant vertical elements, the wrong use of X-braced frames system; excessive stress in vertical elements that led to fractures, to crushing and buckling of the reinforcement.

Except for some instances, one my say that the behavior of recent constructions, build on the basis of a seismic safe concept and design, under satisfactory conditions, was quite good more so when one takes into account the fact that the intensity of the seismic activity of March 4, 1977 has by far exceeded in Bucharest the safety level stipulated by the design and by the official design code regulations.

2. SEISMIC CODE REGULATIONS

The survey of the effects of the recent strong seismic motions on humans and animals, on the seismic waves propagating medium and on constructions of different types and age, all have led to the conclusion that the current code regulations in this respect will have to be fundamentally reconsidered.

Future studies on seismic zoning and microzoning of the country, a work of high complexity and risponsability, will have to be correlated to those of geophysics, geology, geotechnics , hydrology and seismic engineering. In order to develop such maps new and modern investigation criteria are required for these must take into consideration potential strong earthquakes which might have quite different generating mechanisms and spectral compositions, and which in the future might take place at shorter time periods.

As to the seismic code regulations, the records received in Bucharest, the processing and preliminary interpretation of these have shown that the current quantitative regulations, particularly those regarding the variation of the design spectra, do not correspond to the actual findings.

The theory of response spectra accepted by almost all countries subjected to high seismic risk, was found inadequate for the description of the effect produced by an earthquake upon the resistant elements of a structure. Thus, the present seismic design of a structure on the basis of spectral theory does not include the cumulative energetic process due to the cyclic phenomenon, specific of the seismic motion, and the duration of this. This cumulative process is most important and its effects are much more disastrous going beyond the safety measure of providing materials and structures specifically resistant to the peak values of stress and strain. The future codes of regulations will have to take into account all these aspects as well as the necessity to ensure the safety of buildings in at least two next strong earthquakes. It also becomesnecessary to ensure the compulsory obligation of the dynamical approach of the conception, design and building of aseismic structures.

3. SOIL INFLUENCE

Due to the multitude of its specific phenomena, the soil has always been a determinant factor of the effects produced by the seismic motion upon structures. The major problems are related to some specific aspects of the soil, namely: the influence of characteristics of the seismic wave propagation medium under specific geological and lithological conditions; the influence of local geotechnical and dynamical properties related to the site and location; the presence of underground waters; the configuration of the local relief, stratigraphy and the depth of the bedrock; the focusing of seismic waves, the amplification, attenuation or dispersion of these; the possible faulting, landslips, variation of velocities, a.s.o.

The 1977 earthquake produced in Romania has evidenced a particular way of propagation and amplification of seismic waves, in different directions and in areas quite far from the epicentral zone. Also, a marked focusing of seismic waves was found in strongly urban concentrations. The indentification of the bedrock as well as of the nature of the intermediary stratigraphy and of the structure of rocks will help to a quantification and qualitative estimation of the share which the superficial layers may have had in amplifying or attenuating the seismic response of structures. It is most important that the structural design engineer should know well the physical, mechanical and dynamical properties of superficial layers (inclusively the predominant periods) of a certain site, since all of these provide valuable informations on the specific foundation conditions, the potential limitation or even avoidance of amplification, nonuniform settlement and liquefaction phenomena, being thus capable to assume an expected size of the interaction phenomenon between the soil and the structure it bears.

The variety of effects found in and around Bucharest after the March 4, 1977 earthquake have clearly pointed out to the significance of the site characteristics, the knowledge of which involves thorough studies in the field of structural geology, geotechnics, geophysics, seismology, a.s.o., in order to evidence potential tendencies to collapse, landslipping, faulting and alteration of the underground water mirror. At the same time, one of the requirements is the estimation from these points of view of the seismic risk as correlated to the micro- and macrozoning mapping of the country.

The specific features of Romania's March 4, 1977 earthquake , namely the kynetical and spectral ones, have evidenced high predominant periods in the superficial layers, a fact which has led to the amplification of the seismic response of the tall, more flexible, buildings. Although the mirror of underground waters had no important share in tall buildings the interaction phenomenon appeared as a marked rocking of the buildings, leading to ground dislodgings, slight remanent slopes, collisions within the separation gaps as well as to the visible openings of these. No significant foundation damages were found, mostly in those with continuous or raft foundations, a fact which proves the satisfactory design of the Bucharest buildings infrastructure.

4. THE NUMERICAL ANALYSIS

The specific effects found in the resistant structural elements of buildings damaged by the recent earthquakes have evidenced a series of deficiencies regarding the estimation by the numerical analysis - currently used in design - of the stress and strain condition. Also, the reinforced concrete dimensioning methods provided by the official code regulations are inadequate for the short-duration, cyclic and time-cumulative action, specific of the seismic motion.

The design schemes, patterns and hypotheses, stipulated by current code regulations, do not virtually reflect the actual behavior of structures during an earthquake. A reconsideration is required of the design and of the seismic reliance of structures by the approach of a dynamic theory-based analysis and by taking into account the three-dimensional interaction under the conditions of a non-linear behavior and of a post-elastic behavior. Particular attention will have to be paid to the structures local and general design of stiffness, as well as to the ductilities of resistant elements such as to avoid detrimental phenomena brought about by the general torsion and to limitate as much as possible the relative displacements between floors, particularly at the ground floor and lower stories.

It has also been found that current design methods used for the dimensioning of reinforced concrete structures do not adequately ensure the resistance of vertical elements to axial forces and shear stress.

5. CONSTRUCTION

The engineer who designs an aseismic building, conceives and designs a"conventional building" to which he assigns a priori certain properties and characteristics. The seismic safety initially assumed will be seriously altered unless the provisions stipulated by the project are not strictly observed during the process of construction.

The international reports on detrimental effects of earthquakes on some buildings aseismically conceived and designed have evidenced serious deficiencies of building materials and quality of execution.

Reality has unfortunately confirmed that deficiencies of concept and execution in aseismic buildings have led to effects much more serious than some errors of design.

6. RESEARCH

Theoretical investigations carried up to now did not lead to a unitary and general concept of a physical and mathematical model able to reflect in a complex way the ultimate forces which governs the behavior of a structure - regardless of its type and destination - to a strong earthquake.

Scientists concentrate since a long time on the finding of such a model able to allow for a structural analysis and synthesis, and it should further remain a matter of concern. Natural experience offered by real earthquakes has shown in many instances that the real behavior of some buildings refuted the analysis model of design.

Probabilistic analysis, which at the present is particularly centred on the random character of the seismic motion and of the structural parameters, will further be able to elucidate many of the present incertitudes.

Experimental research still can not adequately account for the dynamic properties of materials, for the postelastic behavior of structures, for their behavior to strong cumulative and cyclic motions, for the phenomena of hysteretic damping a.s.o. At the same time, laboratory as well as full scale research work will have to be extended in order to study experimentally the behavior of certain types of elements, units and structures to simulated seismic motions.

The time evolution of physical and mechanical characteristics of materials should be better known as well as the process of ageing and decay which they are subjected to. This will allow for a probabilistic estimation of time-dependent variability of structural characteristics as well as of the expected response to strong shocks acting within predeterminated return periods.

7. PROFESSIONAL EDUCATION

Taking into account the marked seismic activity in many parts of the world, the area it involves, the size and the destructive periodical effects, one can not conceive a structure without the need of highly qualified professionals to design and construct it.

The design and construction of an aseismic structure represents a technical masterpiece with deep social and economic implications.

Thus, the professional education should start at the universitary level and furthered periodically by post-graduate training, having a technical and practical caharacter and providing updating in the field of seismic engineering.

Particular aspects should be particularly studied by fundamental and experimental investigations and by testing models at a laboratory as well as at a full scale level.

In many countries of the seismic-risk areas the lack of qualified professionals in seismic engineering had negative effects, regarding mainly the aseismic design of structures, the interpretation of destructive effects, the aftershock restoring and reinforcement of structures.

x x x

It is only by a permanent and concentrate co-operation of all researchers and engineers from seismic-risk countries that seismic engineering may make such progress as to eliminate, as much as possible, fear and incertitude.

CAPTION S

Photo 1, 2 - Column failure in a building with flexible ground-floor
Photo 3 - Column failure due to discontinuities of stiffness
Photo 4,5,6 - Column failure due to strong axial and shear forces
Photo 7 - Important failure in column due to the absence of stirrups
Photo 8,9,10 - Failure in a non-shear designed column
Photo 11 - Dislocation of a beam-column joint
Photo 12, 13- Local damage at the extremity of a shear wall due to strong compression
Photo 14, 15- Partial collopse of nonseismic designed buildings (built in the '30's)
Photo 16, 17- Span of separation between buildings after the earthquake
Photo 18, 19- Dislocation of frontispiece with great inertial effect in a monumental building
Photo 20 - Damage in masonry walls of a structure in concrete frames (build in the '30's)
Photo 21, 22- Typical crack in bearing walls (build in the '30's)
Photo 23 - Rocking effect due to soil-structure interaction.

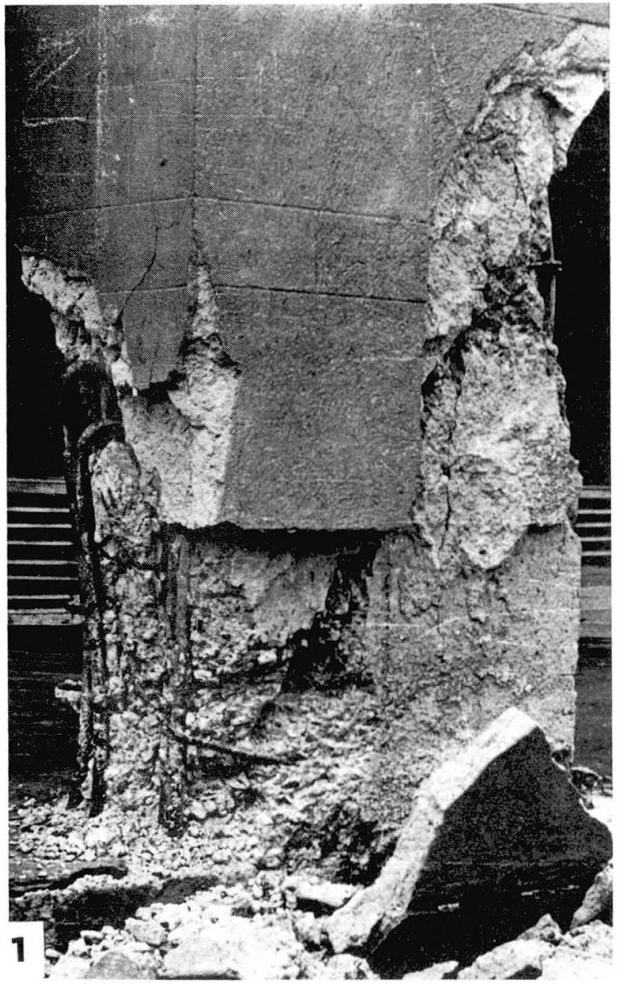

1

• BUCHAREST • 4 MARCH 1977 •

2

• BUCHAREST • 4 MARCH 1977 •

• BUCHAREST • 4 MARCH 1977 •

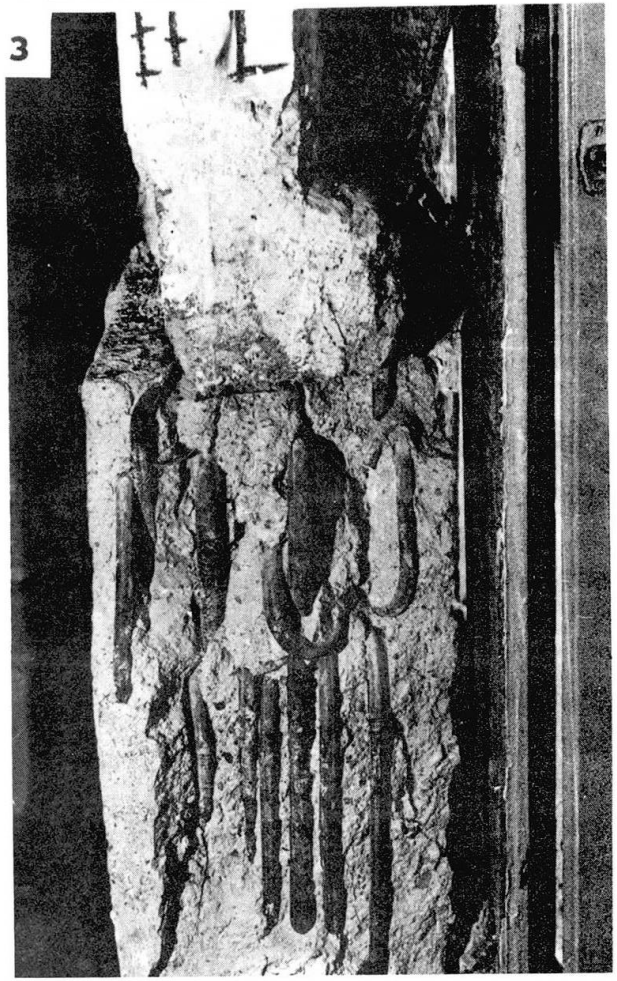

3

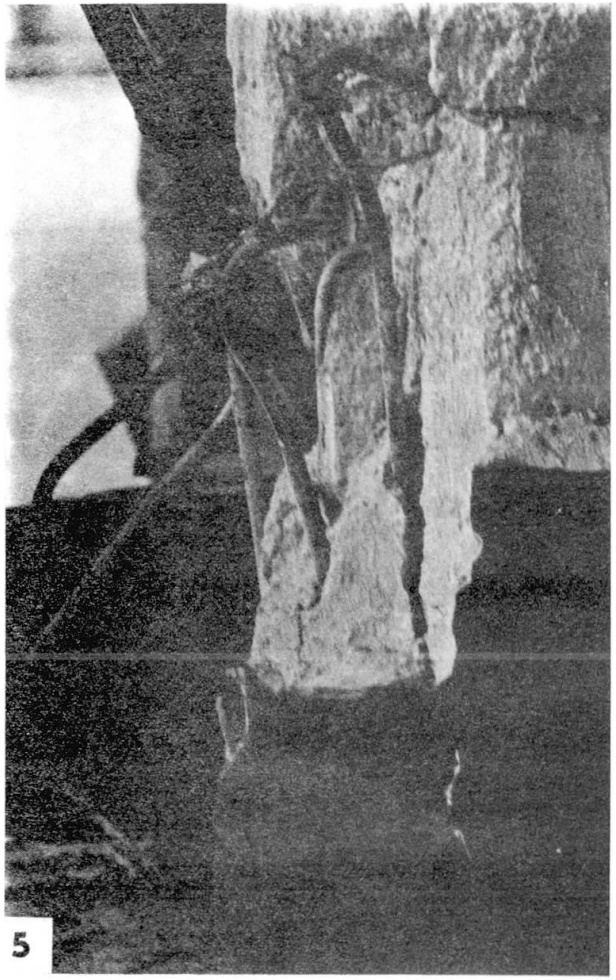

5

• BUCHAREST • 4 MARCH 1977 •

6

• BUCHAREST • 4 MARCH 1977 •

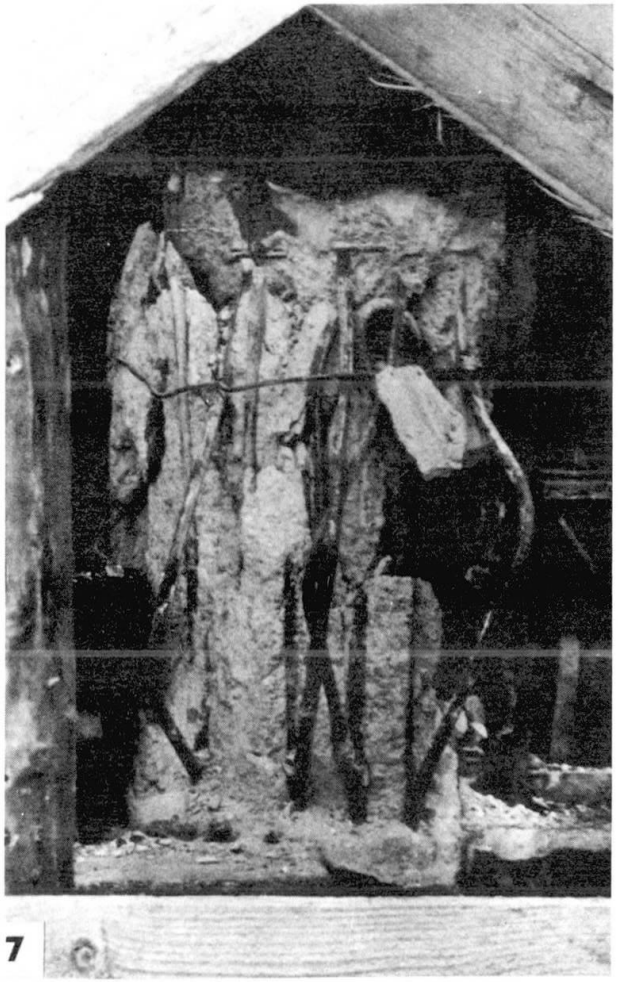

7

• BUCHAREST • 4 MARCH 1977 •

4

• BUCHAREST • 4 MARCH 1977 •

8

• BUCHAREST • 4 MARCH 1977 •

9

• BUCHAREST • 4 MARCH 1977 •

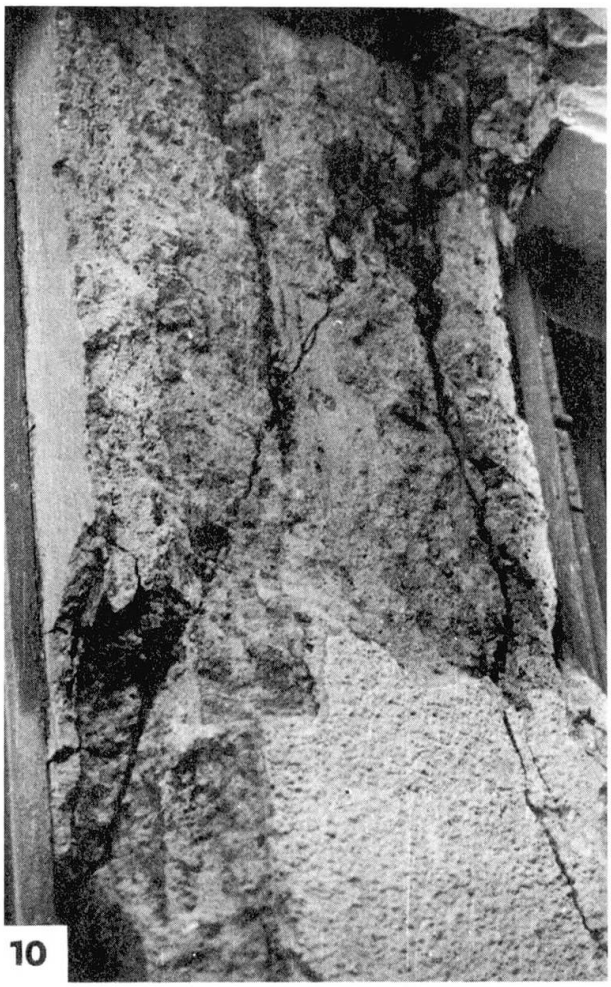

10 • BUCHAREST • 4 MARCH 1977 •

11 • BUCHAREST • 4 MARCH 1977 •

12 • BUCHAREST • 4 MARCH 1977 •

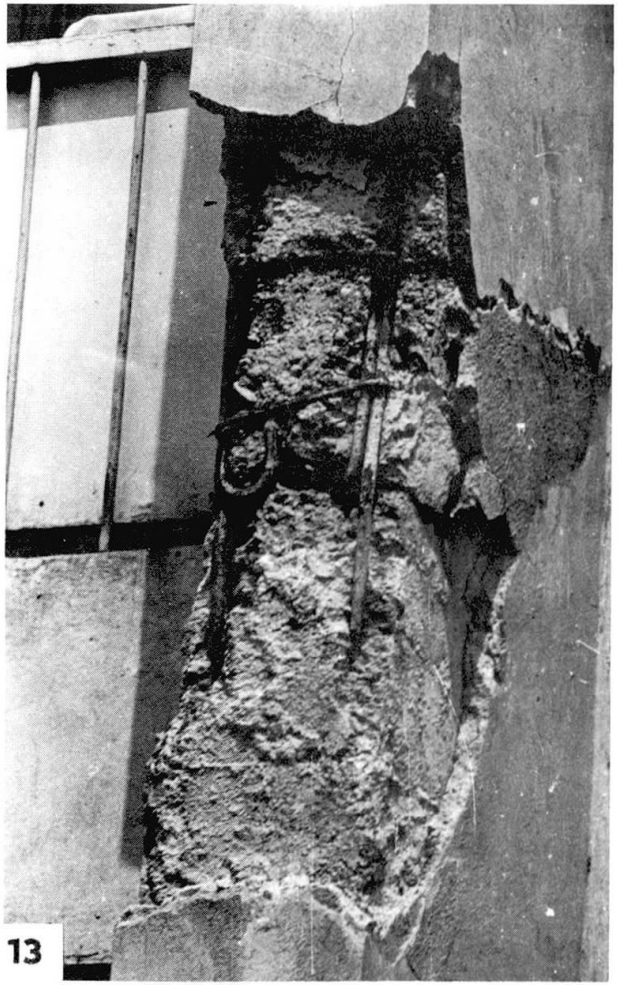

13

• BUCHAREST • 4 MARCH 1977 •

14

• BUCHAREST • 4 MARCH 1977 •

15

• BUCHAREST • 4 MARCH 1977 •

16

• BUCHAREST • 4 MARCH 1977 •

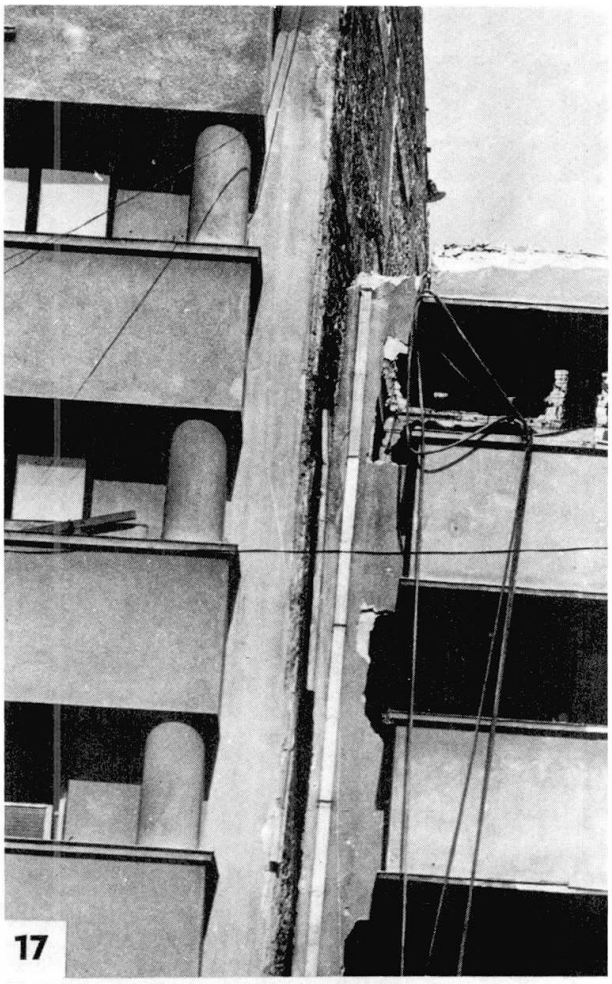

17

• BUCHAREST • 4 MARCH 1977 •

18

• BUCHAREST • 4 MARCH 1977 •

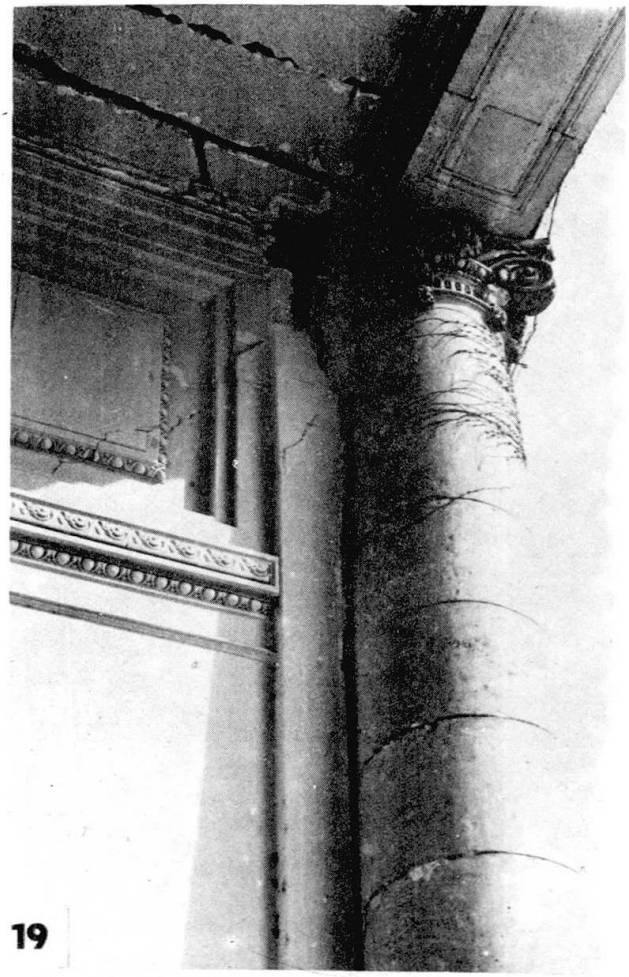

19

• BUCHAREST • 4 MARCH 1977 •

20

• BUCHAREST • 4 MARCH 1977 •

21

• BUCHAREST • 4 MARCH 1977 •

22

• BUCHAREST • 4 MARCH 1977 •

23

• BUCHAREST • 4 MARCH 1977 •

COLUMN UPLIFT DURING SEISMIC RESPONSE OF BUILDINGS

by

Ray W. Clough
Professor of Civil Engineering
University of California
Berkeley, California, U.S.A.

and

Arthur A. Huckelbridge
Assistant Professor of Civil Engineering
Case Western Reserve University
Cleveland, Ohio, U.S.A.

SUMMARY

During severe earthquakes, tall buildings are subjected to overturning moments which may tend to lift the column bases off the foundation. Building codes in California require anchorage of the columns against such uplift, although the cost of anchorage may be high. In this paper, shaking table tests of a 9 story building frame model are described, and the relative behavior with and without anchorage is discussed. Excellent correlations are demonstrated between observed performance and computer predictions.

1. INTRODUCTION

1.1 Overturning Effects during Large Earthquakes

The lateral loading applied to a structure during a major earthquake will often greatly exceed that suggested by current building code seismic provisions. This fact has long been recognized by code committees, and provisions requiring adequate detailing to accommodate local excursions into the nonlinear behavior range have resulted.

No rational provisions have yet been incorporated into codes, however, to consider the effect of the large overturning moments resulting from actual intense seismic loadings. Generally, current code provisions require that whatever overturning moment results from the design calculations must be resisted completely by the structural system, even if supplementary anchorage is indicated. It should be noted, however, that design loadings almost always are lower than the maximum credible seismic loading.

1.2 Implications of Overturning Moment Overloads

If an overturning moment is applied to a structure which exceeds the structure's overturning capacity, a transient uplifting of portions of the structure from its foundation will result. This uplifting response, while not implying imminent toppling of any practical building, is highly nonlinear. Rational consideration of this overload condition, therefore, requires investigation into the category of nonlinear response represented by uplifting systems.

2. UPLIFTING STEEL FRAME TEST PROGRAM

2.1 Preliminary Investigation

Any good structural design must be based on a thorough understanding of the behavior of the structural system when subjected to the anticipated loading conditions. Because severe seismic loading conditions will usually result in a nonlinear response, at least for economical structures, this type of response should be understood as completely as possible. To better understand the nonlinear phenomena associated with uplifting response, a preliminary experimental and analytical investigation was undertaken utilizing a relatively simple single-bay, three-story steel frame superstructure system [1]. In this investigaton the uplifting response was compared to the response of the system when supplementary overturning anchorage was provided, for similar intense excitations. The experimental portion of the investigation was conducted on the U.C. Berkeley shaking table.

The results of this preliminary investigation showed a considerable reduction in applied loading and ductility demand for the uplifting response, when compared to the corresponding fixed base response. In addition, analytical predictions of the uplifting response agreed quite well with the observed experimental results. A mathematical model employing bilinear elastic foundation support elements having zero capacity in the upward direction, combined with a tangent stiffness proportional damping matrix, was utilized in this analytical work.

2.2 Nine-Story Frame Model

As a result of these promising preliminary results, an investigation was undertaken into the uplifting response of a more sophisticated superstructure system, one which would be more representative of an actual prototype structure. The 9 story steel frame model, pictured in Fig. 1 and shown schematically in Fig. 2,

was designed and fabricated for this purpose [2]. As can be seen from the indicated dimensions of the structure in the diagram, the test system was approximately a 1/3 scale model of a realistic, although hypothetical, prototype steel building frame with moment resisting joints. The column base detail which allowed uplift and included a cushioning pad is shown in Fig. 3.

The test structure and the shaking table, described elsewhere by Rea and Penzien [3], were instrumented extensively for the experimental program. A total of 128 data acquisition channels were utilized, with each channel being sampled at a rate of approximately 50 times per second. The resulting data defined the shaking table accelerations and displacements, the accelerations and displacemdnts at the floor levels of the model, its uplift displacements, and selected local member force and deformation quantities, primarily in the lower two floors.

2.3 Experimental Results

One uplift test and one fixed base test utilizing a time-scaled version of the 1971 Pacoima Dam S74W input signal are discussed in this paper. The table accelerations and displacements in the horizontal direction along with the response spectra of these motions for damping ratios of 0.01, 0.02, 0.03 and 0.05 are shown in Figs. 4 and 5. As can be seen in these figures, the table shaking for the two tests was similar and very intense in nature.

The overturning response for the two base conditions is shown in Figs. 6 and 7. Comparison of these figures demonstrates the dramatic effect of column uplift on the response of the structure. The uplift phenomenon performs as a structural "fuse," limiting the overturning forces generally to those values which initiate uplift. Transient excursions beyond this limiting value of load do occur, primarily at instants when the column bases impact with the foundation. However, these very short-lived impulses, such as that seen at about 3.8 seconds in the uplift time history of Fig. 7, appear to be resisted largely by the inertia of the system; these impulses are not so evident in the local element force records.

2.4 Analytical Results: Uplift Test

The analytical results for the uplift test are shown in Figs. 8 through 11; in these figures the analytical quantities are plotted as solid curves together with the corresponding experimental data presented as dashed curves, in order to facilitate comparison of the two. For this analytical work the uplift response was included in the mathematical model through the use of bilinear elastic foundation elements as described for the preliminary tests. In addition a tangent stiffness proportional viscous damping matrix giving a linear 1st mode damping ratio of 0.007 was employed.

As can be seen from the relative horizontal floor displacements of Fig. 8 and the uplift displacements of Fig. 9, the global structural response was predicted quite accurately by this mathematical model. The local 1st floor column forces of Figs. 10 and 11 also show good correlation. An interesting feature of the column base moments of Fig. 11 is the gradual transition from a fixed-base to a free-base condition as the columns separate from the foundation on one side before the other. In addition, a slight numerical stability problem is evident in the calculated column axial forces in Fig. 10; this impact-associated analytical complication is understandably sensitive to the integration time step employed. A time step of 0.0048 sec. was used for this analysis, and the results seem to be within acceptable engineering resolution.

2.5 Analytical Results: Fixed Base Test

The analytical results for the fixed-base test are shown in Figs. 12 through 14, plotted in a similar manner to the previous results. For this analysis the 1st mode damping ratio was specified to be 0.032, and the integration time step was 0.0096 sec. The longer time step was permissible because of the lack of any impact problem in this test. The response during this test extended slightly into the nonlinear strain range for the beams and columns in the lower two floors; their nonlinear moment-curvature behavior was included in the mathematical model through the use of concentrated bilinear plastic hinges at the ends of the members.

As is shown in Fig. 12, the displacements for this test were again predicted accurately. The displacements for the fixed base tests were only slightly lower than those observed during the uplift test, indicating that the internal structural deformations were considerably higher for the fixed base test because there was no "rigid body" contribution to these displacements. The local column forces of Figs. 13 and 14 again show generally good agreement between experimental and analytical values. It can be seen however, that the 2nd mode response was not predicted nearly as accurately as the 1st mode response. Mathematical models, due to assumptions made during their construction, generally tend to overestimate higher mode frequencies. It is interesting to note that the dynamic column compression forces of the fixed base test in Fig. 13 are higher than those of the uplift test, shown in Fig. 10, demonstrating that the impact effect resulting from uplift is not very severe.

3. PRACTICAL DESIGN IMPLICATIONS

The results of this test program indicate that a structural system including a rationally designed uplifting capability would have an enhanced probability of surviving a severe earthquake in a functional condition. Both the structural frame and the nonstructural exterior and interior walls are subjected to reduced strains and deformations. In order to fully exploit this improvement, it is suggested that the two-level design philosophy be employed in the design of building frames in which uplift is allowed. Under expected moderate earthquake conditions, corresponding to normal building code design requirements, it is probable that the dead weight overturning constraint will not be exceeded, and the design may follow standard procedures, because no uplift will occur.

However, under severe seismic conditions, corresponding to the maximum expectable earthquake at the building site, a dynamic response analysis should be performed to determine whether the structure develops overturning tendencies. If so, a nonlinear dynamic uplift analysis should be made to evaluate the maximum frame stresses which can be expected. As is evident from the results of this investigation, these stresses will be significantly reduced by allowing uplift to take place; in effect, the uplift mechanism absorbs the seismic displacements and greatly reduces the ductility demand on the structure frame.

In designing for uplifting performance, the following factors should be considered.

There should be relatively little restraint to vertical separation of the column bases from the foundation, although a rather flexible energy dissipation mechanism could be incorporated if deemed desirable. Sufficient resistance to steady-state wind loading must, of course, be provided.

A reliable "shear key" is required to prevent the columns from walking off the foundation during uplift response. The flexure plate concept used in the test program seems worthy of serious consideration, but would have to be extended to accommodate a biaxial type of response.

An impact pad must be provided at each column, which will tolerate impact and protect potentially more brittle components.

Flexibility is required in service connections to the structure. A centrally located service core, where little or no separation should occur, would seem a logical design concept.

A reliable nonlinear dynamic analysis which takes account of the uplift response must be made to ensure a tolerable amplitude of uplift motion, even during the most severe credible earthquake.

Looked at in this light, a planned uplift capability can be thought of as a supplement to the current detailing requirements which ensure a safe behavior during overload conditions. Due to the fact that little experience has been acquired with the uplift phenomenon, however, it should be considered explicitly in the design process, through an actual dynamic analysis.

Although this investigation was concerned with a steel moment frame, there is no reason to limit uplift behavior to only that category of structural system. Ductility may be achieved readily in steel moment frames, and systems without thi inherent ductility would have their seismic performance enhanced to an even great degree by the inclusion of an uplift capability. Achieving a ductile behavior in reinforced concrete frames, for example, requires adequate confinement steel, wit associated increased material and placement costs. Shear wall and braced frame systems also present special problems in achieving high ductility. Eliminating or at least substantially reducing the ductility demand for those systems could easily lead to considerable savings in the superstructure system, and simultaneously provide enhanced safety for the occupants.

As an added economy to these mentioned above, potential foundation savings could result in structural systems for which current code overturning provisions requir supplementary anchorage. Such overturning anchorage can be exceedingly expensive requiring deep piles or caissons to provide the required tensile capacity.

4. CONCLUSIONS

This research presents strong evidence for including a rationally planned uplift capability as part of a dual seismic performance criterion. By this approach increased safety can potentially be coupled with increased economy. Analytical tool are presently available to accurately predict this type of nonlinear response; indeed this catagory of nonlinearity lends itself very well to analysis, due to its inherently simple nature.

ACKNOWLEDGEMENTS

The research described in this paper was supported by the American Iron and Steel Institute Project 177 (Seismic Resistance of Steel Frames), and National Science Foundation Grant ENV76-04262, (Seismic Behavior of Complete Structural Systems). The continuing interest and support of both these organizations is gratefully acknowledged.

REFERENCES

1. CLOUGH, R. W. and HUCKELBRIDGE, A. A., "Preliminary Experimental Study of Seismic Uplift of a Steel Frame," U.C. Berkeley Earthquake Engineering Center Report, UCB/EERC-77/22, August 1977.

2. HUCKELBRIDGE, A. A., "Earthquake Simulation Tests of a Nine-Story Steel Frame with Columns Allowed to Uplift," Thesis presented to the University of California, Berkeley, California, in 1977, in partial fulfillment of the requirements for the degree of Doctor of Engineering, UCB/EERC-77/23

3. REA, D., and PENZIEN, J., "Dynamic Response of a 20' x 20' Shaking Table," Proceedings of the 5th World Conference on Earthquake Engineering, Rome, 1973.

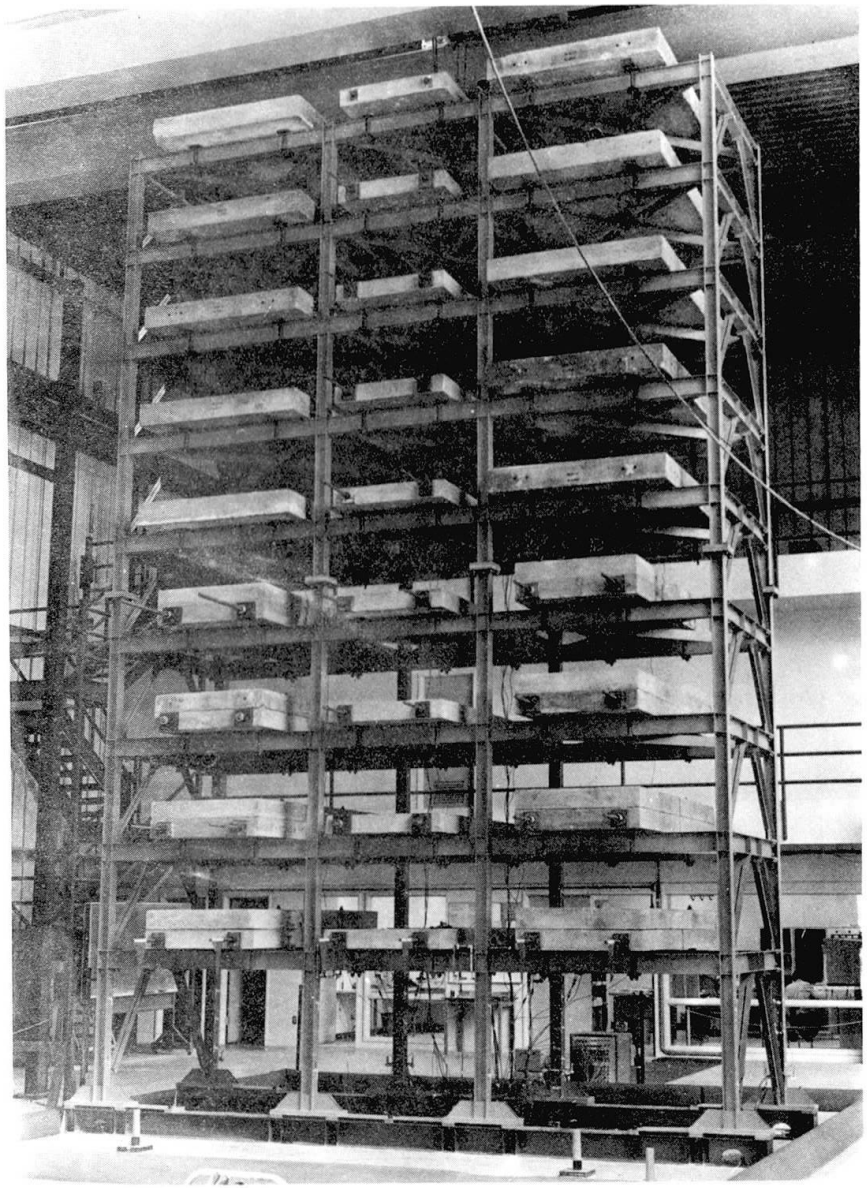

Fig. 1 Test Structure on the Shaking Table

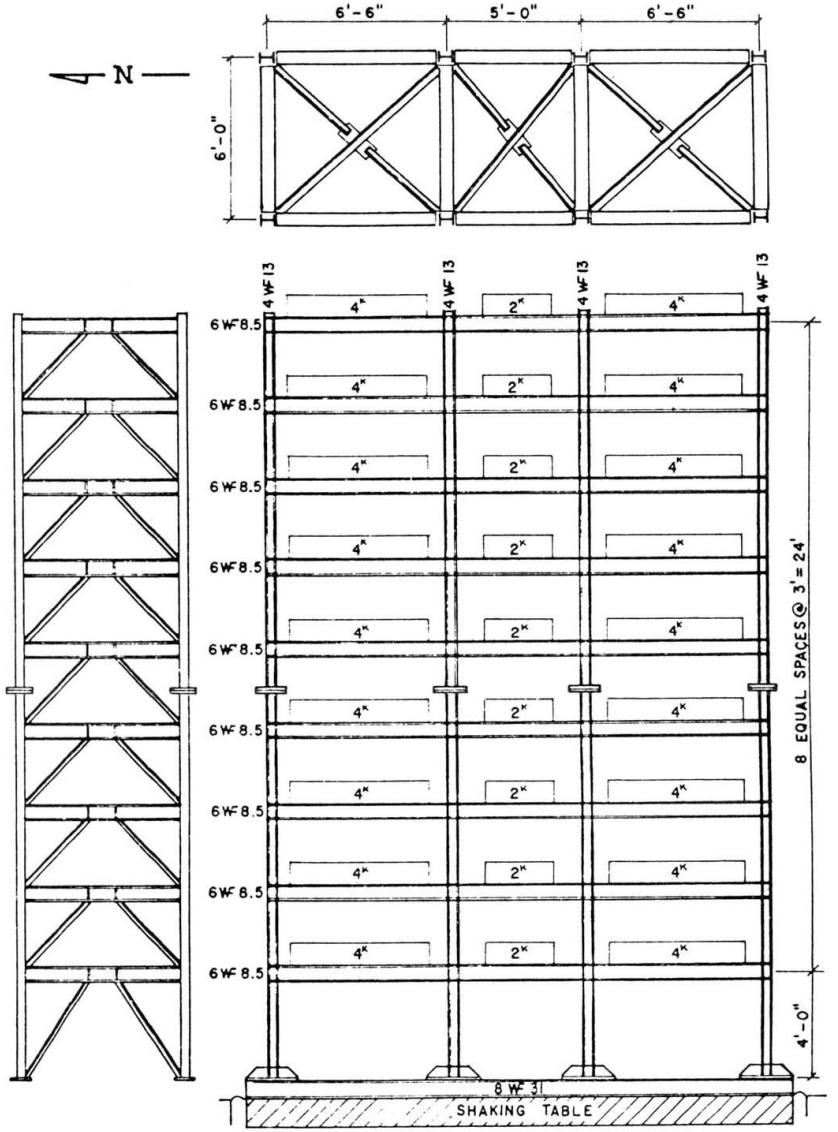

9 STORY STEEL TEST FRAME

Fig. 2 Test Model Schematic

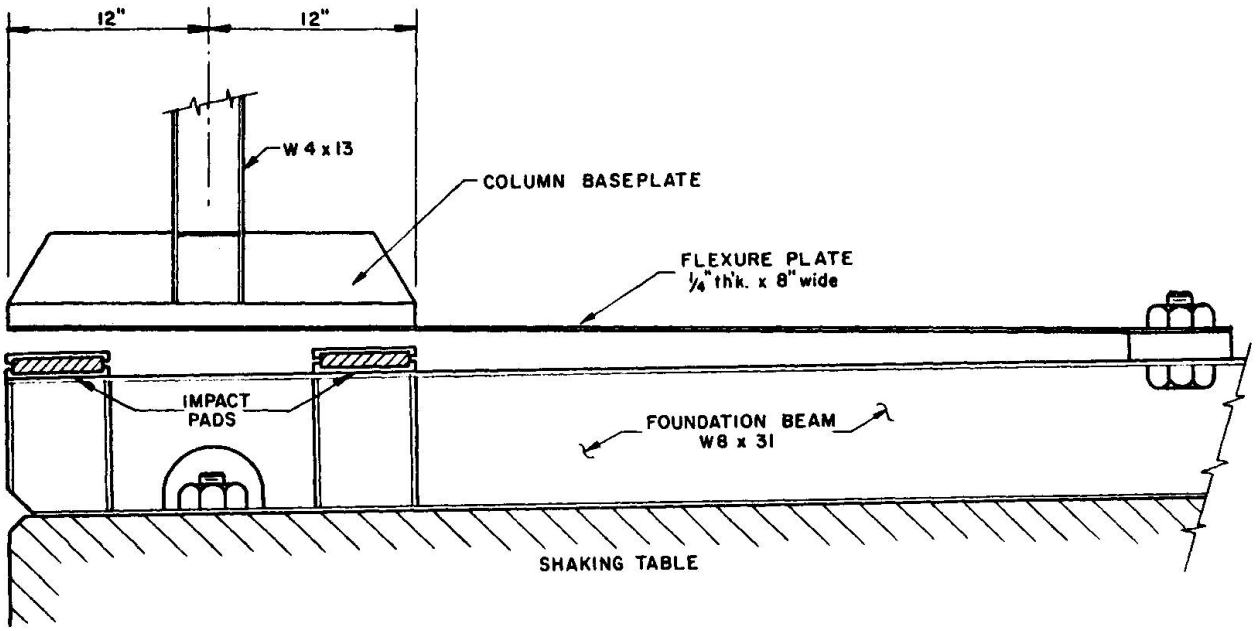

Fig. 3 Uplifting Column Base Detail

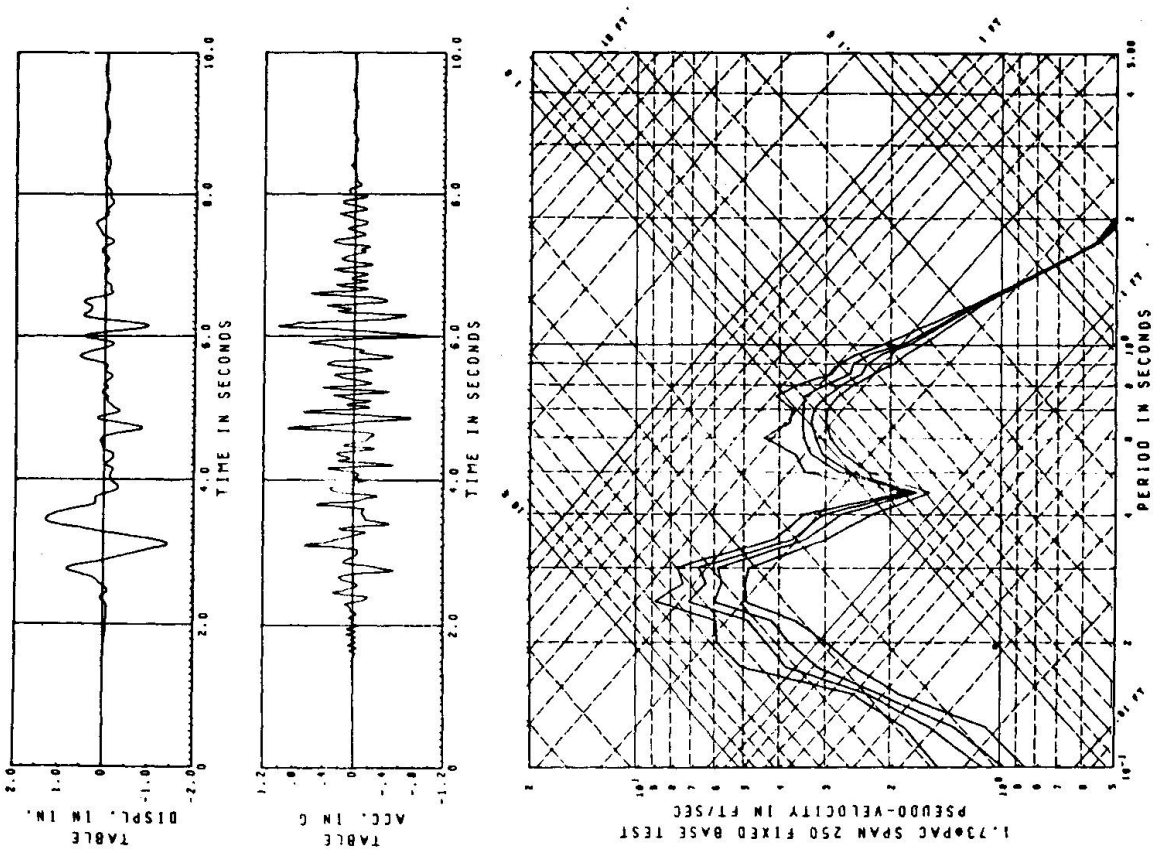

Fig. 4 Fixed Base Test Horizontal Table Motion

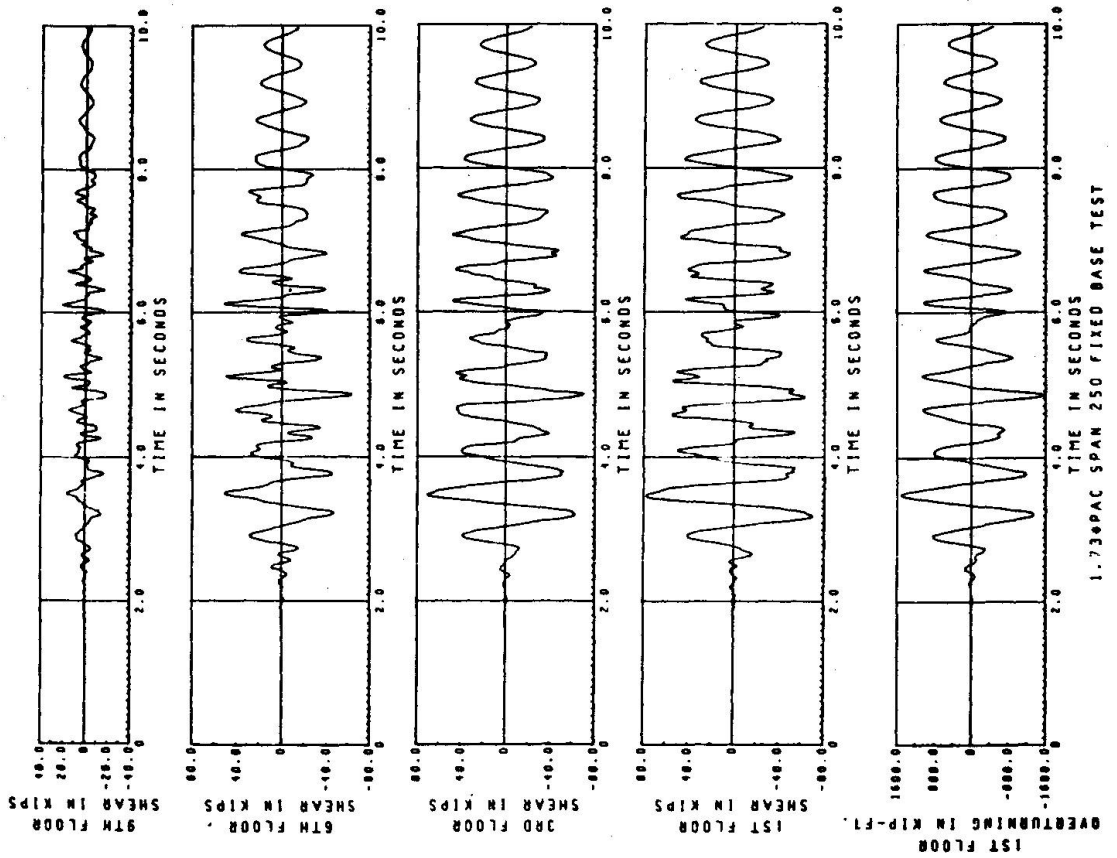

Fig. 6 Fixed Base Story Shears and Base Overturning

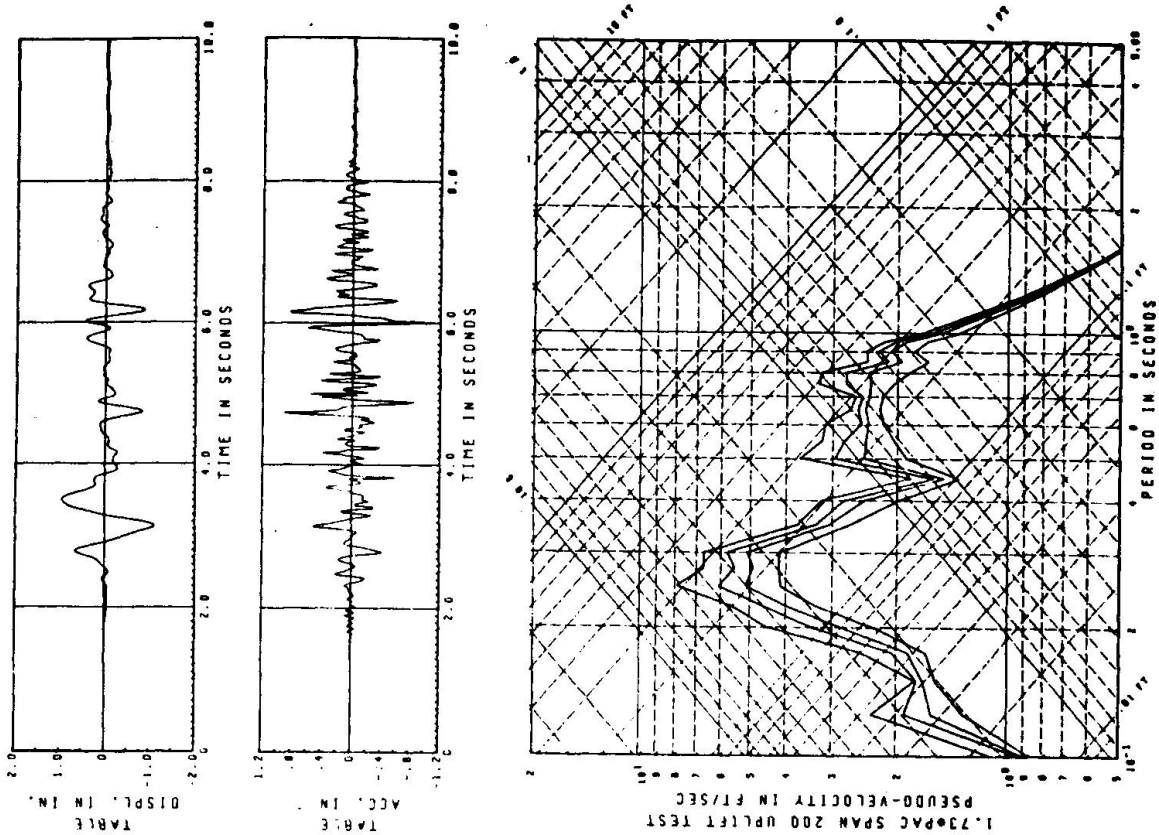

Fig. 5 Uplift Test Horizontal Table Motion

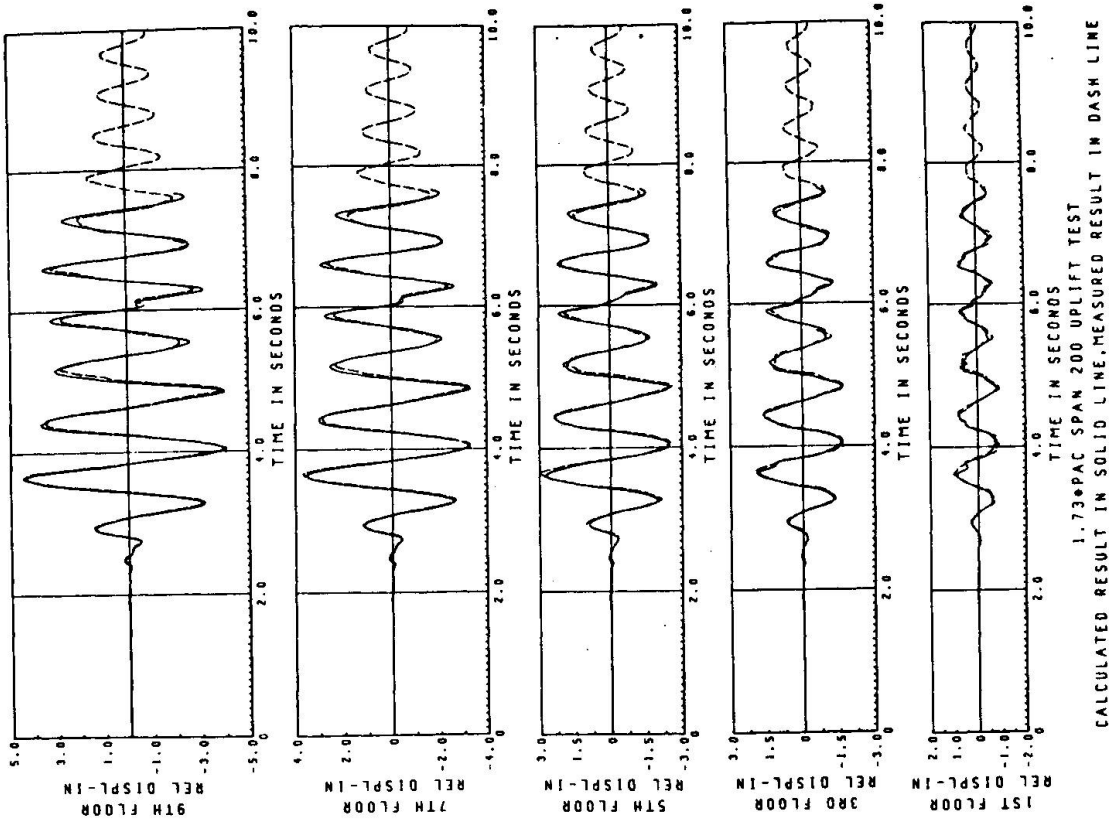

Fig. 8 Uplift Test Results; β = .0011, Δt = .0048 sec.

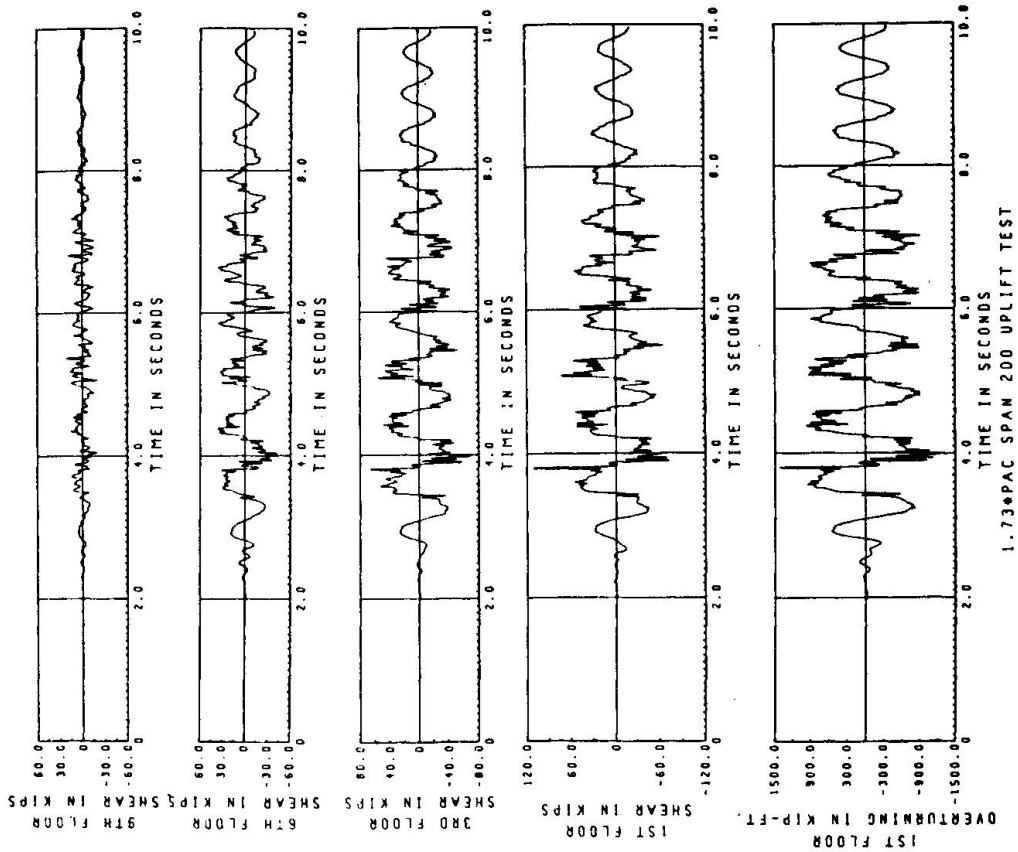

Fig. 7 Uplift Story Shears and Overturning

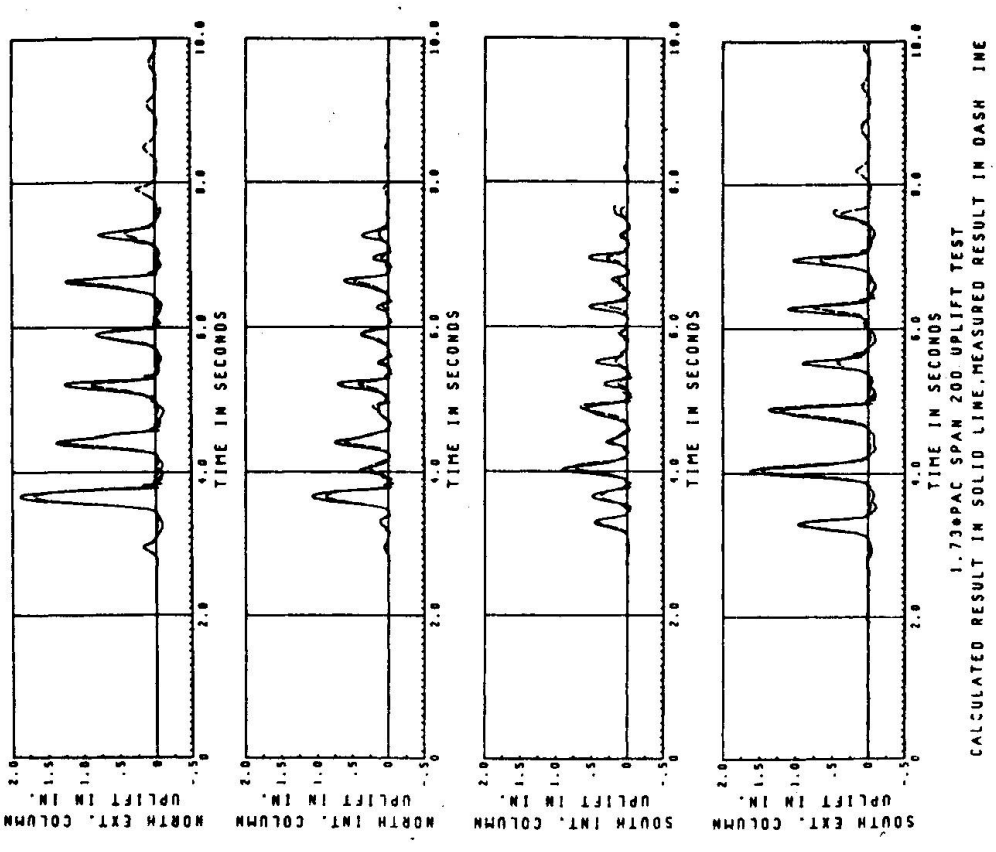

Fig. 9 Uplift Test Results; β = .0011, Δt = .0048 sec.

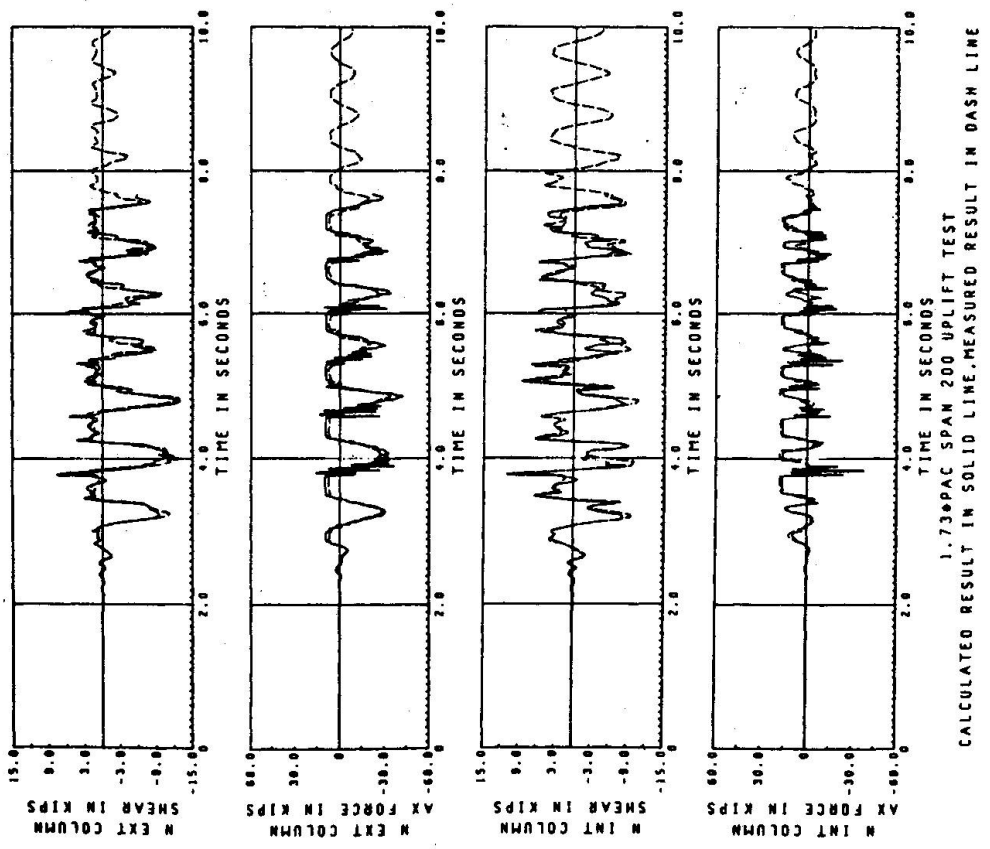

Fig. 10 Uplift Test 1st Floor Column Forces; β = .0011; Δt = .0048 sec.

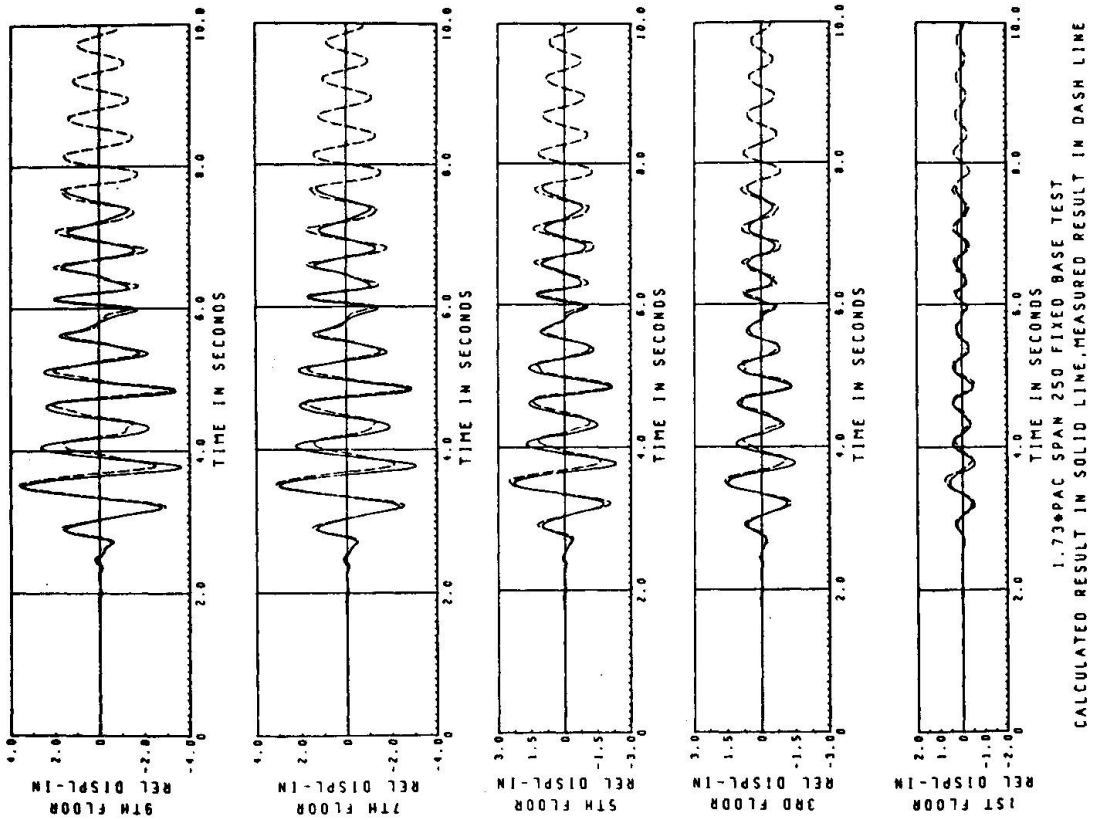

Fig. 12 Fixed Base Test Results; β = .005127; Δt = .0096 sec.

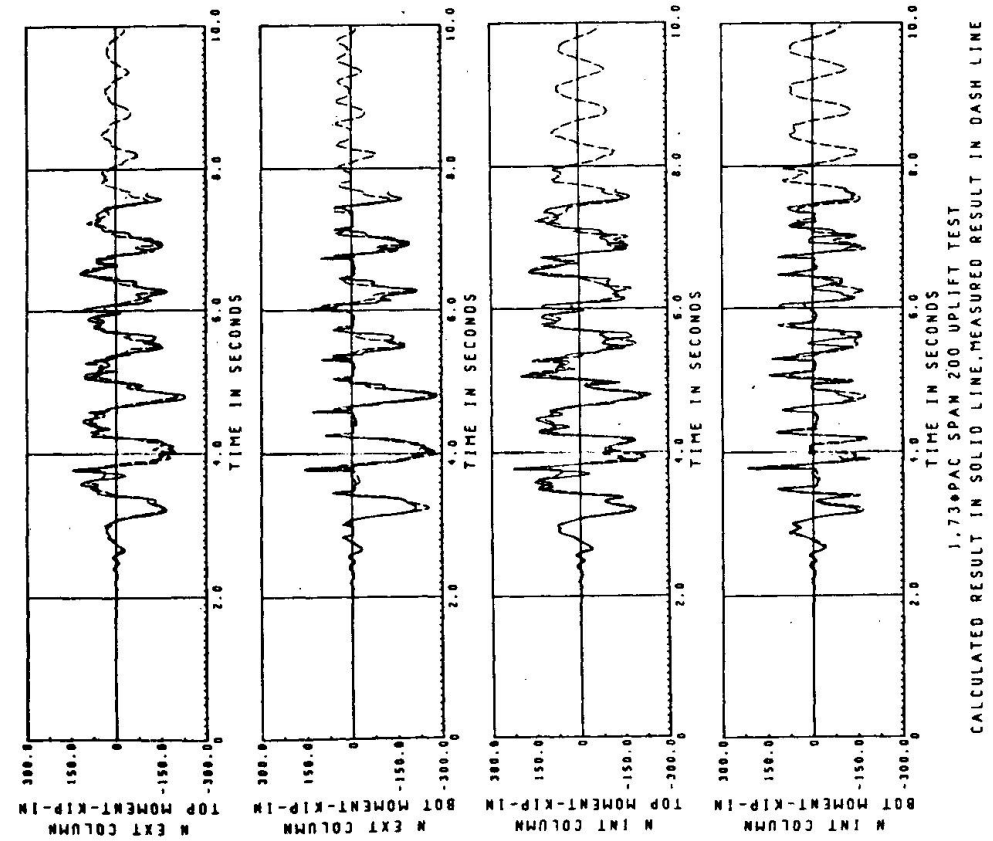

Fig. 11 Uplift Test 1st Floor Column Moments; β = .0011, Δt = .0048 sec.

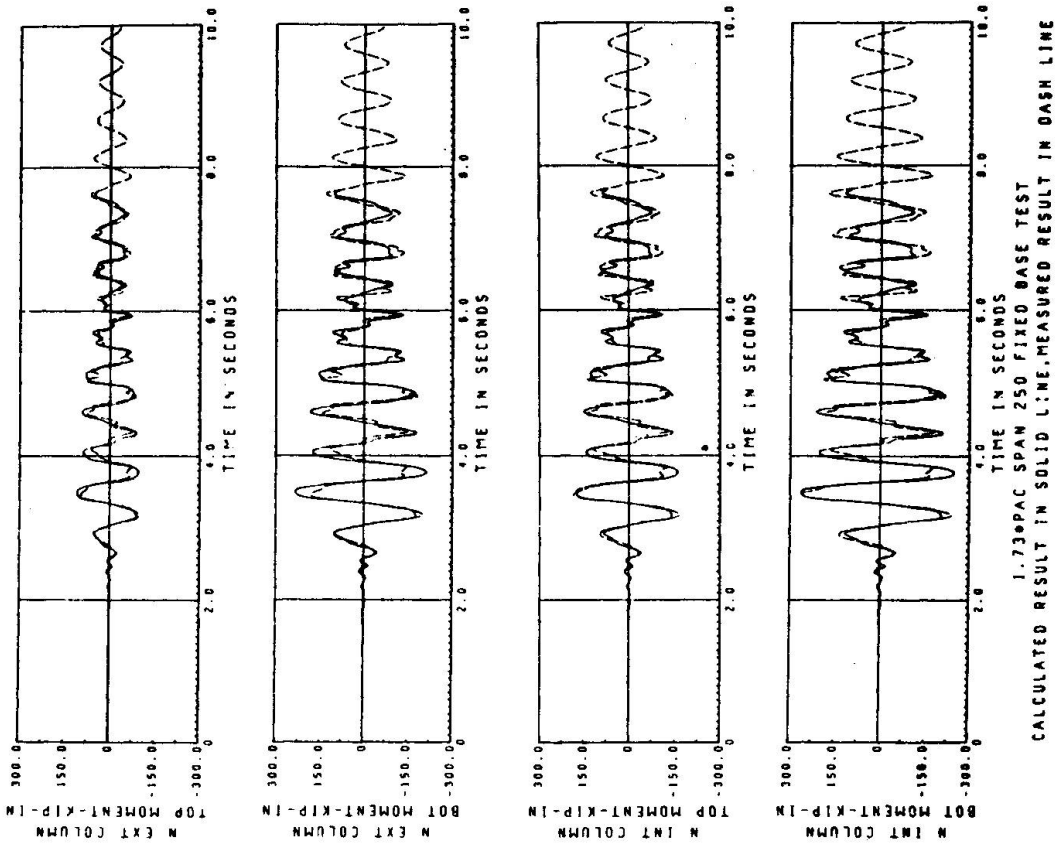

Fig. 14 Fixed Base 1st Floor Column Moments; β = .005127, Δt = .0096 sec.

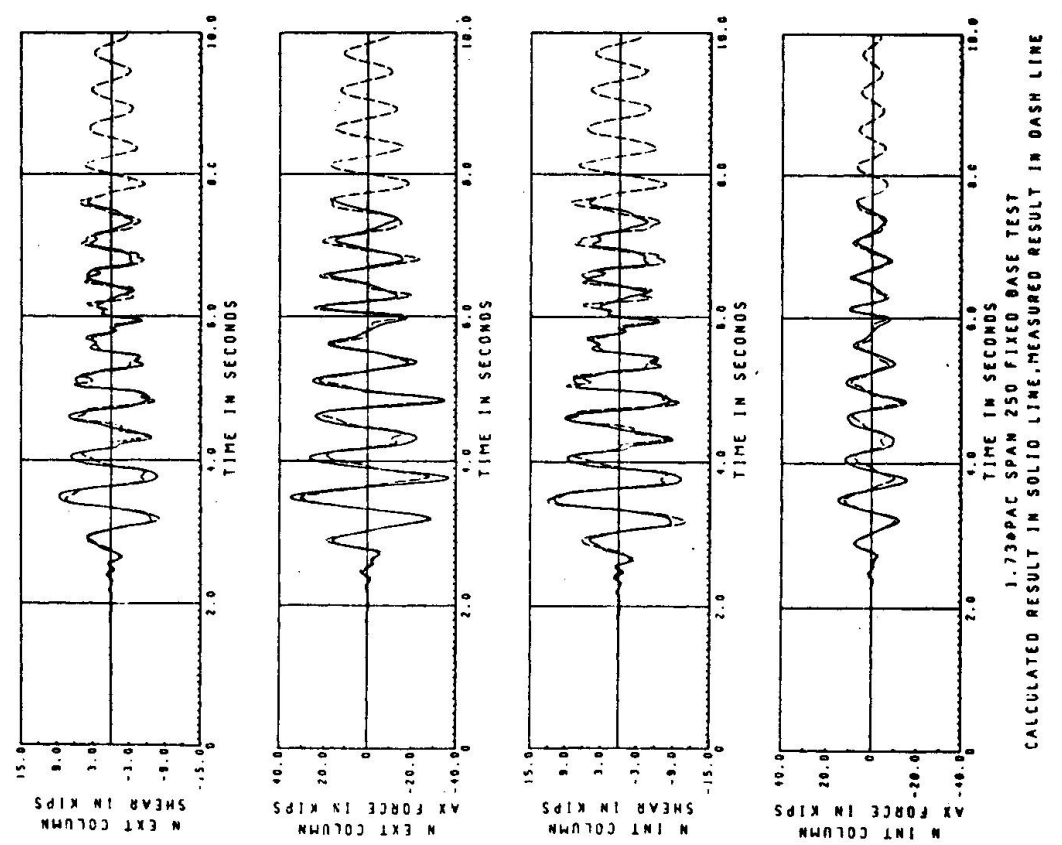

Fig. 13 Fixed Base 1st Floor Column Forces; β = .005127, Δt = .0096 sec.

EFFECT OF CONSTRUCTION JOINTS ON VIBRATIONS OF STRUCTURES

M. Çelebi, Associate Professor Dr., M.E.T.U., Ankara, Turkey
M. Erdik, Assistant Professor Dr., M.E.T.U., Ankara, Turkey
Ö. Yüzügüllü, Assistant Professor Dr., M.E.T.U., Ankara, Turkey

SUMMARY

In this paper two examples are presented with regard to the vibrational behavior of structures with construction joints. A vibration generator system is used to determine experimentally the vibrational characteristics of the structures. First example is a R.C. 14 story building with 3 wings that are located around a core and separated by construction joints. Second is a 6 story high bare R.C. frame structure separated by a construction joint from another building complex. The actual behavior of the structures studied was quite different than expected by assuming functional construction joints. The construction joints constrained the independent vibration of each separate unit.

1. INTRODUCTION

Construction joints have long been used for reasons other than seismic performance considerations. However recent vibration tests of some multistory buildings brought to open the importance of looking into actual behavior of construction joints as against those functions or behavior assumed or predicted from their ideal and theoretical design considerations.

Vibration tests of several structures have been accomplished by various investigators. They studied the dynamic characterists of structures such as multistory building {1}, dams {2}, and nuclear reactors {3}. As one expects these experimental studies were performed to verify the mathematical model of the structures being tested.

These purpose of the presentation made herein is to put actual observed behavior of two multistory building vibration test results and discuss the implications of the construction joints to the seismic performance of these buildings.

2. OBSERVED BEHAVIOR OF STRUCTURES WITH CONSTRUCTION JOINTS

In this section the description and the test results of two structures within the framwork of research project is presented. The results will be further elaborated to bring forth the method of analysis and testing and to help draw conclusions.

2.1. Building A

The geometrical description of Building A is given in Table I and the plan of the building is given in Fig.I.

TABLE I. DESCRIPTION OF BUILDING A

HEIGHT OF THE STRUCTURE (m)	44.1
TYPE OF THE STRUCTURE	Reinforced Concrete Shear Wall
FLOOR SYSTEM	Slab Plate
FOUNDATION SYSTEM	Continous Ribbed Slab
CONCRETE USED	B225 Assumed $E = 2.1 \times 10^5$ kg/cm^2

This particular structure was constructed as a reinforced concrete shearwall structure by using prismoidal tunnel forms originally developed in France {4}. Doors, windows and other functional openings were realized by use of standardized frame forms embedded into the wall, and the floor thickness were defined by the adjacent tunnel forms. The face panels and the stairways of the building were precast independently and later attached to the main body of the structure by means of the existing dowels. At the time of vibration tests the present face panels were not attached to the structure yet.

According to the test results obtained, it has been found out that the building vibrated as a monolithic unit as opposed to the ideal design considerations that considers four independent sections. As seen in Fig. I the building is designed in separate units with 3 identical wings located around a central core unit. Each wing is separated from the core by a construction joint.

It should be noted that, the performance of the structure vibrating as a whole unit would not have been noticed without such a test.

- Analytical Results

After the test, to provide correlation with the experimental values, the structural characteristics are based on the following assumptions :

In the computation of the lateral stiffness, only the contribution of the panels denoted by thick lines in Fig.I are considered.

Door and window openings are neglected in the computation of the equivalent areas.

In each wing, the corridor slab is considered to be a slab with hinges at the ends, connecting the two units on both sides.

Reinforcement is neglected in the computation of the sectional properties.

The structure is modelled as a continuous cantilever beam. The rigidities computed at the center of rigidity are :

$k_x = 105797$ t/m, $k_y = 100440$ t/m, $k_\theta = 4.66 \times 10^7$ t/m.

the uncoupled natural frequencies are then :

$f_{x1} = 2.50$ cps.

$f_{\theta 1} = 2.04$ cps.

The coupled frequencies are computed from the following equation :

$$\left(\frac{f_n}{f_x}\right)^4 \left\{1 - \left(\frac{e_y}{r_{CR}}\right)^2\right\} - \left(\frac{f_n}{f_x}\right)^2 \left\{1 + \left(\frac{f_\theta}{f_x}\right)^2\right\} + \left(\frac{f_\theta}{f_x}\right)^2 = 0 \quad \text{Eq. EI.20 \{5\}}$$

using $\frac{f_\theta}{f_x} = 0.82$ and $\frac{e_y}{r_{CR}} = 0.21$,

$f_1 = 1.98$ Hz. and $f_2 = 2.63$ Hz. are found.

- Experimental Results

The locations of the vibration generator and the accelerometers A1 and A2 on the 14th floor (floor below the roof) are shown in Fig.I and the frequency response curves corresponding to the above mentioned accelerometers A1 and A2 are given in Figs. II and III. The resonant frequency obtained from the tests is 1.525 Hz and percentage of critical is $\xi = 1.47\%$.

- Design Period

During the design of the structure the following period formula was used {4} :

$$T = \frac{0.06H}{\sqrt{L_x}} \sqrt{\frac{H}{2L_x + H}},$$ with $H = 44.1$ m and $L_x = 19.08$ m, the first natural period corresponding to one wing is computed as $T_1 = 0.4435$ sec (or $f_1 = 2.25$ Hz).

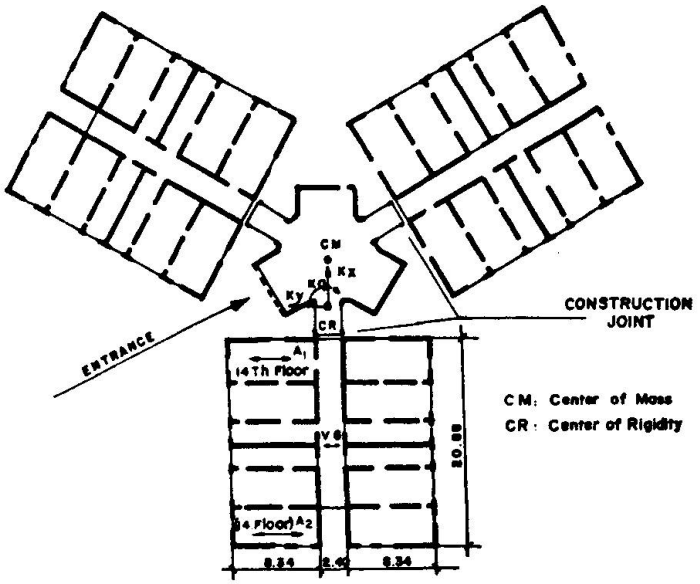

FIG. I PLAN OF BUILDING A

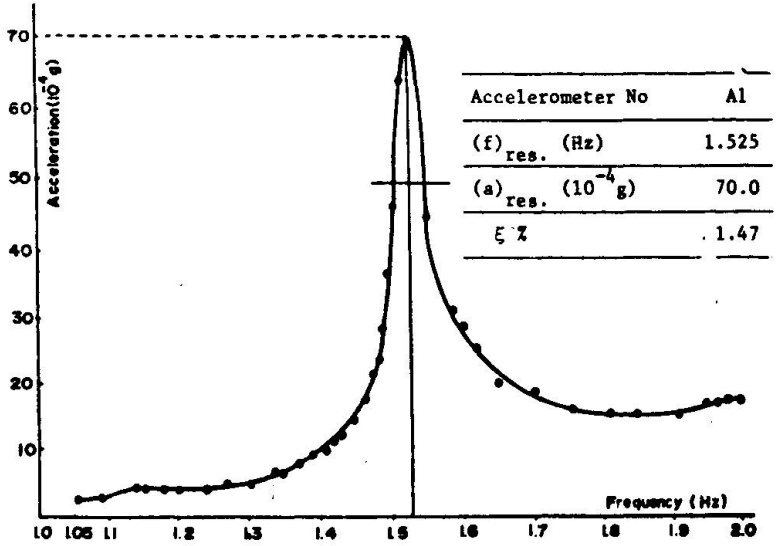

Accelerometer No	A1
$(f)_{res.}$ (Hz)	1.525
$(a)_{res.}$ (10^{-4}g)	70.0
ξ %	1.47

FIG. II FREQUENCY-ACCELERATION CURVE

Accelerometer No	A2
$(f)_{res.}$ (Hz)	1.525
$(a)_{res.}$ (10^{-4}g)	181.44
ξ %	1.47

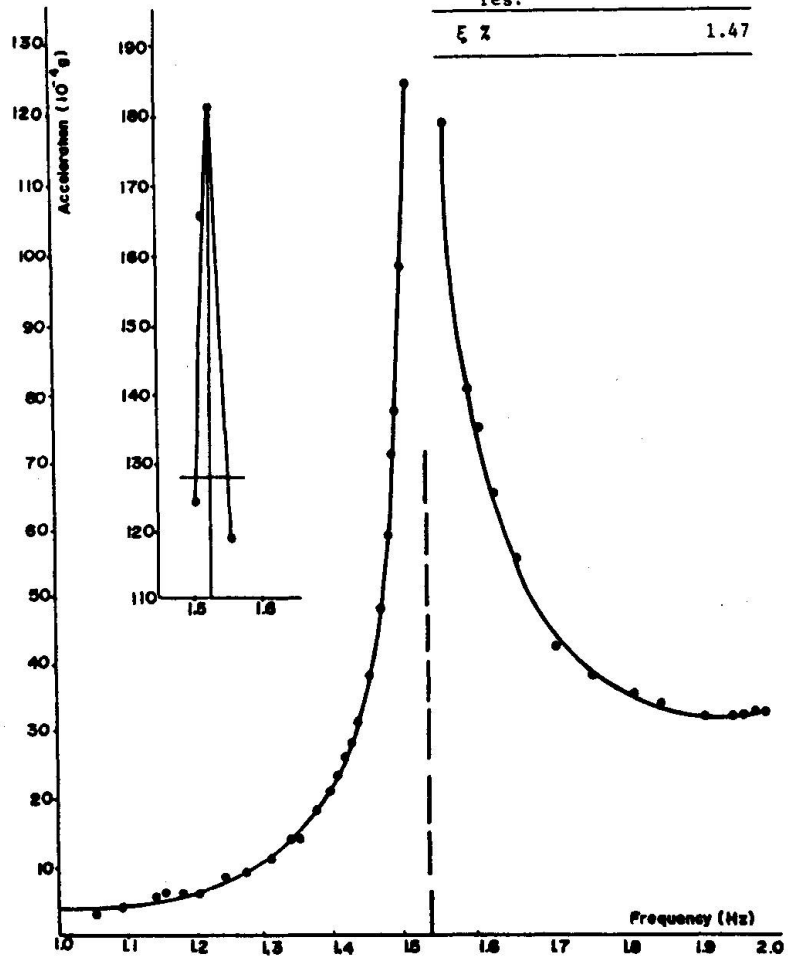

FIG. III FREQUENCY-ACCELERATION CURVE

- Comparison of the Results

Using a procedure developed by WHITMAN {6} it is possible to include the effect of soil-structure interaction on the frequency of vibration. After such a computation analytically obtained first coupled frequency f_1 reduces from 1.98 to 1.72 Hz. This is a 13% reduction, and it is a better result when compared with the experimentally obtained value of 1.525 Hz. It should be noted that the design frequency f_1 = 2.25 Hz obtained for one wing is two much in error when compared with the experimentally obtained value 1.525 Hz, indicating the effect of non-performance of the construction joints.

2.2. Building B

Building B is a six-story reinforced concrete goverment building as described in Table II.

TABLE II. DESCRIPTION OF BUILDING B

HEIGHT OF THE STRUCTURE (m)	H = 20.40
PLAN DIMENSIONS (m)	D = 15.26 B = 48.30
TYPE OF THE STRUCTURE	R.C. Frame
FLOOR SYSTEM	Two-way R.C. Plates
FOUNDATION SYSTEM	Combined column and wall Footings, tied together
CONCRETE USED	B225

As of the day of testing the 7th story of the structure and all outer and partition walls had not been completed. The block was separated from the complex by an expansion joint at the western side. Fig. IV is the N-S section and Fig. V is a typical story plan of the structure. The location of the vibration generator accelerometers, center of mass and center of rigidity are indicated on the typical story plan.

A theoretical dynamic analysis of the structure is carried out through the use of the approximate method developed in {7}. Assuming a rigid foundation, theoretically, first and second coupled natural frequencies are computed to be f_1=3.21 Hz and f_2 = 4.0 Hz respectively. Using WHITMAN's {6} procedure for the soil-structure interaction again, the above frequencies are reduced to the following values :

f_1 = 3.21 Hz and f_2 = 2.69 Hz,

indicating a reduction of 16% in the first lateral frequency of vibration and are very close to the experimentally obtained values which are 2.60 Hz for the first mode and 3.03 Hz for the second mode.

Fig. VI is a comparison of the theoretical and experimental centers of rotation. As one should notice, due to the constraining effect of the construction joint, the experimental centers of rotation are nearer to the construction joint than the theoretical centers.

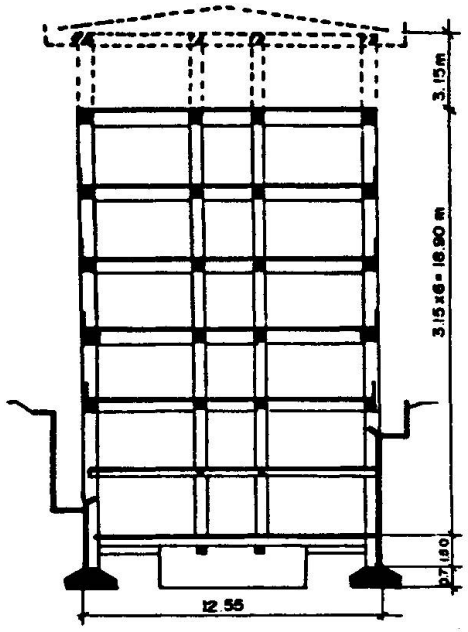

FIG. IV ELEVATION OF BUILDING B

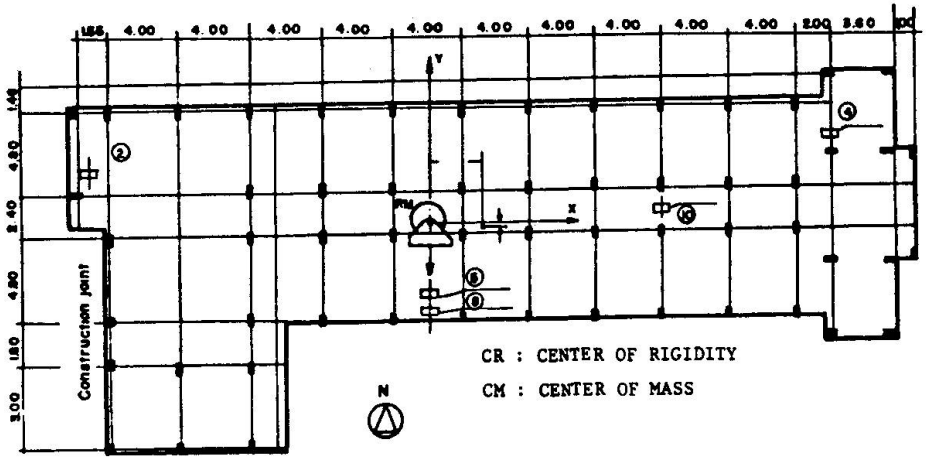

FIG V PLAN OF BUILDING B

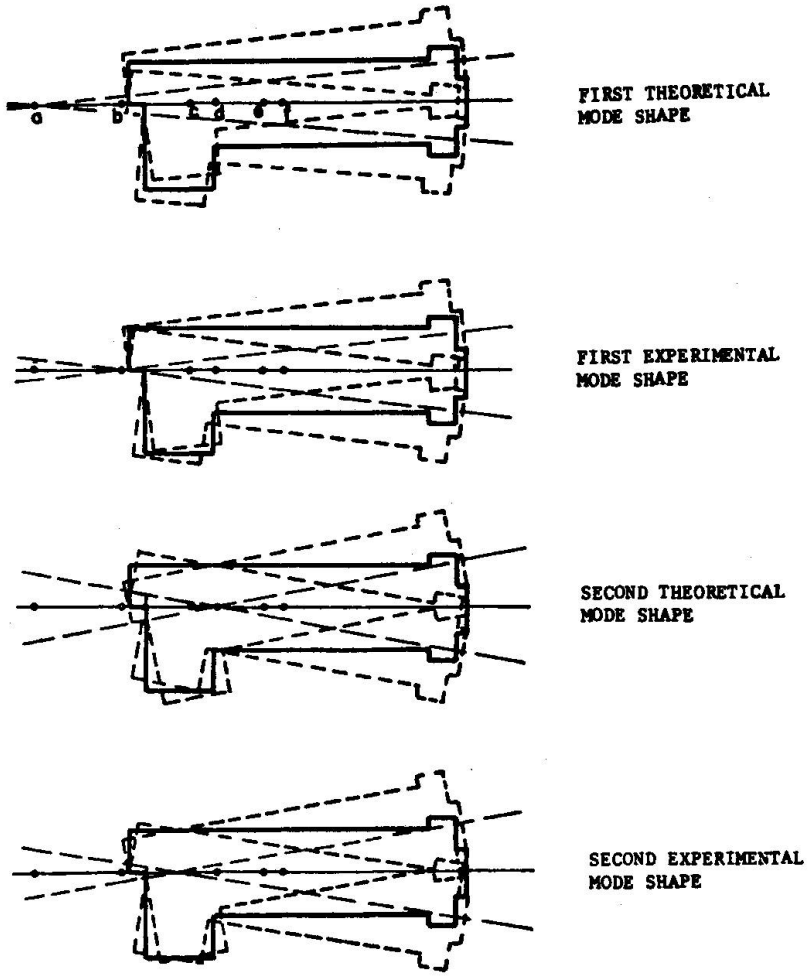

a = THEORETICAL CENTER OF ROTATION IN THE FIRST MODE
b = EXPERIMENTAL CENTER OF ROTATION IN THE FIRST MODE
c = EXPERIMENTAL CENTER OF ROTATION IN THE SECOND MODE
d = THEORETICAL CENTER OF ROTATION IN THE SECOND MODE
e = CENTER OF RIGIDITY
f = CENTER OF MASS

FIG. VI FIRST TWO MODAL SHAPES OF BUILDING B

3. CONCLUSIONS

In the light of the two example structures investigated in this paper and also of someother tests that have been carried out the following practical implications and conclusions can be drawn.

- The effects and the function of the construction joints on the vibrational characteristics of the buildings should be kept in mind during the planning phase and design of the structure.

- Two avoid seismic interaction between parts of the building and to secure the fundamental design considerations on the seismic performance of structure proper care and attention should be paid to the actual construction of the construction joints.

- In both of the structures presented herein, torsional modes have been excited because of the inoperative construction joints. This way totally unexpected and not foreseen in actual design considerations.

- Since the forces that will be emposed on the structure during a seismic exposure will be for above those imposed by vibration generator system the re-operation or (forced operation) of the construction joints may be speculated. However, it can be shown that, especially for building parts with similar dynamic properties, the shearing forces that develop on both sides of the construction joint will most likely be in phase and thus the differential shear may not exceed the value required to rupture and re-operate the construction joint.

NOTATIONS

$f_n = (f_1, f_2)$	coupled frequencies
f_x	uncoupled frequency in x-direction
f_θ	uncoupled frequency in θ-direction
e_y	eccentiricity in y-direction
r_{RC}	radius of gyration with respect to the center of rigidity.

REFERENCES

1. FOUTCH, D.A.: A Study of the Vibrational Characteristics of Two Multistory Buildings, EERL, California Institute of Technology, Pasadena, California, 1976.
2. KEIGHTLEY, W.O.: A Dynamic Investigation of Bouquet Canyon Dam, EERL, California Institute of Technology, Pasadena, California, 1964.
3. SMITH, C.B., and MATTHIESEN,R.B.: Forced Vibration Tests of the Experimental Gas Cooled Reactor Earthquake Engineering and Structures Lab. and Nuclear Energy Lab., University of California, Los Angeles, 1969.
4. DIVER, M. : Calcul Pratique Des Tours En Beton Arme, Dunod, 1972.
5. ÇELEBİ, M., ERDİK, M., YÜZÜGÜLLÜ, Ö.: Vibration of Multistory R.C. Structure Cast in by Tunnel Forms, METU-EERI Report, No.77-6, June 1977.
6. WHITMAN, R.V.: Soil-Structure Interaction Seismic Design for Nuclear Power Plants, ed. HOUSEN, R.J., MIT Pres., Cambridge, Mass., 1970.
7. ÇELEBİ, M., ERDİK, M., YÜZÜGÜLLÜ, Ö.: Vibration of a R.C. Frame w/o Infill Walls, METU-EERI Report No:77-3, April 1977.

Leere Seite
Blank page
Page vide

SEISMIC RESISTANCE OF REINFORCED CONCRETE HIGH RISE BUILDINGS STRUCTURAL ELEMENTS

by

Drazen Anicic *)

SUMMARY

Plastic design elements of reinforced concrete structures under monotonic and cycliy loading as simulation of earthquake conditions are presented. The mechanism of stiffness degrading and same principles for high-rise buildings with shear wall system are analysed. On the basis of the results of experiments coried out by the authers on large models conclusions are offered on the behavior of joints under cyclic loading.

RESUMÉ

On presente les elements du calcul plastique des section du beton armé exposés an forces monothones et cicliques somme la simulation des forces sismiques. On à donné une analise du mechanisme de la deterioration du rigidité et les principes du projet des bâtiments houts avec les mûres portants. Quelques conclusions de comportement des joints exposés an forces cicliques de resultats des experiments propres sont donnés.

ZUSAMMENFASSUNG

Die Elemente plastischer Berechnungen von Stahlbetonschnitten, welche mit nachgeahmter seizmischen Belastung einförmigen und zyklischen Belastungen ausgesetzt wurden, werden hier vorgeführt. Der Mechanismus des streifhcitsverlustes und die grundsätze der Hochbauprojektirung mit Tragwänden werden ferner analysiert. Auf grund eigener Versuchsergebnisse auf grossen Modelen werden Beschlüsse über das Betragen von Verbindungsstellen bei zyklischer Belastung dargeboten.

*) Head, Structural Research Laboratory, Institute of Civil Engineering, University of Zagreb, P.O.Box 165, ZAGREB, Yugoslavia

1. INTRODUCTION

Reinforced concrete residential and office buildings in Yugoslavia are constructed shear wall system in both ortogonal directions with various technological procedures applied (slide form,tunnel form, large panel system etc). Skeleton structures with rigid walls or core are used infrequently while the skeletons without rigid walls are almost unknown. This is very different from the practice in the U.S.A. where the frequency of these structural system increases in reversed order.

Only after strong earthquake ground motions in Caracas in 1967 and Managua in 1972 and the damages of non-structural elements in framework structures without rigid walls, i.e. partition walls, equipments, installations and furnitures which are often more valuable than the structure itself, the necessity of limited displacement as well as a sufficient strength for a building was accepted (5). Security of this kind can be achieved by decreasing the story drift or by increasing the stiffness with reinforced concrete shear walls. Research of behaviour of shear walls under seismic forces is still under way in the world.

The reinforced concrete walls are almost always constructed mutually bound by connecting beams. As the damage of those beams in strong earthquakes does not jeopardize the stability of building as a structural assemblage for bearing vertical load, it is desirable to direct the forming of plastic hinges to the beams.

2. PLASTIC DESIGN OF REINFORCED CONCRETE UNDER SEISMIC CONDITIONS

Since the plastic design of reinforced concrete in non-seismic conditions has been introduced and applied in many countries, the basic assumptions of the design will not be elaborated herein. For seismic conditions it is necessary to extend some assumptions and separate the computation for monotonic and cyclic loading.

2.1. Monotonic loading

Stress-strain curve for concrete and steel shall be extended beyond conventional limits. After publications of numerous researchers in the period between 1928 and 1933 it is well known that the deformability of concrete with lateral deformation prevented, is several times greater than that of concrete with free lateral deformation. Should the concrete be successfully confined by using dense strirrups, the stress-strain curve for concrete will be extended several times over. The stress-strain curve thus becomes dependent on the ratio of confinement which can be expressed as a volume percentage of reinforcement by transverse bar. The analityc equations for such a diagram were given by Park (6) and are shown hereafter. Fig. 1. represents the stress-strain curve for concrete.

Region AB $\quad \varepsilon_c \leq 0{,}002 \qquad f_c = f'_c \left[\frac{2\varepsilon_c}{0{,}002} - \left(\frac{\varepsilon_c}{0{,}002} \right)^2 \right]$

Region BC $\quad 0{,}002 \leq \varepsilon_c \leq \varepsilon_{20c} \qquad f_c = f'_c \left[1 - Z\,(\varepsilon_c - 0{,}002) \right]$

Region CD $\quad \varepsilon_{20c} < \varepsilon_c \qquad f_c = 0{,}2\, f'_c$ where

$$Z = \frac{0,5}{\varepsilon_{50n}+\varepsilon_{50h}-0,002} \qquad \varepsilon_{50n} = \frac{3+0,002\, f_c'}{f_c'-1000} \qquad (f_c' \text{ u psi})$$

$$\varepsilon_{50h} = \frac{3}{4}\rho \cdot \sqrt{\frac{b''}{s}}$$

ρ is the ratio of volume of transverse reinforcement to volume of concrete core i.e. confinement ratio $\rho = A_v/b''.s$, where b" is the with of confined core, s - spacing of stirrups, A_v - area of stirrups, Z - parameter defining the slope of assmed stress-strain curve.

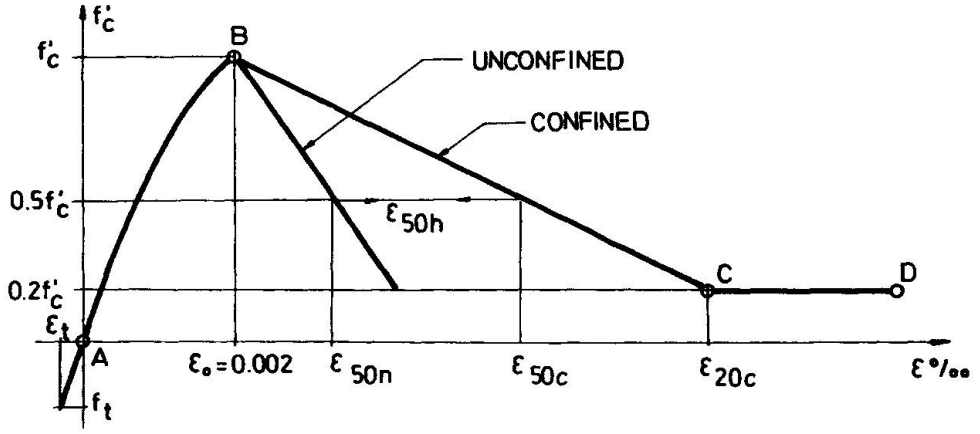

Fig. 1. Stress-strain curve for confined concrete

The stress-strain curve for steel, wich including the whole range of stress-strain relationships can be comparatively simply defined by a schematic representation of the diagram found when testing the steel. Fig. 2.

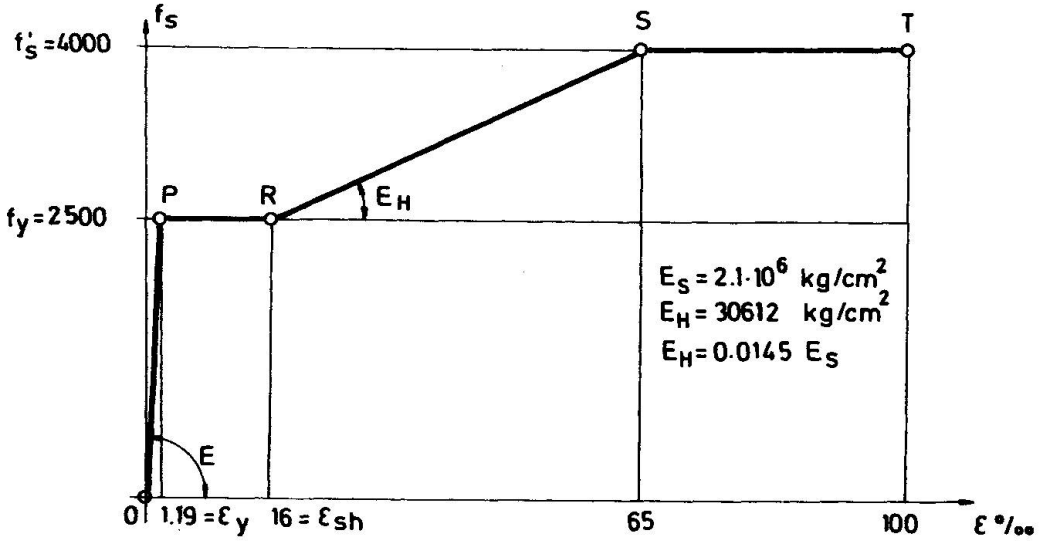

Fig.2. Idealization for stress-strain curve for steel (trilinear approximate)

For the ultimate stress and ultimate strain, the stress-strain curve for concrete and steel as shown in Fig.1 and 2. have to be used as well as the basic assumptions of the plastic design method

(the tensile strength of the concrete may be neglected; Bernoulli-Navier's hypothesis of plane sections is valid for plastic range also; the equilibrium of external and internal forces shall be established). The computation of M-Ø relationship of one bending section is shown in Fig. 3.

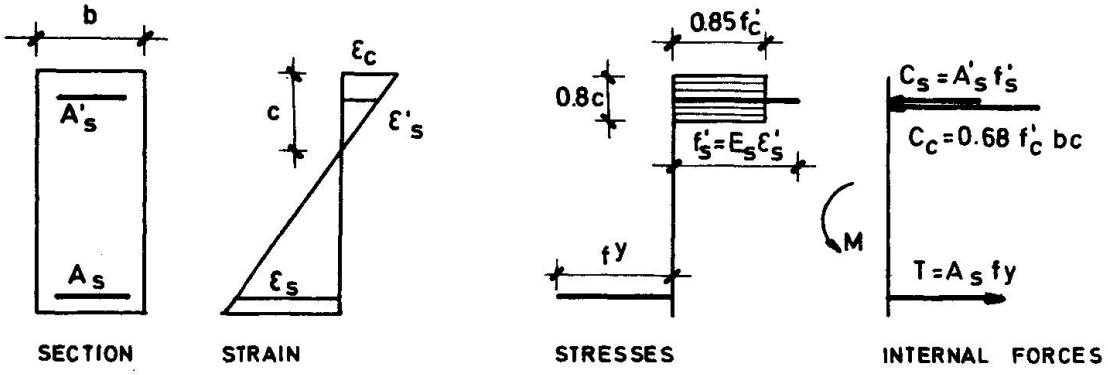

Fig. 3. Scheme for computation of a monotonously loaded reinforced concrete section

For a given value of concrete strain ε_c the value for c shall be selected and the strains for steel ε_s and ε_s' found using the diagram in Fig.2. Corresponding stresses can be obtained from stress-strain curve for concrete and steel according to Fig.1. and 2. The values of internal forces T, C_c and C_s may be determined multiplying the stress by areas. If the equilibrium is no satisfied i.e. $\Sigma H \neq 0$ and $\Sigma M \neq 0$, the computation shall be repeated with a different value for c. When the equilibrium is obtained, the curvature can be obtained from the expression $\emptyset = \varepsilon_c / c$. In the case of weakly and moderately reinforced sections, the relation ship M-Ø will be similar in form to the stress-strain curve for steel.

2.2. Cyclic loading

A idealized stress-strain curve for confined concrete under monotonic loading is the envelope curve of the stress-strain curves for cyclic loading. The shape of $f_c - \varepsilon_c$ curve for cyclic loading can be idealized in several ways in order to approximate actual behaviour as experimentally found by Sinha, Gerstle and Tulin (8). It is considered that a more complicated equations for representation of hysteresis loops because of a dominant influence of the steel response in hysteresis of reinforced concrete. Fig. 4 shows one possible idealized representation of the stress-strain curve of concrete with cyclic loading, according to Park (6). Analytic equations must be given for each of the region AB, BC, CD and FG, HE.

The stress-strain curve for steel under cyclic loading is a function of virgin properties of material, previous stresses, loading run number and some other factors. The first cycle after the first yield exursion, the $f_s - \varepsilon_s$ relationship becomes, due to softening of material, a flat curve with no prominent yield-point. Fig. 5. shows the idealized stress-strain curve for steel.

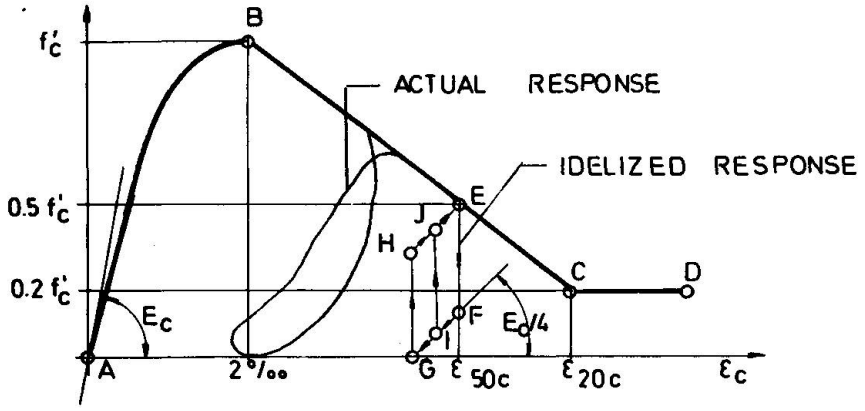

Fig.4. Stress-strain behavior of concrete with cyclic loading

The right-hand diagram in Fig.5. can be used as more favourable because it coresponde better with actual curve. The loading parts of the stress-strain curve is reprezented by the following form of the Ramberg-Osgood function.

$$\varepsilon_s - \varepsilon_{si} = \frac{f_s}{E_s}\left(1 + \left|\frac{f_s}{f_{ch}}\right|^{r-1}\right) \qquad \text{where}$$

ε_s - steel strain, ε_{si} - steel strain at begining of loading run, f_s - steel stress, E_s - modul of elasticity of steel, f_{ch}-characteristic stress of steel in Ramberg-Osgood function, r - loading run number.

For computer programs for cyclically loaded reinforced concrete section, it is necessary to divide the concrete section into a number of discrete elements. The points on M-Ø curves are obtained by previously described procedure of equilirium of the forces and in accordance with Fig. 5.

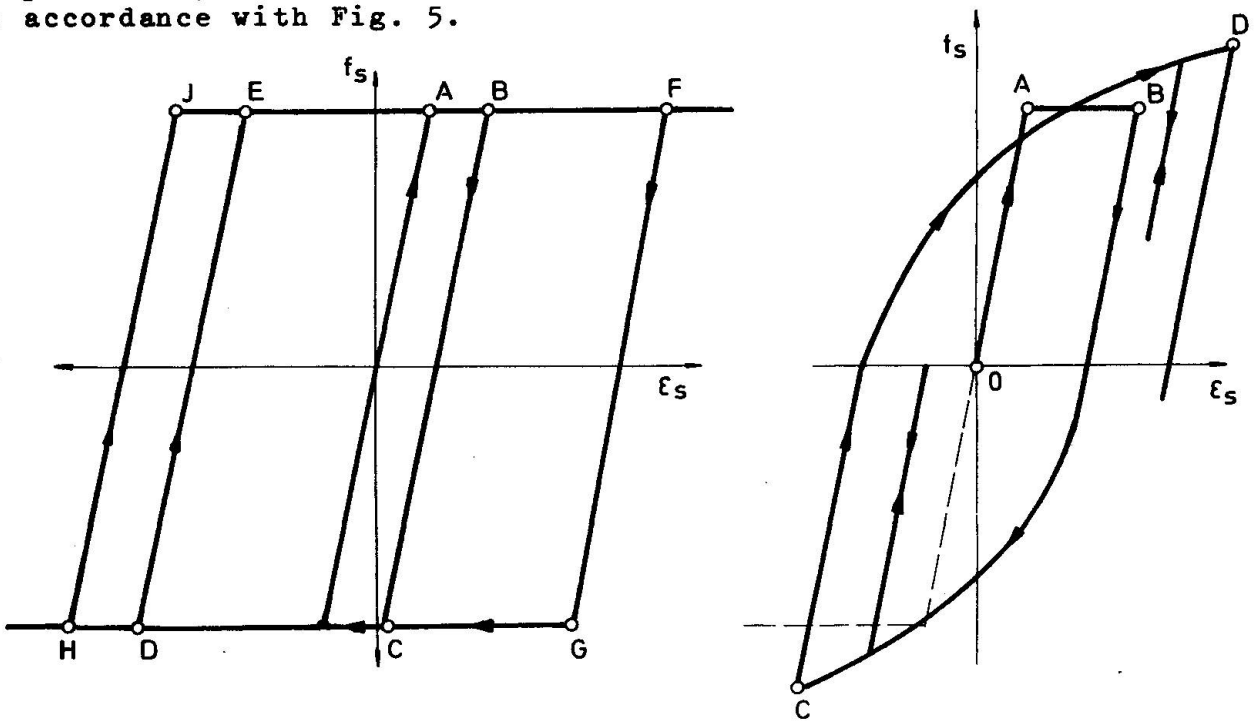

Fig.5. Idealized stress-strain curve for steel with cyclic loading

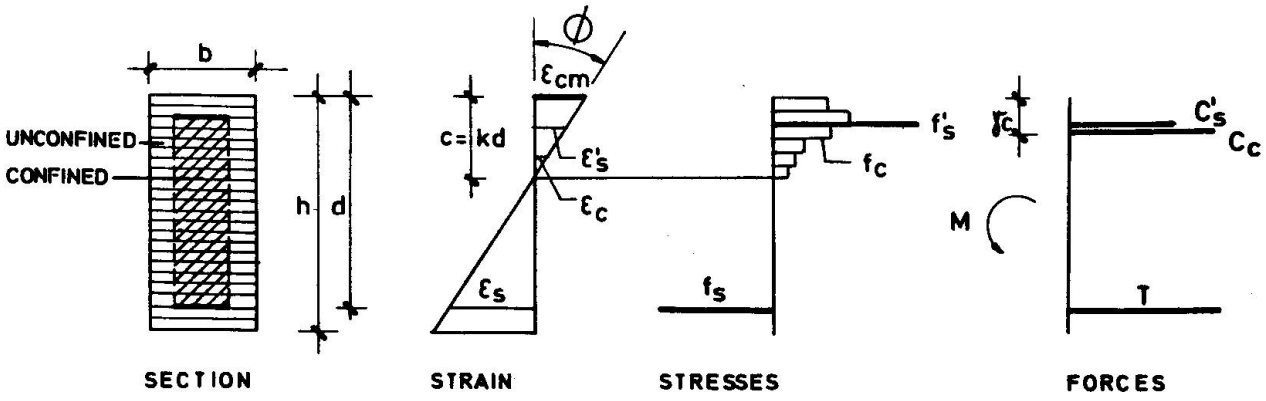

Fig.6. Schemes for computation of cyclically loaded reinforced concrete section

For each element, the corresponding f_c from assumptioned strain ε_c is determined from the stress-strain curve for concrete with cyclic loading, and the ε_s-f_s relationship is found from stress-strain curve for steel. The previous state of strain should be known for each element in order to follow $f - \varepsilon$ curves. It is quite clear that such a procedure is possible only through the use of electronic computer.

3. THE MECHANISM OF STIFFNESS DEGRADING

The plastic deformations in a building exposed to strong earthquake disturbances are usually localized to certain critical region. In case of shear wall system it can be expected that the critical zones will be the sections above the foundations and the sections at places where connecting beams join the walls. In those beam sections, well-defined plastic hinges will be formed only in case of long connecting beams. If short and deep beams are constructed, which occurs more frequently, a system of diagonal cracks will appear under alternating loads due to decisive influence of transversal forces. Hysteresis loops will show instability i.e. trends of degrading stiffness. The main factors that cause that are the cracks in concrete, aplitting of concrete between surface and stirrups, the steel is at the yielding stress, partial or complete cessation of reinforcement anchorage effect, simultaneous influence of shear and flexural deformations etc. Symetrically doubl reinforced section with repated cyclic loading will behave similarly to steel section represented by tensile and compressive reinforcement.

The problem of loading history arises when simulating the effects of an earthquake on a structure or structural assemblage in laboratory. Except when the experiment is carried out with a pre-programmed shaking table where a lifelike simulation is possible,the simulation of loading history for an earthquake is not easily feasible, but it is not necessary either. The testing of structural assemblage in quasy dinamic way is performed with slowly changing dynamic loading. The sequence of cycles does not conform to actual earthquake because the purpose of test is to assess total plastic capability of the assemblage tested. The usual loading history is to, increase deflections or loads as fixed and determined variables.

The reversed order can be adopted too - first the maximal deflections which then decrease. Depending on assemblage tested, different loading history will give upper or lower envelope of strength and energy dissipation (3). The total number of cycles the assemblage will be exposed to must correspond to the number which can be expected in actual earthquake. According to contemporary research, the total number of cycles which cause big plastic deformations is in the range of 20 to 100.

The loading velocity of model, in laboratory conditions always smaller than in earthquake, does not have much import on the results of quasidynamic testing. The principal effect of velocity is the increase of beasing capacity in the first cycle, i.e. first yielding of steel if load is applied very rapidly. Due to Bauschinger effect this "gain" is lostin succeding cycles and can be disregarded in elements exposed to bending (4). The effect of loading velocity for elements loaded with great lateral and axial forces has not been investigated yet.

4. SOME DESIGN PRINCIPLES FOR BUILDINGS WITH SHEAR WALL SYSTEM

The concept of ductility frame, introduced in the U.S.A. at the beginning of the sixties and widely used up to day, has proved to be unsuitable for infilled rigid walls which cannot follow big frame deformations and are thus damaged. The pure framework structure withour rigid walls is therefore considered to be relatively inadequate structural system for buildings with many nonstructural elements, which may have up to 80 % of total value with "non-structual characteristics" (5). Experience from recent earthquakes shows that buildings with shear walls have sufficient strength and considerably greater stiffness, which in turn gives necessary damage control. Ductility and energy absorption capability can be attained by connecting the walls with beams which can be made suitable for this by special reinforcement methods.

The uniform distribution of reinforcement over the whole wall region cannot be deemed correct under seismic conditions. The reinforcement should be concentrated near the edges and densely wound by stirrups in order to get confined concrete effect in compressive area. At the same time, densely placed stirrups will prevent local buckling of longitudinal reinforcement under alternating load. It is also necessary to prevent shear failure in order to get desired ductile behaviour of the wall. Therefore, sufficient number of transversal bars is required to prevent steel yielding.

The maximal resistance of walls with one row of vertical openings is attained when the structure turns into mechanism, i.e. when plastic hinges are formed, one pair in each beam and one in each wall. The sequence in which plastic hinges form depends on mutual relation of stiffness and strength of individual structural elements. It is of primary importance to attain previously determined sequence of openning of plastic hinges during the earthquake. Those joints must have great capacility for energy absorption under alternating load, without significant loss of strength. Satisfactory sequence of openning of plastic hinges is one that permits the walls to turn to plastic range only after the majority of beams already became plastic. Desired plastic properties of short and deep beams cannot be attained by conventional reinforcement, but

through diagonal reinforcement in both directions. This diagonal reinforcement is constructed in the form of a basket with very dense stirrups or spiral. Experiments performed on so reinforced short beams gave very high ductility and energy absorption factors (7).

5. AUTHOR EXPERIMENTS

Laboratory tests for structural elements on ten large models of a typical high-rise building constructed by slide form system in Yugoslavia were performed. The building has nineteen storeys,with ground-plan measures 20x20 m and reinforced concrete shear walls of constant thickness of 20 cm set in two orthogonal directions. The walls are mutually connected by beams over door and window openings and by solid slabs. The models tested were constructed to represent the parts of wall above and beneath the slab and the beam which connects them. The models were done to 1:2 scale. The procedure of testing was minutely described in other reports (1,2).

The loading history was quasidynamic with symetric cycles on x-axis. Deflections cause yielding of reinforcement immediately after the beginning and the damage of models increases. Electrohydraulic equipment has been employed during the test. The deflection was used as controlled varibale and hysteresis loops were directly registered.

The tested joints of beams and walls were damaged predominantly by bending moment because the beams were "long". Some of the conclusions drawn from analysis of experimental data are:

- long beams, conventionally reinforced, have shown high capability of plastification through forming of plastic hinges in the section at wall connection points.
- relative deformations of main reinforcement considerably overshoot conventional yield-point and can reach more than 1,0 %.
- lateral reinforcement is not strained because the beams are not working in tri-axial state of strain and the failure is caused by bending.
- the stiffness decreases with the increase of load and deformation according to adopted loading history. Substantial loss of stiffness appears when ductility ratio reaches values of more than 10.
- the collapse and real failure did not occur during the testing and so it appears that the damages can be technically easily repaired. If real building should be damaged in such a way, it's stability for vertical load would not be jeopardized.
- the beams are able to absorb considerable amount of energy, which has a favourable effect on the behaviour of building as a structural assemblage.

6. REFERENCES

1. ANICIC,D., ZAMOLO,M. - Stiffness Deterioration of Cyclic Loaded RC Structural Elements,Proceedings of the Fifth European Concference on Earthquake Engineering, Istanbul, Sept. 1975.
2. ANICIC,D., ZAMOLO,M. - Structural Assemblage of Shear Wall High-Rise Building Exposed to Cyclic Loading,Proceedings of the Sixth World Conference on Earthquake Engineering, New Delhi,Jan.1977.
3. BERTERO,V.V. - Experimental Studies Concerning RC Structures and their Elements,AIPC,Symposium on Resistance and Ultimate Deformability of Structures Acted on by Well Defined Repeted Loads, Lisboa,1973.
4. BERTERO,V.V., REA,D. - Rate of Loading Effects on Uncracked and Repaired Reinforced Concrete Members,Proceedings of the Fifth World Conference on Earthquake Engineering,Rome,1973.,P 182.

5. FINTEL,M. - Ductile Shear Walls in Earthquake Resistant Multi-story Buildings,Journal of the American Concrete Institute,Detroit, USA, Juna 1974.
6. PARK,R. & al.-Reinforced Concrete Members with Cyclic Loading, Proceedings of the ASCE, Journal of the Str.Div., New York,July 1972.
7. PARK,R., PAULAY,T. - Reinforced Concrete Structures,J.Wiley & Sons, New York, 1975.
8. SINHA,B.P., GERSTLE,K.H., TULIN L.G.-Stress-Strain Relationships for Concrete under Cyclic Loading, Journal of the American Concrete Institute,Detroit, USA, Feb. 1964.

Leere Seite
Blank page
Page vide

LOW COST SEISMIC DESIGN AND CONSTRUCTION

PREISWERTE SEISMISCHE WANDKONSTRUKTION

Thomas S. Tarpy, Jr.
Research Associate Professor
Vanderbilt University
Nashville, Tennessee, U.S.A.
Structural Engineer
Stanley D. Lindsey and Associates, Limited
Nashville, Tennessee, U.S.A.

Cynthia S. McCreless
Associate Engineer
EXXON Corporation
Los Angeles, California, U.S.A.
Former Graduate Student
Vanderbilt University
Nashville, Tennessee, U.S.A.

Stephen F. Hauenstein
Graduate Student
Vanderbilt University
Nashville, Tennessee, U.S.A.

This paper presents the results of a full scale test program for determining the shear resistance and acceptable deflection level for composite light gauge steel stud and gypsum wall panels under lateral loads. Special emphasis is placed on the wall attachment and anchorage details as they apply to seismic conditions. Application of the results for the design of low cost seismic design and construction is presented. General observations are made on the ability of the wall panel to effectively function as a lateral load or shear resisting element in building design.

In diesem Vortrag werden die Ergebnisse eines Versuchsprogrammes zur Bestimmung der Schubwiderstandes und annehmbarer Verformungen von Vollwandpanelen beschrieben. Die Panele bestehen aus dünnwandigen Stahlstützen mit Gipskartonplatten in Verbundskonstruktion, welche horizontal in der Wandebene belastet werden. Besonderer Nachdruck wurde auf die Befestigungs- und Verankerungsdetaillierung mit Hinblick auf die seismische Belastung gelegt. Anwendungen des Ergebnisse für den seismischen Entwurf von preiswerten Wandkonstruktionen werden presentiert. Auch allgemeine Schlussfolgerungen, die sich auf die Schubfähigkeit der Wandpanele in Bauwerken beziehen, sind dargelegt.

1. INTRODUCTION

The three basic framing systems commonly used in building design for resisting lateral loads caused by seismic action, wind loads, etc. are the unbraced frame, the braced frame, and the vertical diaphragm. The relative advantages of one of these framing systems over another depends to a large degree on the allowable lateral drift, the ductility requirements, and potential problems with uplift or overturning. That is, any of these framing systems can be used economically for certain classes of problems provided adequate design recommendations and precautions are followed.

The design of low rise structures of four stories or less presents a special challenge to the structural engineer as to the proper selection of an economical framing system. For this particular application, the writers wish to present the use of the vertical diaphragm system or wall system composed of gypsum wallboard for the diaphragm and light gage steel studs for the framing members. This framing system corresponds to wood diaphragms currently used in many areas of construction. When lateral loads are applied to the diaphragm, they are resisted primarily by shear stresses generated in the plane of the diaphragm. Due to the brittleness of the gypsum and the ductility of the steel stud, the resulting composite wall system possesses a limited amount of ductility, the exact amount being dependent upon the degree of attachment of the gypsum to the studs and the resulting anchorage of the wall system to the rest of the structure. Its resistance to overturning depends largely on its height to width ratio which for most wall configurations is usually not a problem.

From a dynamic load viewpoint, the composite wall system offers considerable savings in weight over conventional systems in that the lateral forces exerted are directly proportional to the mass of the structure. The mass of the composite gypsum-steel stud wall system is approximately 24 kg/m^2. Hence, due to the lighter wall weight over that of other materials, the resulting structure has a better chance of surviving an earthquake than a heavier structure. The primary caution is to keep the failure out of the diaphragm and the connections and to adequately tie the structure together.

Several building codes permit the use of wall panels composed of wood studs and gypsum as vertical shear diaphragms provided the height to width ratio does not exceed unity and the deflection between supports does not exceed L/240. The gypsum panel attachment to the wood studs is restricted to a maximum spacing of 178 mm for an allowable shear value of 1095 N/m. The option of using steel studs in lieu of wood studs is not covered in the codes due primarily to the lack of supportive performance data.

While the economic advantages of using composite steel stud-gypsum wallboard partitions appear numerous, very little design information is available on the shear strength and stiffness of the panels or damage threshold load level of the gypsum. These values are best determined experimentally due to the complexity of trying to model the composite system constructed of both steel and gypsum. The availability of this information permits the use of this system in building design.

The earliest known research project involving composite shear wall partitions was conducted by URS/John A. Blume and Associates beginning in the mid-sixties. They developed and conducted a testing program for composite wall panels subjected to racking loads (1,2,3,4). Several 2.44 m x 2.44 m wall panels with both wood and drywall studs were tested. The majority of the panels were constructed of gypsum wallboard, but plaster, plywood, concrete block and combination plywood and gypsum wallboards were also tested. Pop-rivets and friction

connections were used to attach the steel studs to the track. Both static loading and cyclic load reversals were used in testing.

Additional small scale tests involving composite steel stud-gypsum wallboard partitions were performed at Cornell University to study the behavior of steel stud wall diaphragms (6). Results of these tests indicate that commonly used gypsum wallboard significantly increases the load carrying capacity of steel studs.

While the research to date has provided many valuable results on the behavior of composite wall systems very little structural design information is available to assist in the design of the wall panels for possible usage to resist lateral loads. The purpose of this paper is to present the results of a test program aimed at establishing design information for typical interior steel stud gypsum wallboard partitions commonly encountered in building construction.

The objective of the test program is two-fold. The first is to determine the effect of various construction techniques on the shear strength and shear resistance of composite steel stud-gypsum wallboard partitions. The second is to determine the degree of panel distortion possible before major wall panel damage of the gypsum occurs for asthetic as well as structural purposes.

The experimental test program consists of testing several full size wall panels of varying wallboard attachment and wall panel anchorage details. Displacements are measured at critical locations on the wall for varying load levels and load displacement curves are plotted. Shear strength and shear stiffness are calculated from the test results.

2. EXPERIMENTAL TEST PROGRAM AND PROCEDURE

The shear strength and stiffness of the panels are determined by racking a panel from a rectangle to a parallelogram. This is accomplished by fixing the base of the wall and applying a force along the top of the wall parallel to the plane of the wall. The forces required to rack the wall and the corresponding displacements at increasing load intervals are measured. The shear strength and stiffness of the panels are then calculated from the load deflection curves.

Testing is performed in accordance with ASTM # 564 - 76. This method is a static load procedure designed to evaluate the shear resistance of framed walls for buildings. The recommended test assembly is shown in Figure 1. Specifications are not made regarding the type of connection system used except to duplicate as nearly as possible the system intended for use in actual building construction. The wall may be tested vertically or horizontally and the panel size should not be less than 2.44 m high by 2.44 m wide.

The shear strength and shear stiffness are obtained from the test results. The ultimate shear strength (N/m) is determined by dividing the ultimate load (i.e. the last load that gage deflections were recorded) by the length of the wall panel parallel to the application of the load. The shear stiffness (KN/m) is determined as one-third the ultimate load divided by the total deflection including shear deflection and that contributed by bending of the panel at that load level times the aspect ratio of the wall panel.

For this investigation a series of interior wall panels with various construction details as shown in Table 1 were tested. The variables considered were the wallboard attachment centers and the type of wall panel anchorage to the base. Based on previous research (5,7), these conditions were felt to

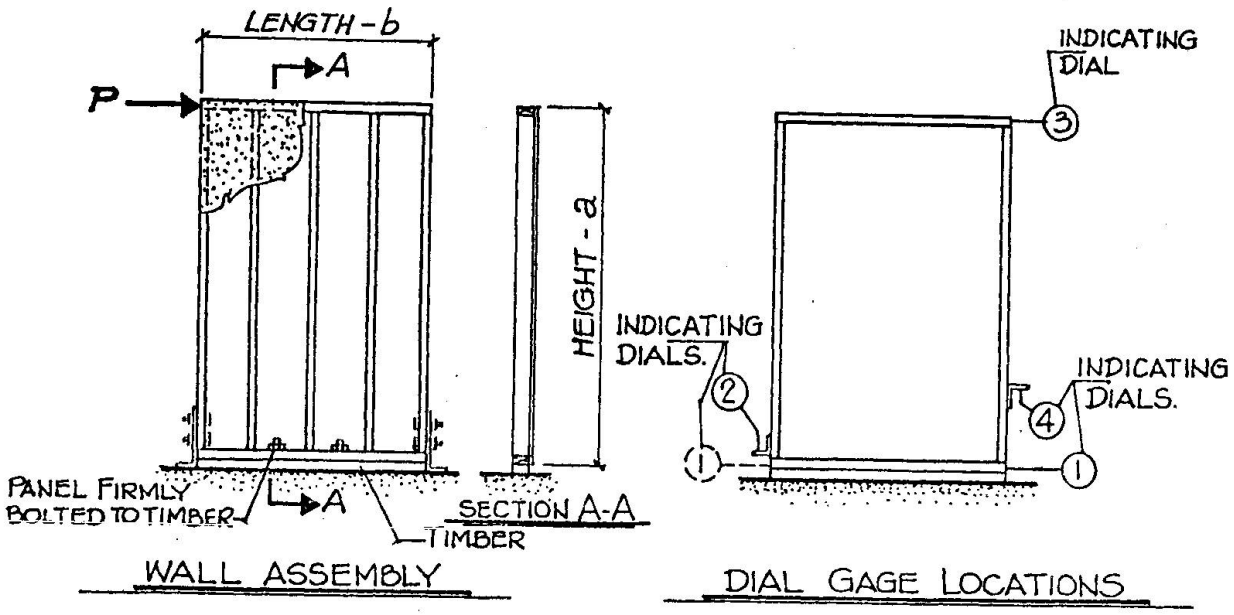

Figure 1. Racking Load Assembly ASTM E 564 - 76.

TABLE 1

WALL ASSEMBLY

WALL TYPE	WALL HEIGHT (m)	WALL WIDTH (m)	TYPE WALLBOARD	STUD SPACING	WALL FASTENER SPACING	WALL ATTACHMENT	STUD ATTACHMENT	WALLBOARD ATTACHMENT
A	2.44	2.44	12.7 mm Gypsum Each Face	610 mm-o.c. Steel	305 m-o.c.	Clips at 1.22 m-o.c.	#10x12.7 mm Low Profile Head Screws	#6x25.4 mm Bugle Head Screws
B	2.44	2.44	"	"	153 mm-o.c. perimeter Balance @ 305 m-o.c.	"	"	"
C	2.44	2.44	"	"	5 at 153 mm-o.c. at corners Balance @ 305 m-o.c.	"	"	"
D	2.44	2.44	"	"	305 mm-o.c.	Bolt & Washer @ 1.22 m-o.c.	"	"
E	2.44	3.66	"	"	"	Clips at 1.22 m-o.c.	"	"
F	2.44	3.66	"	"	"	Clips at Ends Bolt & Washer @ 1.22 m-o.c.	"	"

have the greatest influnece on the wall performance. The panels were tested horizontally in a steel load frame assembly designed especially for the series of tests. The connections used to attach the wall panel to the frame and prevent overturning of the wall were located at 1.22 m o.c. For the clip angle detail, one face of the angle was bolted to the stud and the other face of the angle was bolted through the track to the load frame. A digital strain indicator in combination with a linear load cell was used to apply the load.

Each wall panel was constructed of 89 mm by 1 mm thick structural "C" studs spread 610 mm o.c. The steel studs were attached to 92 mm web by 38 mm flange by 1 mm thick structural track with #10 x 12.7 mm long low profile head screws. Care was taken to avoid gaps between the studs and track. The studs were attached by screws to both flanges of the track.

The use of screws provides a permanent means of attachment of the steel frame. This eliminates the collapse failure that occurs with friction connections or the breaking of pop rivets.

Gypsum wallboard 12.7 mm thick, was positioned horizontally and attached to one side of the stud panels with #6 x 25.4 mm long Bugle head self-drilling screws. The standard spacing for the fasteners was 305 mm o.c. over the entire face of the panel along both studs and runner tracks for all wall types except B and C. Wall type C had fasteners spaced 153 mm around the perimeter, while wall type C has fasteners spaced 153 mm o.c. within 610 mm of the corners along the perimeter with the balance of the fasteners spaced 305 mm o.c. The gypsum wallboard seams were then caulked and taped to complete the construction of one face of the wall panel. A minimum curing time of 24 hours was maintained before the wall panel was moved to allow the joint compound to harden properly.

Once the wall panel had cured it was mounted horizontally in the load frame by either clip angles or bolts and washers. Wall types A, B, C and E were anchored to the test frame assembly by clip angles located 1.22 m o.c. Wall type D was anchored by bolts and washers located at 1.22 m o.c., and wall type F had clip angles locat-d at the corners of the wall panel and bolts and washers at the two interior attachment points. A bearing block and structural steel joist was then attached at the top of the steel stud panel to uniformly distribute the load along thelength of the wall.

After the connections were completed the remaining face was covered with gypsum and taped as described before. It was felt that by constructing the wall panel in this manner the laboratory construction would represent as closely as possible actual field installation. The only exception being the jack bearing block and steel joist assembly. In actual construction, this assembly simulates the support furnished by the gravity supporting frame systems. The completed wall assembly located in the load frame and interior wall panel details are shown in Figures 2.

Displacement indicating dials were located on the test frame assembly at points shown in Figure 1. The horizontal dial gage at the lower right measures the slippage of the panel in the test frame. The two vertical dial gages measure panel rotation and the dial at the upper right measures the same readings as the other dial gages plus the lateral deformation of the panel.

Prior to starting a test the ultimate load was estimated and loading increments determined to guarantee a minimum of ten readings. A preload of ten percent of the estimated ultimate load was initially applied to the wall panel for five minutes to set all connections. The load was then removed and all the dial gages set to zero. The load was then applied incrementally to the wall and

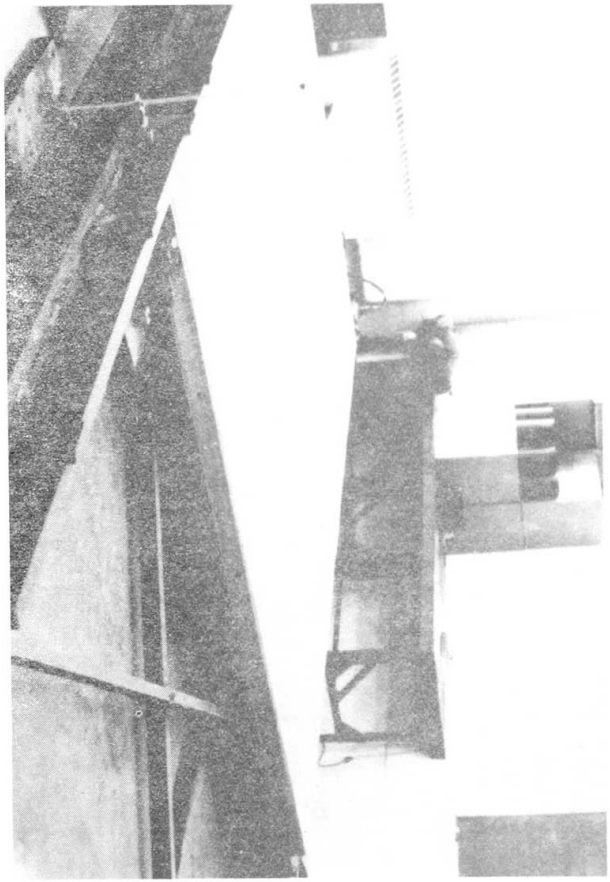

a) Completed Wall Assembly

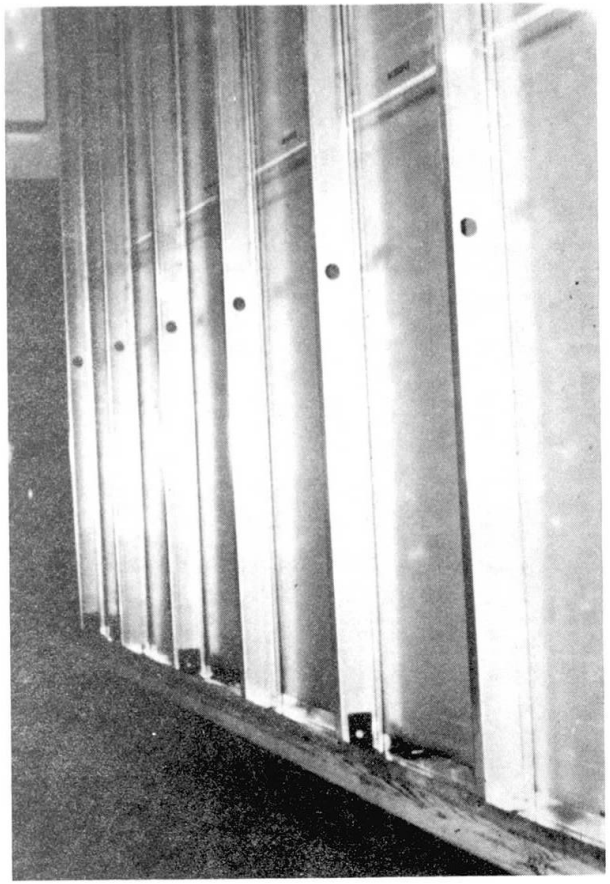

b) Interior of Wall Assembly

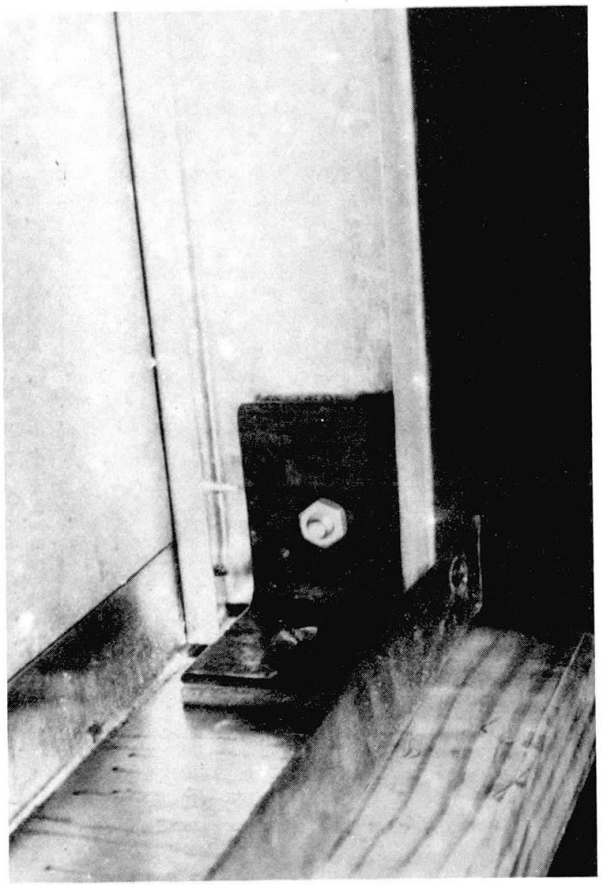

c) Clip Angle

Figure 2. Completed Wall Assembly and Typical Details.

displacement measurements recorded after a two minute hold to allow the wall to stabilize. At load levels of one-third and two-thirds of the estimated ultimate load, the load was fully removed and the wall recovery recorded after a five minute duration. The load was then re-applied to the next increment above the back-off load. Loading continued in this manner until the panel was no longer capable of holding additional load. The last load held for two minutes with displacement measurements recorded is defined as the ultimate load.

As discussed earlier the information obtained from the test results are load-deflection curves, ultimate shear strength, ultimate shear stiffness, and damage threshold levels. The load-deflection curve is a plot of the applied load versus the corresponding wall deflection. The ultimate shear strentth is determined from the ultimate load and the ultimate shear stiffness is determined from the load-deflection curves. The damage threshold is a visual observation and is defined as the level of loading which causes critical and major damage to the gypsum wall panel; that is, the gypsum is no longer structurally effective.

ASTM recommends that the total deflection or a combination of shear and bending deflection be used in all computations. The total deflection of the wall panels or drift is determined by subtracting the base slippage from the total lateral deflection.

The ultimate shear strength of the wall is defined as the highest load level held long enough to record gage measurements divided by the length of the wall panel.

The shear stiffness is obtained from the corresponding load-deflection curve. A reference load in the elastic range of the load-deflection curve at one-third ultimate is recommended by ASTM and that load and corresponding deflection used in the calculations. The shear stiffness computed from the total deflection is defined as the load at the one-third reference point divided by the corresponding total deflection times the aspect ratio of the wall.

3. DISCUSSION OF RESULTS

Table 2 shows the gypsum damage thresholds observed during testing. The first noticeable damage is the point where the first hairline cracks in the wallboard materila were observed and furnishes an indication of the effect of shearing of the brittle gypsum and paper material. Major damage is defined as the point where the damage to the wall was extensive and unrepairable. That is, the gypsum tore through the sheet. Human judgement is a primary factor in the determination of these values and varies from one observer to another. As such, the values reported are based on the general observations of several individuals involved in the testing.

The visible signs of yielding for all wall types followed the same general pattern. The first sign was one of the wall base track deforming around the exterior corner tension uplift anchorage point. As the load was increased cracking of the gypsum wallboard occurred at the same corner screw location. This process continued with increased deformation in the track and increased cracking of the wallboard until yielding due to excessive rotation of the panel occurred. For structural purposes the load level and corresponding deflection at first cracking of the gypsum wallboard is the controlling design factor. For this case, it is noted from Table 2 for wall type C that for a slight increase in the number of fasteners in the corners the load level doubles and by adding the fasteners at 143 mm around the perimeter in wall type B increases

TABLE 2

GYPSUM DAMAGE THRESHOLDS

WALL TYPE	WALL HEIGHT (m)	WALL WIDTH (m)	INITIAL CRACKING		REAL DAMAGE	
			LOAD LEVEL (KN)	TOTAL DEFLECTION (mm)	LOAD LEVEL (KN)	TOTAL DEFLECTION (mm)
A	2.44	2.44	7.6	7.6	11.1	10.2
B	2.44	2.44	18.2	17.6	20.5	22.9
C	2.44	2.44	14.7	12.7	16.9	17.8
D	2.44	2.44	8.9	17.8	9.8	22.9
E	2.44	3.66	14.7	10.2	18.7	17.8
F	2.44	3.66	16.9	10.2	18.7	12.7

TABLE 3

TEST RESULTS

WALL TYPE	WALL HEIGHT (m)	WALL WIDTH (m)	ULT. SHEAR STRENGTH (N/m)	MAX. TOTAL DEFLECTION (mm)	SHEAR STIFFNESS (KN/m)
A	2.44	2.44	5983	24.9	1699
B	2.44	2.44	9778	36.6	1681
C	2.44	2.44	8756	34.5	1856
D	2.44	2.44	4524	30.5	718
E	2.44	3.66	5838	16.8	1891
F	2.44	3.66	5473	16.3	2452

the load level one hundred and forty percent. This increase in wall panel load capacity and corresponding deflection is significant from a seismic viewpoint as all connections must be designed for 1.25 times the allowable design loads for a braced system.

The effect of eliminating the clip angles on the damage threshold appear to be minimal. However, it is the writers opinion that the two end angles should be maintained to reduce the potential of track deformation that occurs around the bolt and washer.

The calculated shear strength, total deflection and shear stiffness are summarized in Table 3 for the different wall panel sizes considered. The calculated shear strength of the wall panels indicates that the shear strength is essentially independent of aspect ratio. The total deflection, on the other hand, is a function of the anchorage details. This is reasonable in that the wall behaves as a cantilever system with larger deflection for the walls without the corner clips or with closer wallboard fastener spacings.

It can be noted from Table 3 that shear strength is highly dependent upon the construction details of the wall systems. Basically, an increase in the number of wall fasteners or a decrease in fastener spacing causes an increase in shear strength, while the replacement of clip angles with bolts and washers lead to a decrease in strength. The total shear stiffness was also found to be dependent upon wall assembly anchorage, but was almont entirely independent of wall fastener spacing. The complete replacement of clips with bolts and washers lead to a pronounced decrease in total shear stiffness, while a decrease in the wall fastener spacing had no noticeable effect on this stiffness value. This effect was not as pronounced when the end clip angles were maintained.

4. CONCLUSIONS

The results of the test program indicate that composite steel stud-gypsum wallboard partitions can offer an economical framing system for resisting lateral loads in building construciton for seismic and hurricane forces provided appropriate factors of safety and anchorage details are maintained. This conclusion is based on the ultimate shear strength of the panels as well as the level of loading at first cracking of the gypsum wallboard. Based on these test results theoptimum installation details would be wall type B with fasteners at 153 mm around the perimeter and with clip angles at the ends. This offers the ideal maximum load and deflection for the gypsum and the wall panel.

Previous tests (5,7) run by the writers on wall type A with different aspect ratios indicated that the performance of steel stud wall panels is dependent on the panel aspect ratio. From the results of these tests design curves for total shear stiffness, shear strength, and load level at initial damage of the gypsum wallboard for walls of varying aspect ratios were developed. While it is expected that walls using different types of construction details with varying aspect ratios would produce design curves similar to those produced from the previous tests, it is the opinion of the writers that the extension may not necessarily be straight-forward. Therefore, additional tests should be run on wall type B with the anchorage details modified as discussed herein.

5. ACKNOWLEDGMENT

The research reported herein was sponsored at Vanderbilt University, Nashville, Tennessee by the American Iron and Steel Institute and the United States Steel Corporation. For their sponsorship and the assistance of the advisory task group chaired by Karl Klippstein for AISI and George Ratliff for U.S.S. Corp. the writers are extremely grateful. The steel studs, joists and track used in the tests were furnished by the U.S.Steel Corporation.

REFERENCES

1. BLUME, J.A., "First Progress Report on Racking Tests of Wall Panels," NVO-99-15, John A. Blume and Associates Research Division, San Francisco, August 1966.

2. BLUME, J.A., "Second Progress Report on Racking Tests of Wall Panels," JAB-99-34, John A. Blume and Associates Research Division, San Francisco, July 1968.

3. FREEMAN, S.A., "Third Progress Report on Racking Tests of Wall Panels," JAB-99-54, John A. Blume and Associates Research Division, San Francisco, December 1971.

4. FREEMAN, S.A., "Fourth Progress Report on Racking Tests of Wall Panels," JAB-99-55, John A. Blume and Associates Research Division, San Francisco, September 1974.

5. MCCRELESS, C.S., "Shear Resistance Tests on Steel Stud Wall Panels," Masters Thesis, Vanderbilt University, May 1977.

6. SIMAAN, A., and PEKOZ, T., "Diaphragm Braced Members and Design of Wall Studs," Proceedings ASCE, Vol. 102, ST1, January 1976.

7. TARPY, T.S. and MCCRELESS, C.S., "Shear Resistance Tests on Steel Stud Wall Panels," CE-USS-1, Report submitted to the United States Steel Corporation, December 1976.

8. TARPY, T.S., and HAUENSTEIN, S.F., "Effect of Construction Details on Shear Resistance of Steel Stud Wall Panels," CE-AISI-1, Report submitted to the American Iron and Steel Institute, November 1977.

ENGINEERING DECISIONS AND SEISMIC RISK PREVENTION[1]

by

E. Grandori[2], G. Grandori[2] and V. Petrini[2]

Abstract - A mathematical model leading to the marginal cost of a saved life at a site exposed to seismic risk is presented. The site is assumed included in an ideal seismic zone, with uniform distribution of epicenters and with constant depth of focuses. The anlysis is carried out on the basis of four different magnitude-frequency laws: "linear", "truncated-linear", "quadratic" and "truncated-quadratic".

Resume' - On présent un modèle mathématique pour le calcul du cout marginal d'une vie sauvée dans un lieu expose' au risque sismique. On suppose que le site soit compris dans une zone idéalisée dans la quelle la distribution des épicentres est uniforme et la profondeur des hypocentres est constante. Le calcul est conduit sur la base de quatre different hypothèses à propos de la corrélation entre la magnitude et la fréquence: "lineaire", "lineaire-tronquée", "parabolique", "parabolique-tronquée".

Zusammenfassung - Ein mathematisches Modell für die Berechnung des Lebensbewahrungzusatzkostenpreis in einem erdbebengefährdeten Ort vorgeschlagen wird. Mit der Annahme dass der Ort in einer Region liegt wo die Epizentrenverteilung gleichmässig ist und die Epizentrentiefe konstant ist, die Rechnung entwickelt wird mit vier verschiedenen Magnitude-Frequenz Zusammenhängen (linear, linear mit Beschränkung, parabolisch und parabolisch mit Beschränkung).

---

1 Research carried out in the frame of CNR's Italian Geodynamics Project. Publ. n. 67.

2 Professor, Politecnico di Milano, Milano, Italy.

1. INTRODUCTION

The occurrence of earthquakes in a given zone is generally represented by means of the average number N(m) of earthquakes with magnitude greater than m in a year. A classic assumption about the function N(m) is:

$$\log_{10} N(m) = a - bm, \tag{1}$$

with a, b constant coefficients depending on the zone.

It has been observed by many Authors that the use of eq. (1) in elaborating statistical data normally overestimates the occurrence of large events. An improvement of the "linear" magnitude-frequency law (1) can be obtained either assuming a "truncated-linear" law (i.e. imposing an upper bound m_1 on m) or assuming a "non-linear" law leading to lower values of N(m) for large events in respect of eq. (1). In this second case the "non-linear" law can also be truncated. Shlien and Toksöz [1] used a "quadratic" form for the magnitude frequency law:

$$\log_{10} N(m) = a + b'm + b''m^2. \tag{2}$$

Merz and Cornell [2] carried out an analysis with both a linear and a quadratic magnitude-frequency law for a fault-site configuration, concluding that the difference in the prediction of local seismicity is significant in the high-ground-acceleration region.

The aim of the present paper is to develop the model contained in [2] in order to include in it the effects of the earthquakes on the buildings, taking into account both the economical aspects of the problem and the expected number of victims. The model thus obtained can be useful when the differences in local seismicity, depending on the alternative assumptions about the magnitude-frequency law, must be discussed from the point of view of engineering decisions in the field of seismic risk prevention.

The first step is the calculation of the local seismicity at a site contained in an ideal seismic zone, with uniform distribution of epicenters and with constant depth of focuses, starting from four different mangitude-frequency laws: linear, truncated linear, quadratic, truncated-quadratic. Thus four different expressions giving the local seismicity at the considered site are obtained. For this first step the mathematical treatment is essentially the same as in [2], adapted to the particular hypothesis about the distribution of potential earthquake sources.

The second step is based on the following assumptions: 1) the decisions regarding seismic risk prevention are mostly condensed in the design value of the lateral force coefficient C; 2) the consequences of alternative designs are well represented by the marginal

cost of a saved life, $\Delta D/\Delta L$, which is a function of C [3]. Therefore the function $\Delta D/\Delta L(C)$ is calculated for the considered site starting from the different expressions of the local seismicity previously defined.

2. LOCAL SEISMICITY

2.1 First Case

Consider an ideal seismic zone with uniform distribution of epicenters, with constant depth of focuses, and where the peak ground acceleration y at the distance r from the epicenter of an earthquake of magnitude m depends only on r and m. Consider the earthquakes with $m>m_o$ (m_o being the value below which earthquakes are not of engineering importance and/or the statistical data are not reliable). Then the linear magnitude-frequency law (1) can be written:

$$N^{(1)}(m) = \begin{cases} \lambda & ; \quad m \leq m_o \\ \lambda e^{-\beta(m-m_o)} & ; \quad m > m_o \end{cases} \tag{3}$$

Let $F_M(m)$ be the distribution function of the random variable M. Then the assumption (2) implies for a single earthquake:

$$P[M>m] = 1 - F_M^{(1)}(m) = \begin{cases} 1 & ; \quad m \leq m_o \\ e^{-\beta(m-m_o)} & ; \quad m > m_o \end{cases} \tag{4}$$

The corresponding probability density is:

$$f^{(1)}(m) = \begin{cases} 0 & ; \quad m \leq m_o \\ \beta e^{-\beta(m-m_o)} & ; \quad m > m_o \end{cases} \tag{5}$$

Observe that the coefficient β defines the distribution function $F_M(m)$: it does not depend on the total average number of earthquakes λ.

Consider one site sufficiently far from the border of the zone and assume that for an earthquake with M = m at distance R = r from the site, the peak ground acceleration at the site is:

$$y = \begin{cases} b_1 e^{b_2 m} r_o^{-2} & r \leq r_o \\ b_1 e^{b_2 m} r^{-2} & r > r_o \end{cases} \tag{6}$$

Then for an earthquake at distance R = r, from eq. (4) and (6) we obtain the probability of exceeding the acceleration y at the site:

$$P[Y>y/R=r]=p_{y/r}=1-F_M^{(1)}[m(y,r)]=\begin{cases}\left(\frac{y}{b_1 r_0^2}\right)^{-\beta/b_2} e^{\beta m_0} & ; r\le r_0 \\ \left(\frac{y}{b_1 r^2}\right)^{-\beta/b_2} e^{\beta m_0} & ; r>r_0\end{cases} \quad (7)$$

and for an earthquake at random distance $R \le r_1$ (r_1 being the distance at which an earthquake is not of engineering importance):

$$p_y=\int_0^{r_1} p_{y/r}\, f(r)\, dr \quad (8)$$

where f(r) is the probability density of the random variable R; i. e., due to the uniform distribution of the epicenters:

$$f(r)dr=\frac{2\pi r\, dr}{\pi r_1^2} \quad (9)$$

Assume now that the number of earthquakes in a year is a Poisson distributed random variable with mean λ. The seismicity at the site is then represented by:

$$P[Y>y]_{one\ year}=1-F_Y(y)=1-e^{-\lambda p_y}\simeq \lambda p_y=N(y) \quad (10)$$

where the approximation is valid for small probabilities and N(y) is the annual average number of earthquakes with Y>y. For the present first fase, from eq. (7), (8), (9), (10) we obtain:

$$N^{(1)}(y)=1-F_Y^{(1)}(y)=A\, y^{-\beta/b_2} \quad (11)$$

where

$$A=\frac{\lambda\cdot e^{\beta m_0} b_1^{\beta/b_2}}{(1-\beta/b_2)\, r_1^2}\left(r_{max}^{2-2\beta/b_2}-\frac{\beta}{b_2} r_0^{2-2\beta/b_2}\right) \quad (12)$$

In eq. (12) the distance r_{max} coincides with r_1. The different symbol has been choosen because in the analogous expressions for the second and the fourth cases, in which m is truncated, r_{max} will be a function of y, and hence different from r_1.

The probability density $f^{(1)}(y)$ is given by:

$$f^{(1)}(y) = A \frac{\beta}{b_2} y^{-\frac{\beta}{b_2}-1} \tag{13}$$

2.2 Second Case

If an upper bound m_1 is imposed on m the probability density f(m) must be changed. Assuming that the new probability density $f^{(2)}(m)$ is proportional to $f^{(1)}(m)$ in the range $m_0 < m \leq m_1$, the normalization of $f^{(2)}(m)$ leads to:

$$\int_{m_0}^{m_1} K f^{(1)}(m)\, dm = 1,$$

and hence:

$$K = \frac{1}{1 - e^{-\beta(m_1 - m_0)}}$$

This implies

$$1 - F_M^{(2)}(m) = \begin{cases} 1 & ; \ m \leq m_0 \\ K\left[1 - F_M^{(1)}(m)\right] + 1 - K & ; \ m_0 < m \leq m_1 \\ 0 & ; \ m > m_1 \end{cases} \tag{14}$$

Hence:

$$N^{(2)}(m) = K N^{(1)}(m) + \lambda (1 - K) \tag{15}$$

As regards the calculation of $N^{(2)}(y)$ we can start from the equation:

$$1 - F_Y^{(2)}(y) = \lambda \int_0^{r(y)} \left\{1 - F_M^{(2)}[m(y,r)]\right\} f(r)\, dr \tag{16}$$

where the limit r(y) of the integral is given by:

$$r(y) = b_1^{1/2} e^{b_2 m_1/2} y^{-1/2} \tag{17}$$

In fact, as observed by Cornell [4], earthquakes beyond a distance defined by solving

$$y = b_1 e^{b_2 m_1} r^{-2}$$

cannot possibly cause a peak acceleration at the site greater than y since their magnitude cannot exceed m_1.

From eq. (11), (12), (16), (17) we obtain:

$$1-F_Y^{(2)}(y)=N^{(2)}(y)=K\left[N^{(1)}(y)\right]_{r_{max}=r(y)}+\lambda(1-K)\frac{r^2(y)}{r_1^2} \tag{18}$$

The probability density $f^{(2)}(y)$ is given by:

$$f^{(2)}(y)=-\lambda\frac{d}{dy}\int_0^{r(y)}\left\{1-F_M^{(2)}[m(y,r)]\right\}f(r)dr=$$

$$=-\frac{\lambda}{r_1^2}\int_0^{r_0}\frac{\partial}{\partial y}K\left\{1-F_M^{(1)}[m(y,r_0)]\right\}2rdr-\frac{\lambda}{r_1^2}\int_{r_0}^{r(y)}\frac{\partial}{\partial y}K\left\{1-F_M^{(1)}[m(y,r)]\right\}2rdr+ \tag{19}$$

$$-\frac{\lambda}{r_1^2}\left\{1-F_M^{(2)}[m(y,r(y))]\right\}2r(y)\frac{dr(y)}{dy}-\frac{\lambda}{r_1^2}(1-K)\frac{dr^2(y)}{dy}.$$

Taking into account that

$$m[y,r(y)]=m_1,$$

and $K[1-F_M^{(1)}(m_1)]+1-K=P[M>m_1]=0$,
the eq. (19) becomes:

$$f^{(2)}(y)=K\left[f^{(1)}(y)\right]_{r_{max}=r(y)} \tag{20}$$

2.3 Third Case

Assume:

$$N^{(3)}(m)=\lambda e^{\beta_1(m-m_0)+\beta_2(m^2-m_0^2)} \tag{21}$$

This implies that, for a single earthquake:

$$P[M>m]=1-F_M^{(3)}(m)=\begin{cases}1 & ;\quad m\le m_0\\ e^{\beta_1(m-m_0)+\beta_2(m^2-m_0^2)} & ;\quad m>m_0\end{cases} \tag{22}$$

Maintaining the remaining hypotheses as in the first case, the seismicity at the site for the present third case is:

$$N^{(3)}(y) = 1 - F_Y^{(3)}(y) = B\, y^{\beta_1/b_2}\left[r_0^{2+2\beta_1/b_2} e^{\varphi(y,r_0)} + 2\int_{r_0}^{r_{max}} r^{2\frac{\beta_1}{b_1}+1} e^{\varphi(y,r)} dr\right] \quad (23)$$

where

$$B = \frac{\lambda}{r_1^2}\, b_1^{-\beta_1/b_2}\, e^{-\beta_1 m_0 - \beta_2 m_0^2} \quad (24)$$

$$\varphi(y,r) = \frac{\beta_2}{b_2^2}\, ln^2\left(\frac{y}{b_1} r^2\right) \quad (25)$$

The probability density $f^{(3)}(y)$ is:

$$f^{(3)}(y) = -B\, y^{\frac{\beta_1}{b_2}-1}\left\{r_0^{2+2\frac{\beta_1}{b_2}} e^{\varphi(y,r_0)}\left[\frac{\beta_1}{b_2} + \frac{\beta_2}{b_2^2} 2ln\left(\frac{y}{b_1} r_0^2\right) - 1\right] + \right.$$
$$\left. + r_{max}^{2\frac{\beta_1}{b_2}+2} e^{\varphi(y,r_{max})} - 2\int_{r_0}^{r_{max}} r^{2\frac{\beta_1}{b_2}+1} e^{\varphi(y,r)} dr\right\}. \quad (26)$$

In eq. (23), (26), as for the first case, $r_{max} = r_1$.

2.4 Fourth Case

If the magnitude-frequency law (21) is truncated at m_1 we get:

$$1 - F_M^{(4)}(m) = \begin{cases} 1 & m \le m_0 \\ K_1\left[1 - F_M^{(3)}(m)\right] + 1 - K_1 ; & m_0 < m \le m_1 \\ 0 & m > m_1 \end{cases} \quad (27)$$

where

$$K_1 = \frac{1}{1 - e^{\beta_1(m_1 - m_0) + \beta_2(m_1^2 - m_0^2)}}. \quad (28)$$

Moreover, the equations (18), (20) become:

$$N^{(4)}(y) = K_1 \left[N^{(3)}(y) \right]_{r_{max} = r(y)} + \lambda (1 - K_1) \frac{r^2(y)}{r_1^2}, \qquad (29)$$

$$f^{(4)}(y) = K_1 \left[f^{(3)}(y) \right]_{r_{max} = r(y)} \qquad (30)$$

3. MARGINAL COST OF A SAVED LIFE

The mathematical model leading to the calculation of the marginal cost of saved life $\Delta D/\Delta L$ is based on the following assumptions:

- The amount of damage due to an earthquake with peak ground acceleration y is obtained from the total cost of the building multiplied by a factor d(y, C) which depends on y and on the design lateral force coefficient C:

$$d(y,C) = \begin{cases} 0 & ; \quad y \le y_i \\ \dfrac{y - y_i}{y_c - y_i} & ; \quad y_i < y \le y_c \\ 1 & ; \quad y_c < y \end{cases} \qquad (31)$$

where y_i is the value of y for which damage caused by an earthquake will begin to be appreciable and is given by:

$$y_i = \gamma + C \qquad (32)$$

y_c is the value of y corresponding to the collapse of the structure and is given by:

$$y_c = \xi C + \zeta. \qquad (33)$$

- The total monetary damage is supposed to be the one just described multiplied by 1.5 in order to take into account the indirect damage. Thus the cost of damage in liras/year person is given by:

$$D_1 = 1.5 \varrho \int_0^{y_{max}} d(y,C) f(y)\, dy, \qquad (34)$$

where ρ is the initial cost of the building per person, and y_{max} is the maximum possible peak ground acceleration at the site:

$$y_{max} = b_1 e^{b_2 m_1 r_0^{-2}} \tag{35}$$

which becomes ∞ in the first and in the third case.

- The additional construction cost due to seismic design (expressed in liras/year/person taking into account the interest on the invested capital) is given by:

$$D_2 = \rho(hC + \theta), \qquad C \geq 0.01 \tag{36}$$

- The expected number V of victims/year/person is proportional to the number of failures:

$$V = p\,N(y_c) \tag{37}$$

Under the foregoing assumptions, the marginal cost $\Delta D/\Delta L$ can be expressed in terms of the derivatives of the total cost $D = D_1 + D_2$ and of the expected number of victims V in respect of C. Assuming D_m as new symbol for the marginal cost of a saved life, we get:

$$D_m = \frac{\frac{d(D_1+D_2)}{dC}}{-\frac{dV}{dC}} \quad ;$$

or also:

$$D_m = D_{m,1} + D_{m,2} \ ,$$

where $D_{m,1}$ and $D_{m,2}$ are the marginal costs of a saved life calculated, respectively, only with the cost of damage D_1 and only with the additional cost for seismic design D_2.

Taking into account that:

$$\frac{d}{dC}\int_{y_i}^{y_{max}} d(y,C)f(y)\,dy = \int_{y_i}^{y_c} \frac{\partial}{\partial C} d(y,C)f(y)\,dy + \int_{y_c}^{y_{max}} \frac{\partial}{\partial C} d(y,C)f(y)\,dy +$$

$$+ d(y_c,C)f(y_c)\xi - d(y_i,C)f(y_i) - d(y_c,C)f(y_c)\xi \ ,$$

and that:

$$\frac{\partial}{\partial c} d(y,c) = 0 \qquad \text{when} \quad y > y_c$$

$$d(y_i, c) = 0,$$

we get:

$$\frac{d}{dc} \int_{y_i}^{y_{max}} d(y,c) f(y)\, dy = \int_{y_i}^{y_c} \frac{\partial}{\partial c} d(y,c) f(y)\, dy.$$

Hence the marginal cost $D_{m,1}$ is given by:

$$D_{m,1} = \frac{1.5 \rho \int_{y_i}^{y_c} \frac{\partial}{\partial c} d(y,c) f(y)\, dy}{n \xi f(y_c)}, \tag{38}$$

while the marginal cost $D_{m,2}$ is obviously:

$$D_{m,2} = \frac{\rho \Theta}{n \xi f(y_c)} \tag{39}$$

It is interesting to observe:

- that in force of eq. (10) the marginal cost $D_{m,1}$ (due to damage) depends on the earthquakes with y contained in the interval $[y_i, y_c]$, but is does not depend on the earthquakes with $y > y_c$;
- that the marginal cost $D_{m,1}$ does not depend on the total number of earthquakes λ; as both D_1 and V are proportional to λ;
- that when $D_m^{(1)}$ and $D_m^{(3)}$ are calculated for the first and the third case, the marginal costs $D_m^{(2)}$ and $D_m^{(4)}$ for the corresponding truncated cases are simply given by:

$$D_m^{(2)} = \left[D_{m,1}^{(1)} \right]_{r_{max} = r(y)} + \frac{1}{K} \left[D_{m,2}^{(1)} \right]_{r_{max} = r(y)},$$

$$D_m^{(4)} = \left[D_{m,1}^{(3)} \right]_{r_{max} = r(y)} + \frac{1}{K_1} \left[D_{m,2}^{(3)} \right]_{r_{max} = r(y)}$$

Just to give an example of a complete numerical application of the mathematical model, the linear and the quadratic magnitude-frequency laws contained in [2] have been considered (without truncation in both cases):

$$\log_{10} N(m) = a_o - 0.98\,(m - m_o)$$

$$\log_{10} N(m) = a_o + 1.076\,(m - m_o) - 0.218\,(m^2 - m_o^2)$$

The coefficient a_o referred to the area πr_1^2 has been derived from an assumed value a=6 referred to 10^6 km^2.

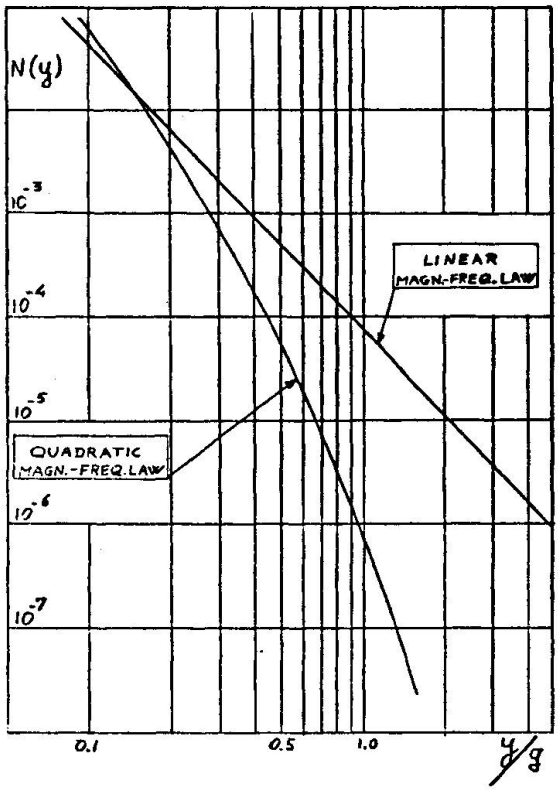

Fig. 1 - Seismicity at a site included in an ideal homogeneous seismic zone with two different magnitude-frequency laws taken from Merz and Cornell [2].

The remaining coefficients of the model have been assumed as follows:

eq. 32 $\gamma = 0.05$

eq. 33 $\xi = 6$, $\zeta = 0.375$

eq. 34 $\varrho = 7.5 \cdot 10^6$ lines/person

eq. 35 $b_1 = 1200/981$ km^2 $b_2 = 0.8$, $r_o = 25$ km

eq. 36 $h = 0.0778$ year^{-1}, $\vartheta = -0.000778$ year^{-1}

eq. 37 $p = 0.3$

The results of the calculation are shown in the figures 1 and 2. Fig. 1 shows the seismicity at the site. Fig. 2 shows the influence of the alternative seismicities on the marginal cost of a saved life. The influence, in this case, is very large. However it must be observed that a quantitative discussion will be possible only on the basis of linear and quadratic magnitude-frequency laws, derived from the same set of statistical data possibly referred to an approximately homogeneous distribution of potential earthquake sources.

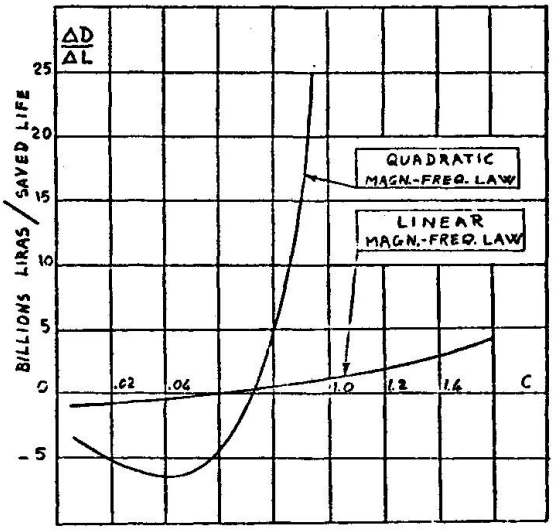

Fig. 2 - Marginal cost of a saved life versus design coefficient C for the site of fig. 1.

REFERENCES

[1] SHLIEN, S. and TOKSÖZ, M.N.: Frequency-magnitude statistics of earthquake occurrence. Earthquake Notes (Eastern Section of the Seismological Society of America), 1970, 41, 5-18.

[2] MERZ, H.A. and CORNELL, C.A.: Seismic risk analysis based on a quadratic magnitude-frequency law. B.S.S.A., 1973, vol. 63, n.6.

[3] GRANDORI, G.: Seismic zoning as a problem of optimization. 2nd Int. Conference on Structural Safety and Reliability, Munich, Sept. 1977.

[4] CORNELL, C.A.: Probabilistic analysis of damage to structures under seismic loads. in Dynamic Waves in Civil Engineering; D. A. Howells, I.P. Haigh and C. Taylor, Editors, John Wiley, London, 1971.

THE GAPEC SYSTEM : A NEW ASEISMIC BUILDING METHOD FOUNDED ON OLD PRINCIPLES

BY GILLES C.DELFOSSE
Civil Engineer , Docteur ès-Sciences
Head of the Structural Dynamics Section
C.N.R.S./L.M.A. - FRANCE

SYNOPSIS

The GAPEC system is a new aseismic system of the soft-story type experimented at the Centre National de la Recherche Scientifique, (C.N.R.S.) in Marseille, France. With this system, a building is standing on energy-absorption isolators set between the first story and the basement or the soil if no basement. Large scale experiments performed on a shaking-table and designs of typical high or intermediate buildings show that using the GAPEC system divides the accelerations response, shears and overturning-moments by a factor of 5 to 8. Practical applications have begun in 1978 with three buildings fitted with the GAPEC system.

Le système GAPEC est un nouveau système antisismique du type "étage mou" expérimenté au Centre National de la Recherche Scientifique (C.N.R.S.) à Marseille France. Avec ce procédé, un immeuble repose sur des isolateurs placés entre le premier étage et les caves ou le sol si l'immeuble n'en possède pas. Des essais effectués à grande échelle sur une table vibrante et le calcul d'immeubles typiques de hauteur élevée ou moyenne montrent que l'emploi du système GAPEC divise la réponse en accélération, les efforts tranchants et les moments de renversement par un facteur de 5 à 8. Les applications pratiques ont commencé en 1978 avec trois immeubles équipés du système GAPEC.

1.- INTRODUCTION.

A new trend for earthquake - resistant structures has developed for several years, which intends to confine the seismic energy in a limited area of the structure acting as a shock absorber. In the 1930's, Martel, Green and Jacobsen presented some aspects of a flexible first story and Fintel and Khan (1968) wrote about a shock-absorbing soft story concept [1]. These authors obverved that the upper stories of many buildings submitted to strong earthquakes had suffered but small damage when the first story was flexible enough to accomodate large distorsions. In the Fintel and Khan's method, the entire building should remain within the elastic range, except the soft story which undergoes elasto-plastic behaviour. As a consequence, the building would stay in a displaced position after the quake and would have generally to be demolished.

A further step is to implement a soft perfectly elastic story so that the building remains in its original position after the seismic event. The laws of the structural dynamics show us that such a story would increase the natural periods of the buildings and decrease correspondingly the acceleration response. In another way, the recent developments of rubber technology allow us to conceive such a perfectly elastic story. This old knowledge joined to this new technology has given rise to the GAPEC system.

2.- FUNDAMENTALS OF THE GAPEC SYSTEM. (G.S.)

The GAPEC system is a new aseismic system experimented at the "Centre National de la Recherche Scientifique " (C.N.R.S.) in Marseille, France, since 1973. With the GAPEC system a building is standing on energy absorption devices called isolators and located between the first floor and the basement (fig.1). These devices consist of a laminated rubber-and-steel sandwich manufactured with a new and special design. Their main feature is a relatively high stiffness in the vertical plan and about the two horizontal principal axes of the building and a low stiffness in the horizontal plan and about the vertical axis. Transverse stiffness of the isolators is currently a hundred times less than the vertical one and two hundred times less than that of the concrete columns of the first story. They constitute a very soft and short story. Isolators have a general nonlinear elastic behaviour ; the fig.2 shows typical stress-strain compression curves which seem to agree well with the following equation :

$$\sigma = G\, s\, \alpha(\alpha^2 - 3\alpha + 3)/(1 - \alpha)^2 \qquad (1)$$

where

$$s = 1 + 0.103\ (a/e_o)^2 \qquad (2)$$

G is the shear-modulus of rubber, a the side or diameter of the cross-section of rubber and e_o the thickness of a rubber-layer.

Fo tall buildings, the transverse flexibility of the isolators can introduce some discomfort to the occupants under wind action. For this reason simple mechanical devices called wind-stabilizers inserted at the same level as the isolators are designed to fix the building against ordinary wind loads. When the base shear reaches a minimum designed value, the wind-stabilizers are automatically disconnected from the structure which becomes free on the isolators. After the earthquake, the wind-stabilizers are easily re-connected to the building.

3.- HIGH EFFICIENCY OF THE GAPEC SYSTEM.

The GAPEC system allows engineers to control three essential parameters of the behaviour of a building submitted to an earthquake shock, which are the lateral, vertical and torsional responses.

3.1.- Lateral response.

Due to their low stiffness, the isolators act mainly in the horizontal plane as low-pass filters by increasing the natural periods of the building. As we know, the maximum response of a structure to a ground acceleration a(t) can be found by response spectrum analysis ; thus the maximum absolute acceleration-vector is written as :

$$X(t) = \sum_j \gamma_j \, x_j \, Saj \qquad (3)$$

where

$$Saj = \omega_j \left| \int_o^t a(\tau) \exp.[-\xi_j \omega_j (t - \tau)] \sin \omega_j (t - \tau) d\tau \right|_{max} \qquad (4)$$

represents the spectral acceleration in the j th mode x_j and γ_j , ω_j and ξ_j are respectively the modal participation factor, the natural circular frequency and the equivalent viscous damping ratio of the j th mode. A typical acceleration-response spectrum is shown on the fig.3 and we can see that increasing the natural period above 2s results in a large decrease of the horizontal response acceleration. Numerous experiments were performed on the shaking-table of the Laboratory of Mechanics and Acoustics of the C.N.R.S. in Marseille with a 20-story scale model measuring 1.20m x 0.68m in plan ; height is 3.10m and weight 9 380 N ; it is excited by the 1952 Taft California earthquake, N21 E component, normally to the longer side with a maximum ground acceleration of 0.1 g. The table 1 shows the maximum measured values with and without isolators ; we can see that using the GAPEC system in the scale model divides the accelerations, shears and overturning moments by a factor of more than 8. In addition, some typical buildings were designed using the normal mode method with a complete history of the response and the design values found confirm well the excellence of the new system. For example, the fig.4 shows the designed values of the Enaluf Building in Managua, Nicaragua, which was badly damaged by the earthquake of December 23, 1972 ; the design was performed with and without the GAPEC system and we can see on the fig.4 that (a) the first predominant mode shape of the building fitted with G.S. is practically a straight line almost parallel to the undeflected vertical axis (fig.4a) ; this means, in fact, that the building moves on the isolators like a quasi-rigid body with a very small overall-bending (b) the acceleration response, shears and overturning moments are reduced by a factor of 5 at least when using G.S. (fig.4b,c,d) ; let us emphasize right now that a so large decrease of the overturning moments (fig.4d) will increase the foundation stability proportionally. In this case, the first natural period has grown from 0.86s without G.S. to 3.1s with G.S.. The design shows obviously that the Enaluf Building would have withstood the December 23, 1972 earthquake shock with light damage only if it had been fitted with the GAPEC system. Similar conclusions arise from the design of other building types. The table 2 shows the maximum design values of a typical 20-story building measuring 23.60m x 23.60m in plan excited by the 1940 El Centro California earthquake. N-S component ; we see that, in this case, using GAPEC system divides the acceleration response, shears and overturning moments by more than 8. The fundamental period has grown in this case from 1.15s without G.S. to 5s with G.S..

3.2.- Vertical response.

In the vertical plane the isolators act mainly as dampers with a loss factor of 0.1. Their relatively high vertical stiffness involves a large decrease of the P - Δ effect in the structure and explains the lateral quasi-rigid motion that we mentioned above.

3.3.- Torsional response.

The torsional stiffness of the isolators is currently 2,000 times less than that of the concrete columns of the first story. Consequently the buildings fitted with G.S. also have a very low torsional response acceleration.

4.- THE MAIN ADVANTAGES OF THE GAPEC SYSTEM.

Examining the current aseismic technics, we can see that the GAPEC system has four main advantages related to the foundation stability, safety of the structural and non-structural elements and building coast. We shall discuss these points successively.

4.1.- Foundation stability.

The large overturning moments induced by strong earthquakes in classical aseismic buildings involve an important rocking of the base with high compression stresses in the soil foundation and sometimes alternative states of tension and compression. Large irregular settling can occur resulting in big damage for the structure. As we have seen in the last section, the GAPEC system strongly reduces the shears and overturning moments and consequently decreases the base rocking proportionally. The soil foundation remains reasonably strained during the earthquake and no or little settling is observed. G.S. confers in fact to the building what is certainly the most important parameter of safety, e. g. the base stability.

4.2.- Safety of structural elements.

It is well known [2] that the current aseismic designs are based upon the concept that a structure must be able to resist moderate earthquakes with minor structural and some non-structural damage and resist major catastrophe earthquakes without collapse, but with permissible major structural and non-structural damage. In the best case, this means much expensive repairs and often a complete demolition of the building. The conditions are obviously quite different if the structure is fitted with G.S. Indeed, the large decrease of the seismic forces involves that the structural elements undergo moderate strain only and the building suffers no or minor easily repaired structural damage when undergoing a large earthquake. Moreover, in case of successive shocks, due to the elastic properties of isolators, the building fitted with G.S. perfectly recovers its initial position after each shock and remains quite able to resist the next one.

4.3.- Safety of non-structural elements.

Overall-bending and relative displacements between adjacent floors of classical aseismic buildings are important during strong earthquakes. The non-structural elements are generally unable to accommodate these differential motions and suffer damage usually beyond repair. We have seen in the first section that a building fitted with G.S. behaves nearly like a rigid body ; as a consequence, overall-bending and relative displacements between adjacent floors are reduced to a degree more easily accommodated by non-structural elements which suffer no or small damage. If, as stated in [3], the skeleton in tall buildings is only 20% of the total coast, the high safety given by G.S. to the non-structural elements represents very large savings of money.

4.4.- Building coast.

The general decrease of shears and overturning moments of a building fitted with G.S. results in substantial savings in the size of the structural elements, chiefly in foundation. These savings balance the coast of the devices

of G.S. for a protection against moderate earthquakes. For strong earthquakes, the use of G.S. can introduce a few additionnal per-cents on the coast of the classical aseismic building, depending on the type of building and the country where it is located. However, in view of the fact that, after an earthquake, the building remains in use without important repairs. G.S. is undoubtedly much cheaper than any of the present classical aseismic systems.

5.- THREE BUILDINGS FITTED WITH G.S.

The practical applications of G.S. have begun in 1978 by three buildings located at Saint-Martin de Castillon, near the little town of Apt in the french department of Vaucluse. This is a seismic area classified 2 in the "Règles Parasismiques 1969" which are the french aseismic regulations.

The first building is a dwelling-house, the second one is for technical purposes and the third one a recording studio ; they are spaced of 14cm one from the other with adequate flexible passages between them. They are fitted by 200mm diameter isolators designed and supplied by the company E.R.A. of Marseille [4]. The table 3 shows the physical caracteristics of these buildings. They were designed for a VIII M.M. earthquake according to the french aseismic regulations. The table 4 shows the results of the design performed with and without G.S. ; the comparison is made in the X direction, but we have to notice that the results are practically the same in both directions when the buildings are fitted with G.S. We can see on the table 4 that G.S. applied to low buildings divides the base shear and overturning moments approximatively by 2 ; which is again very satisfying. We observe that the natural periods are increased, in this case, by a factor of about 30.

The coast of the isolators was 7% of the structural works, of which 2% have to be taken off for the savings on the structure resulting of the decrease of seismic forces. The extra-coast was thus 5% of the structural works, which is low for a protection against earthquakes, specially in view of the high amount of additionnal savety brought by the system.

6.- CONCLUSION.

Based on old principles, the ÇAPEC system results of the large improvements made in the rubber technology. It represents presently one of the most efficient way to protect buildings fully against earthquake risk at very reasonable coast.

7.- REFERENCES.

[1] Mark FINTEL, Fazlur R.KHAN. - Shock-absorbing soft story concept for multistory earthquake structures. 64th Annual ACI Convention, Los Angeles, March 7, 1968.

[2] Mark FINTEL. - Resistance to earthquake. Philosophy ductility and details. Publication ACI SP-36. Response of Multistory Concrete Structures to Lateral Forces. Paper SP 36-5 American Concrete Institute, Detroit, 1973.

[3] Mark FINTEL, Ingvar SCHOUSBOE. - Response of Buildings to Lateral Forces. Journal of American Concrete Institute, Proceedings, 68, n°2; Feb. 1971, pp.81-106 ; n°8 Aug. 1971, pp.616-619.

[4] E.R.A., B.P. 182, 13275 Marseille Cedex 2, France.

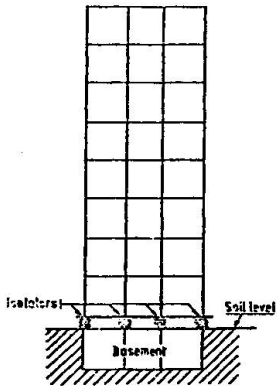

Fig.1. The GAPEC SYSTEM

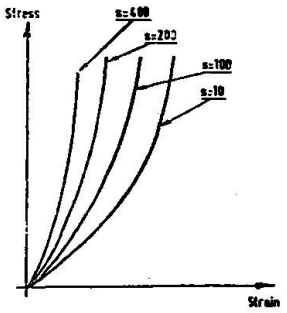

Fig.2. Typical stress-strain compression curves of isolators.

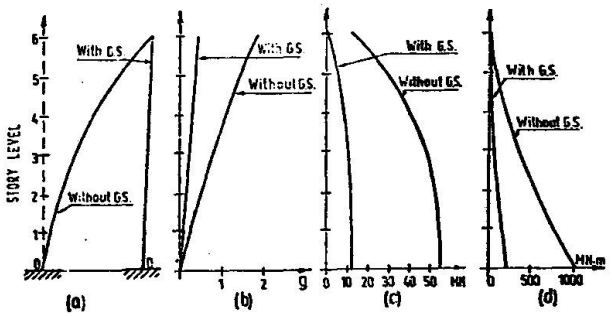

Fig.4 - The Enaluf building in Managua, Nicaragua. Design values, North-South direction, with and without the GAPEC SYSTEM (a) 1rst predominant mode shape (b) acceleration-response; (c) shears; (d) overturning moments.

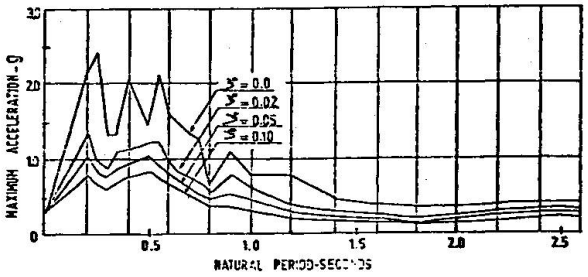

Fig.3.1940 EL CENTRO California Earthquake, N.S component. Acceleration-response spectra with values of damping ratio 0.0, 0.02, 0.05 and 0.10.

	Without G.S.	With G.S.	Ratio Without G.S. / With G.S.	Without G.S.	With G.S.	Ratio Without G.S. / With G.S.
MAX-Acceleration-response (g)	0.170	0.020	8.5	0.28	0.032	8.7
MAX-Shear (N)	1014	123	8.2	43×10^6	4.86×10^6	8.8
MAX-Overturning moment (N.m.)	1570	190	8.3	1383×10^6	161×10^6	8.6

Table 1. The scale-model Accelerations, shears and overturning moments measured with and without G.S.

Table 2. Maximum design values of a typical 20-story building with and without G.S.

Building N°	Sizes in plan (m x m)	No of Stories	Weight (tons)	Number of 200mm isolators	Horizontal stiffness (10^3N/m)
1	13.00x13.10	2	414	21	655
2	9.60x8.20	1	121	11	343
3	9.10x9.80	1	208	10	312

TABLE 3. Main caracteristics of the first three buildings fitted with G.S.

	Building N°	1rst natural period (s)	Max. response acceleration (g)	Max. shear (10^3N)	Max. overturning moment (10^3N.m)
Without G.S.	1	0.063	0.100	414	1536
With G.S.		1.58	0.055	228	728
Ratio		0.04	1.82	1.82	2.11
Without G.S.	2	0.031	0.100	121	220
With G.S.		1.18	0.063	76	101
Ratio		0.03	1.59	1.59	2.18
Without G.S.	3	0.057	0.100	208	568
With G.S.		1.62	0.055	114	285
Ratio		0.03	1.82	1.82	1.99

Table 4. Seismic design of the three buildings with and without G.S.

RECENT NEW ZEALAND DEVELOPMENTS ON BRIDGE SEISMIC DESIGN

DÉVELOPPEMENTS RÉCENTS EN NOUVELLE ZÉLANDE DU DESSEIN SÉISMIQUE DES PONTS

NEUE NEUSEELÄNDISCHE ENTWICKELUNGEN ÜBER DEM ERDBEBENANSCHLAG DER BRÜCKEN

by R.W.G. BLAKELEY* *and* H.E. CHAPMAN*

* Design Engineer, Ministry of Works and Development, Wellington, New Zealand

SUMMARY

Information is presented on recent New Zealand developments in the two main approaches for seismic design of bridges. Most commonly, design is based on ductile flexural yielding of specially detailed members, usually the piers. Research data are shown on ductility demand on reinforced concrete piers and their ductility capability. A design office procedure for assessing available bridge structure ductility is discussed. A recent alternative approach involves isolation of the structure from the worst effects of earthquake ground shaking by a combination of flexible mountings and mechanical energy dissipating devices. Details of the devices, examples of their application and a philosophy of design are presented.

RÉSUMÉ

On présente les informations de developpements récents en Nouvelle Zélande concernant les deux procédés principaux pour le dessein séismique des ponts. Très ordinairement, le dessein s'est basé sur le fléchissement ductile à la flexion des membres avec particularités spécialement arrangées, d'habitude les piliers. On montre des faits de recherches concernant la demande de la ductilité sur les piliers de béton armé et leur capacité de la ductilité. On discute un procédé du bureau de dessein pour estimer la ductilité disponible de la structure des ponts. Un procédé récent et alternatif comporte l'isolement de la structure de plus mauvais effets du tremblement de terre par une combination d'affûts flexibles et appareils mécaniques qui dispersent l'énergie. On présent les détails des appareils, exemples de leur application et une philosophie de dessein.

HAUPTINHALT

Informationen wird über neue neuseeländische Entwickelungen von den zwei Hauptmethoden gegenüber dem Erdbebenanschlag der Brücken vorgelegen. Am gewöhnlichsten, wird der Anschlag auf ziehbare krümmende Nachgebendigkeit von Gliedern mit besonders geordneten Details gegründet, meistens die Pfeiler. Erforschungsunterlagen werden über der Anforderung der Biegsamkeit auf Eisenbetonpfeiler und ihre Fähigkeit der Biegsamkeit dargestellt. Eine Handlungsweise des Anschlagbüros, verfügbare Biegsamkeit in Brückenaufbauten einzuschätzen, wird behandelt. Eine neue, alternative Methode hat zur Folge die Absonderung des Aufbaus von den schlimmsten Folgen des Erdbebengrundschüttelns von einer Zusammensetzung biegsamer Vorbauten und mechanische Apparate, die die Energie zerteilen. Die Einzelheiten der Apparate, Beispiele ihres Gebrauchs und eine Anschlagphilosophie werden vorgelegen.

1. INTRODUCTION

In the past, greater attention has generally been given to development of seismic design procedures for buildings than those for bridges. However, some spectacular collapses of several highway interchange bridges during the San Fernando earthquake of 9 February, 1971 highlighted the needs for research into the seismic response of bridge structures and for the development of improved design methods and details. Over recent years, in New Zealand, considerable efforts have been made to satisfy these needs.

It is well known that, when a structure responds to earthquake induced ground motions, very high forces may be generated if the structure is required to remain elastic. Such a requirement is seldom economically justifiable in view of the rapid increase in the cost of the structure, and the foundations in particular, as the design horizontal load increases. The common design approach is, therefore, to limit, or at least reduce, the horizontal forces induced in the structure. Two methods of achieving this are as follows:

(a) *Ductile Design Approach:* Energy dissipating members of a plastic hinge mechanism are designed to yield at an acceptable intensity of earthquake ground shaking and are detailed to deform in a ductile manner. Other structural elements are provided with sufficient reserve strength capacity to ensure that the chosen energy dissipating mechanism is maintained at near full strength throughout the deformations that may occur under a very severe earthquake. In a bridge structure, the chosen energy dissipating members are usually the piers rather than the foundations, because of the greater accessibility for inspection and repair in the former members.

(b) *Application of Mechanical Energy Dissipating Devices:* The structure is isolated from the worst effects of ground shaking by a combination of flexible mountings, usually in the form of elastomeric bearings, and of specially developed energy dissipating devices.

Method (a) above is the most commonly used approach, but a number of disadvantages must be accepted : design procedures may be complicated; details are expensive and sometimes difficult to fabricate; there is a high probability of some form of earthquake induced damage during the life of a structure and the associated requirement for costly repairs; and there may be difficulties in restoring permanent set deflections. The procedure in method (b) of concentrating energy dissipation in special components allows the structure itself to be protected from damage even in severe earthquakes. There is also potential for simplified design procedures and details. However this method is still in its developmental stages. Recent developments in both of these approaches are described in this paper.

2. DUCTILE DESIGN APPROACH

2.1 General

Because the primary energy dissipating members in a bridge designed according to this approach are the piers, satisfactory design depends on an understanding of the ductility demand on the piers and of their ductility capability. Previous buildings-related research is not necessarily applicable. Ductility demand during dynamic seismic response is dependent on aspects peculiar to bridges, such as foundation and elastomeric bearing characteristics. Knowledge of ductility capability has required recently obtained data for axially loaded piers with shapes, sizes and loads commonly adopted for bridge design. Research inform-

ation must be translated into a form allowing ready use by the designer, and for this purpose a convenient design office procedure for calculating available structure ductility has been developed.

2.2 Ductility Capability of Reinforced Concrete Piers

A programme of testing model bridge piers is proceeding at the University of Canterbury and progress to date has been fully reported by Priestley et al [1]. Five pier units have been tested, all representing variations of the same prototype, namely a single stem octagonal pier 1.5 m wide by 6 m clear height, reinforced vertically with 20 bundles of 3 by 32 mm dia bars giving a steel content of 2.7%.

The first three units were modelled to a scale of $\frac{1}{3}$ full size. Transverse reinforcing was designed to ACI requirements [2], and since the design ultimate axial load was only 0.06 $f'_c A_g$ the requirements for flexural members applied. Within the hinge region minimum requirements governed, namely $A_v d/s = 0.15 A'_s$ or $0.15 A_s$, whichever is the larger, with spacing not to exceed d/4 or 16 bar diameters. In the model this was provided by 6.5 mm dia welded hoops at 65 mm centres, giving a volumetric transverse steel content of 0.44%. The test procedures allowed a variation of the ratio of base moment to shear, and thus piers of different height were simulated in each model. Horizontal load was applied as slow cyclic load reversals of increasing displacement amplitude. The behaviour was generally satisfactory with displacement ductility factors in excess of 5 being achieved for each unit with substantial hysteretic energy dissipation evident. In later cycles hoop steel strains exceeded yield and cover concrete spalled, leading to buckling of compression steel progressively over subsequent cycles with associated moment and stiffness degradation.

The transverse steel of Units 4 and 5 was designed according to the more stringent requirements of ref 3, namely that within the hinge region hoop spacing should not exceed 100 mm, and the volumetric ratio of circular reinforcing should not be less than $0.12 f'_c/f_y$. Unit 4 represented the prototype pier at $\frac{1}{3}$ scale, and hoop steel was 8 mm dia at 34 mm centres. The design office procedure described in Section 2.4[4] results in similar transverse steel requirements. No axial load was applied and horizontal load application was at the equivalent height of 8.25 m on the prototype. This unit behaved exceptionally well. Stable hysteresis loops with only minor load and stiffness degradation were obtained at all displacement levels as indicated in Fig 1. Base moments have been scaled to prototype values and displacements to the effective prototype mass centre. Theoretical ultimate moment capacities based on measured material properties are indicated by dashed lines marked M_u. Displacement ductility factors (DF) were based on a nominal experimental yield displacement found by extrapolation of the post-cracking elastic moment-displacement curve to the theoretical ultimate moment capacity. Maximum recorded hoop steel strains reached 92% of nominal yield based on f_y = 275 MPa and E = 200 GPa, indicating that the design requirement [3] was realistic. Unit 5 was similar in detail to Unit 4 but at $\frac{1}{6}$ scale. It was subjected to sinusoidal and simulated earthquake base accelerations using a MTS

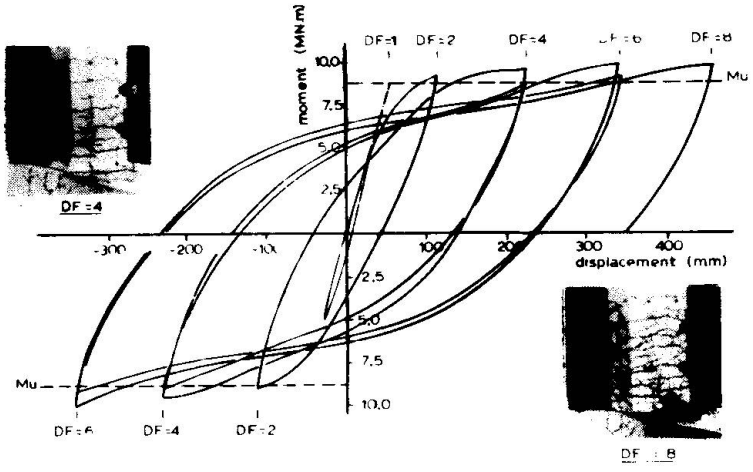

FIG 1: Moment-Displacement Loops for Unit 4, after Priestley et al [1]

electro-hydraulic system coupled to a shaking table. Good agreement was found between moment-displacement curves from Unit 4 tested statically and Unit 5 tested dynamically, giving confidence in the continued investigation of ductility capability using statically tested models.

Research is proceeding at University of Canterbury on ductility of circular and rectangular reinforced concrete bridge piers under combined axial load and bending moment.

2.3 Ductility Demand on Reinforced Concrete Piers

A number of dynamic computer analysis studies have been made [5,6,7,8] of the seismic response of bridge structures, and in particular the ductility demand on reinforced concrete piers. Sharpe [5] used finite element techniques to model a bridge on alluvial soil deposits within a wide valley, and demonstrated the significance of site characteristics on seismic displacement response. Priestley et al [1] computed the theoretical response of Unit 5 described in Section 2.2 above to the El Centro 1940 N-S earthquake record. The results were compared with the experimental response of the model to a displacement time-history form of that record applied to the shaking table, as shown in Fig 2. The theoretical curve was based on the experimentally observed elastic stiffness, a bilinear moment-curvature relationship and a viscous damping of 7%. Agreement is good for the 10 seconds shown and was adequate for the remainder of the earthquake record, although experimental displacements exceed theoretical values, indicating a lower viscous damping at lower levels of response. The corresponding maximum displacement ductility factor demand on the prototype pier was 2.6, and section curvature ductility factor demand was 5.8.

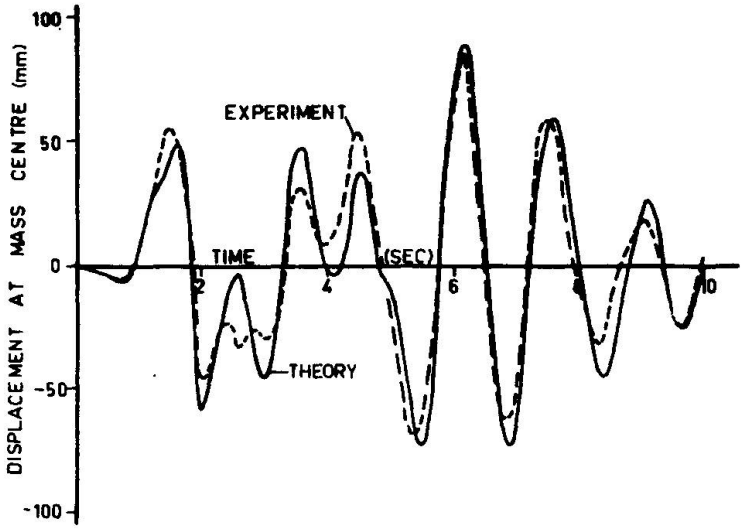

FIG 2: Response of Pier to El Centro 1940 N-S, after Priestley et al [1]

Cameron [7] investigated the sensitivity of the computed response of a reinforced concrete pier to several parameters; namely, the shape of the moment-curvature loop, the contribution of the vertical component of the earthquake ground accelerations, foundation flexibility and different ground acceleration records. Ductility demand decreased moderately with increasing post-yield hardening ratio; inclusion of vertical ground accelerations caused little difference to calculated response values, introduction of foundation flexibility as compared with a fixed base condition caused, in general, a significant reduction in displacement ductility demand but an increase in pier section curvature ductility demand; and ductility requirements varied considerably with different earthquake acceleration records. Analyses of two bridges designed according to current New Zealand requirements [3] and subjected to the El Centro 1940 N-S record showed displacement ductility factor demands of 2 for a portal frame pier and 5 for a single stem pier. Another study [8] of a three-span twin overpass with slab-type piers, analysed with allowance for pier foundation translation and rotation, showed longitudinal displacement ductility factor demands of 2 for the El Centro 1940 N-S record and 4 for the artificial A1 record. Studies are proceeding at University of Canterbury and in Ministry of Works and Development with the objective of defining design ductility requirements taking account of important parameters, in particular foundation and elastomeric bearing flexibilities.

2.4 Design Office Procedure

Design of state highway bridges in New Zealand is governed by the Highway Bridge Brief [3]. Fig 3 shows the recommended seismic design loadings, including importance factors and the basic seismic coefficients applicable to ductile structures for each of the three seismic zones subdividing the country. The seismic coefficients of Fig 3 for Zone A correspond approximately to an elastic response spectrum for the El Centro 1940 N-S earthquake and 5% equivalent viscous damping, divided by a design ductility factor of 6. The corresponding required structure ductility of 6 is regarded as a target and a lower value, with a minimum of 4, is accepted where economics have a strong influence. Less structure ductility is acceptable when the structure has a yield strength exceeding the design value for geometric or other reasons. Research on ductility demand, as discussed in Section 2.3, indicates that the design ductility factor of 6 may be conservatively large, that is that the equal displacement criterion implicit in the assumptions gives an overestimate of displacement response. The figure will be amended, if appropriate, in the light of current research.

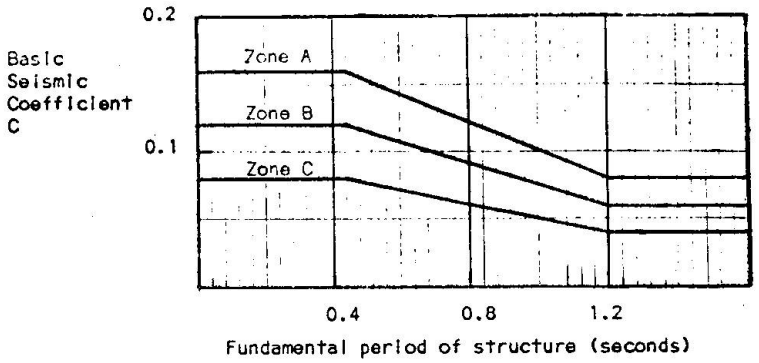

Importance Factors F

Category 1	Motorway under or overpass or bridge carrying more than 2500 vehicles per day.	1.0
Category 2	Bridge carrying between 250 and 2500 vehicles per day.	0.85
Category 3	Bridge carrying less than 250 vehicles per day.	0.7

NOTE

Seismic base shear = V = CxFxM_D x g (gravity) where M_D = mass of structure without live load.

Minimum ultimate strength is required to be adequate to resist 1.35xV

FIG 3: Seismic Design Loadings [3]

The ductile design approach requires for completeness an assessment of the available structure ductility. A convenient design office procedure for this purpose has been developed and is more fully described elsewhere [4,9]. The procedure involves, first, assessment of the ductility capability of each section of pier in which plastic hinging is intended to form and, second, calculation of the consequent structure ductility capability. The design charts cover a range of concrete cylinder strengths from 25 to 35 MPa, and apply to mild steel reinforcement with a yield stress of 275 MPa as appropriate for flexurally yielding piers. The stress/strain idealization used for concrete [10] takes account of the degree of confinement. Reinforcing steel strain hardening is assumed to commence at 11 times yield strain. Both circular and symmetrically reinforced rectangular sections are considered.

The section ductility is defined as the ratio of limit curvature of the section to curvature at yield, ϕ_u/ϕ_y, where deformation at yield is nominated as illustrated in Fig 1. In preparation of the charts, the value of ϕ_u was calculated as the ratio of the limit concrete strain in compression to the depth from the compressive face to the neutral axis when the limit strain is reached. The value of ϕ_y was calculated from the curvature at first yield, being the ratio of the steel tensile strain at first yield in the reinforcement closest to the tensile face to the distance from that steel to the neutral axis, multiplied by a factor depending mainly on the section shape, reinforcement layout, and average axial stress

on the section. The steps required for calculation of ϕ_u/ϕ_y by the designer using the charts are shown in Fig 4. An example calculation for a circular section is shown in Fig 5. It may be seen that the designer can quickly determine section ductility capability taking account of the relevant variables; namely, section shape, concrete strength, reinforcement percentage, volume of confining reinforcement and average axial stress on the section.

The structure ductility, μ, is defined as the ratio of limit displacement of centre of mass of structure to displacement at yield, δ_u/δ_y, where deformation at yield is nominated as illustrated in Fig 1. Structure and section ductilities are related using the concept of equivalent plastic hinge lengths. From a known moment/curvature relationship and section ductility capability for the piers, a force/displacement curve for the centre of mass of the structure may be derived. Examples of the analysis of various structural forms of bridge and suitable design charts are given in ref 4. It is important that due account is taken of the flexibility of foundations and elastomeric bearings.

At present the method incorporates a number of approximations and it is intended that these be gradually reduced by continuing research. At this stage it should not be used for other than basically single degree-of-freedom structures. A future development of the approach could involve an alternative method for defining and predicting limit curvature [10], being the curvature achieved when the moment of resistance has reduced to 85% of the maximum value. Further test results are needed to support the previous analytical studies before the approach can be developed for design office use.

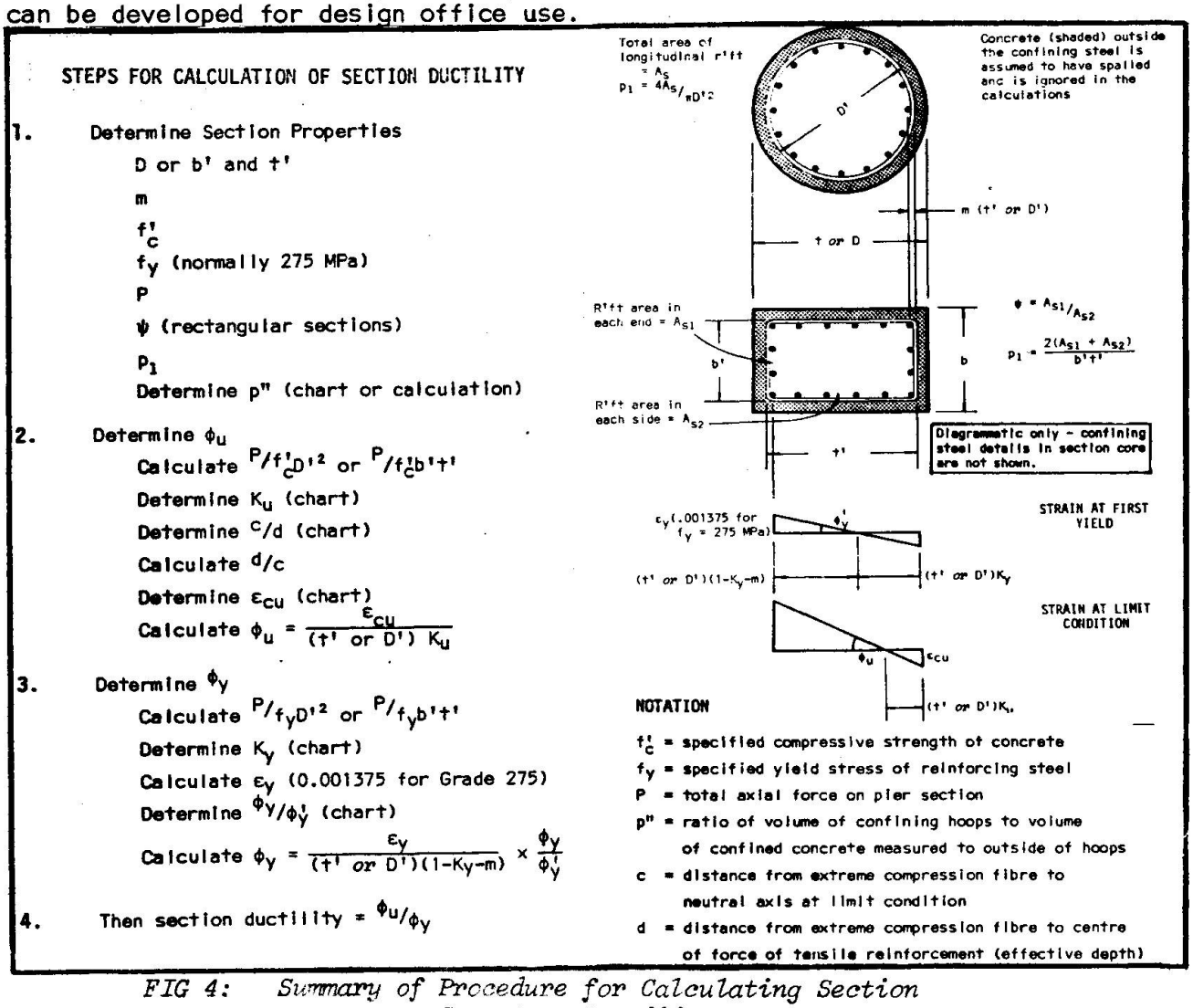

FIG 4: Summary of Procedure for Calculating Section Curvature Ductility.

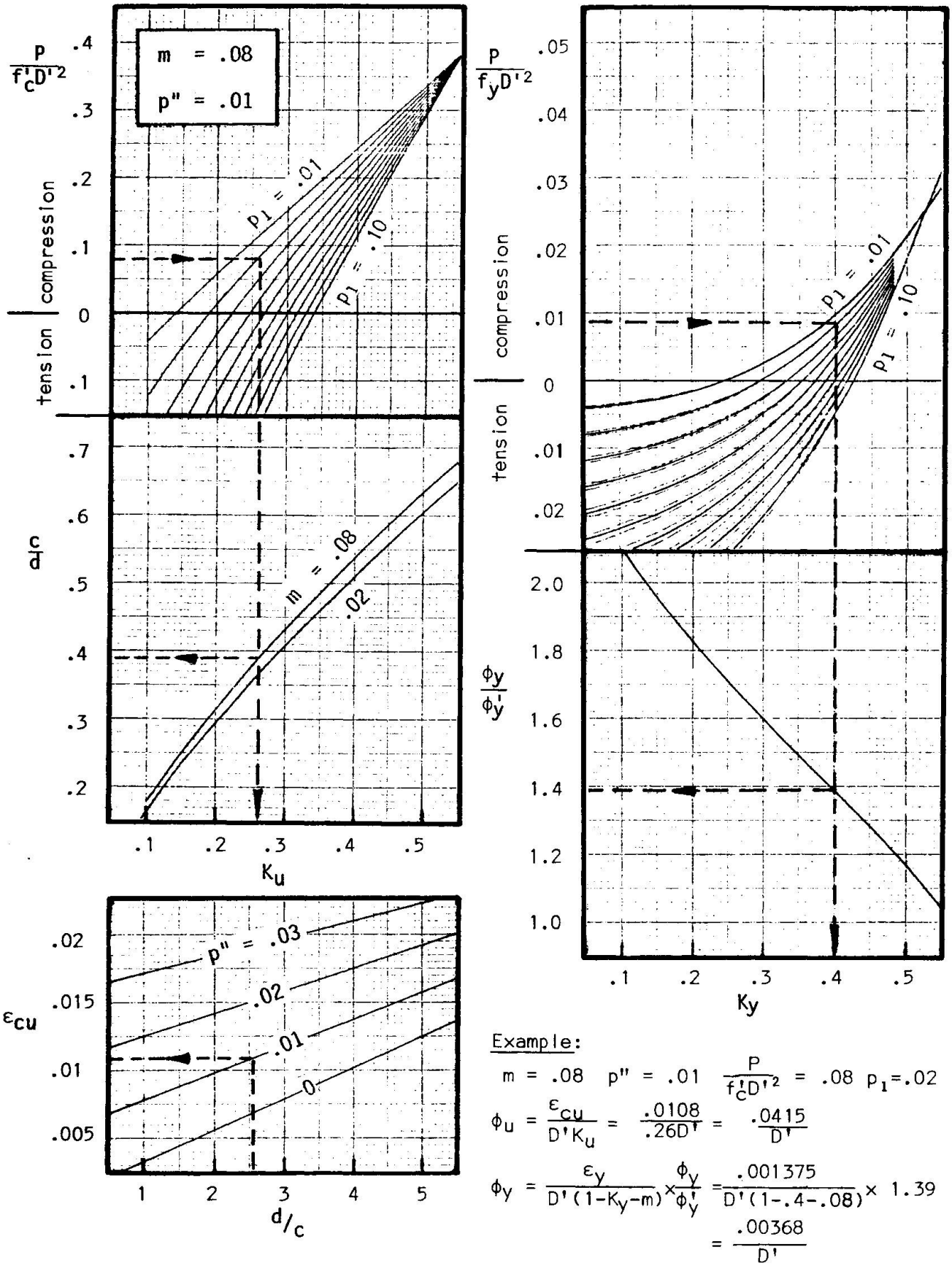

Example:

$m = .08 \quad p'' = .01 \quad \frac{P}{f'_c D'^2} = .08 \quad p_1 = .02$

$$\phi_u = \frac{\varepsilon_{cu}}{D' K_u} = \frac{.0108}{.26D'} = \frac{.0415}{D'}$$

$$\phi_y = \frac{\varepsilon_y}{D'(1-K_y-m)} \times \frac{\phi_y}{\phi'_y} = \frac{.001375}{D'(1-.4-.08)} \times 1.39$$

$$= \frac{.00368}{D'}$$

Section Ductility = $\phi_u/\phi_y = 11.3$

FIG 5: Example Charts for Calculation of Curvature Ductility. Circular Section, f'_c = 30 MPa, f_y = 275 MPa

3. APPLICATION OF MECHANICAL ENERGY DISSIPATING DEVICES

3.1 Details of Devices

In recent years a number of methods of isolating a structure from the effects of ground shaking have been proposed, but have not met general acceptance because of practical deficiencies, in particular the expected excessive displacements under wind or earthquake. However, a system overcoming these deficiencies has been made possible by the development of practical mechanical devices which act as hysteretic dampers. Detailed information on development and testing of these devices is given by Skinner, Robinson et al [11,12].

A number of the devices developed to date are illustrated in Fig 6. Four of the devices shown dissipate energy through cyclic yielding of mild steel elements, in either torsion or flexure. The other two devices rely on "hot working" of lead; during its deformation either in extrusion or in shear the lead recovers most of its mechanical properties almost immediately, and exhibits "coulomb damping" characteristics. All devices have been tested at earthquake-like frequencies and displacement amplitudes and have exhibited stable hysteretic characteristics for several hundred cycles of loading. Although energy is eventually dissipated in the form of heat, the temperature rise in the devices was only of the order of 5-10°C when subjected to the loading expected in a severe earthquake. The devices have been patented by the New Zealand Department of Scientific and Industrial Research and are marketed in this country.

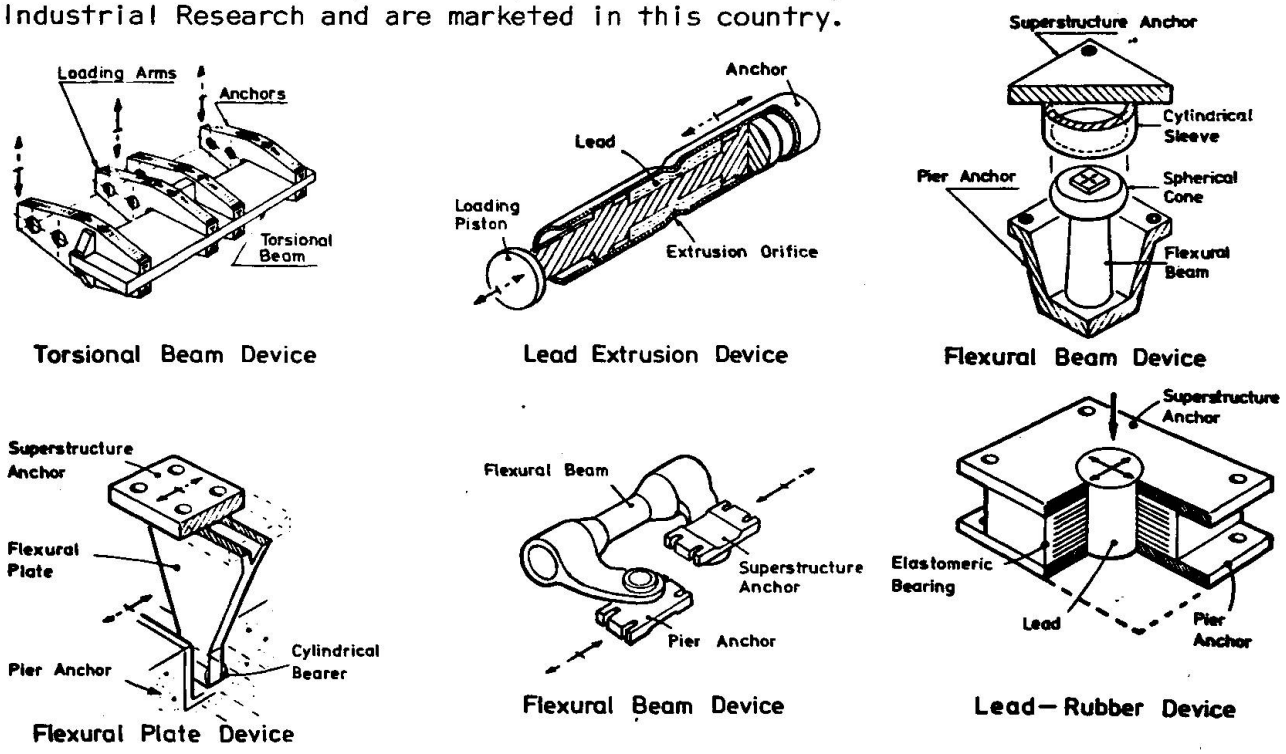

FIG 6: Schematic Drawings of Mechanical Energy Dissipating Devices

3.2 Practical Applications

The application of energy dissipating devices to bridges is shown in Fig 7 with respect to four examples. In general the cost of the devices and associated details is of the order of 1% of the bridge cost. Details are as follows:

(a) This six span prestressed concrete box girder railway bridge on tall reinforced concrete piers is currently under construction. The design concept is

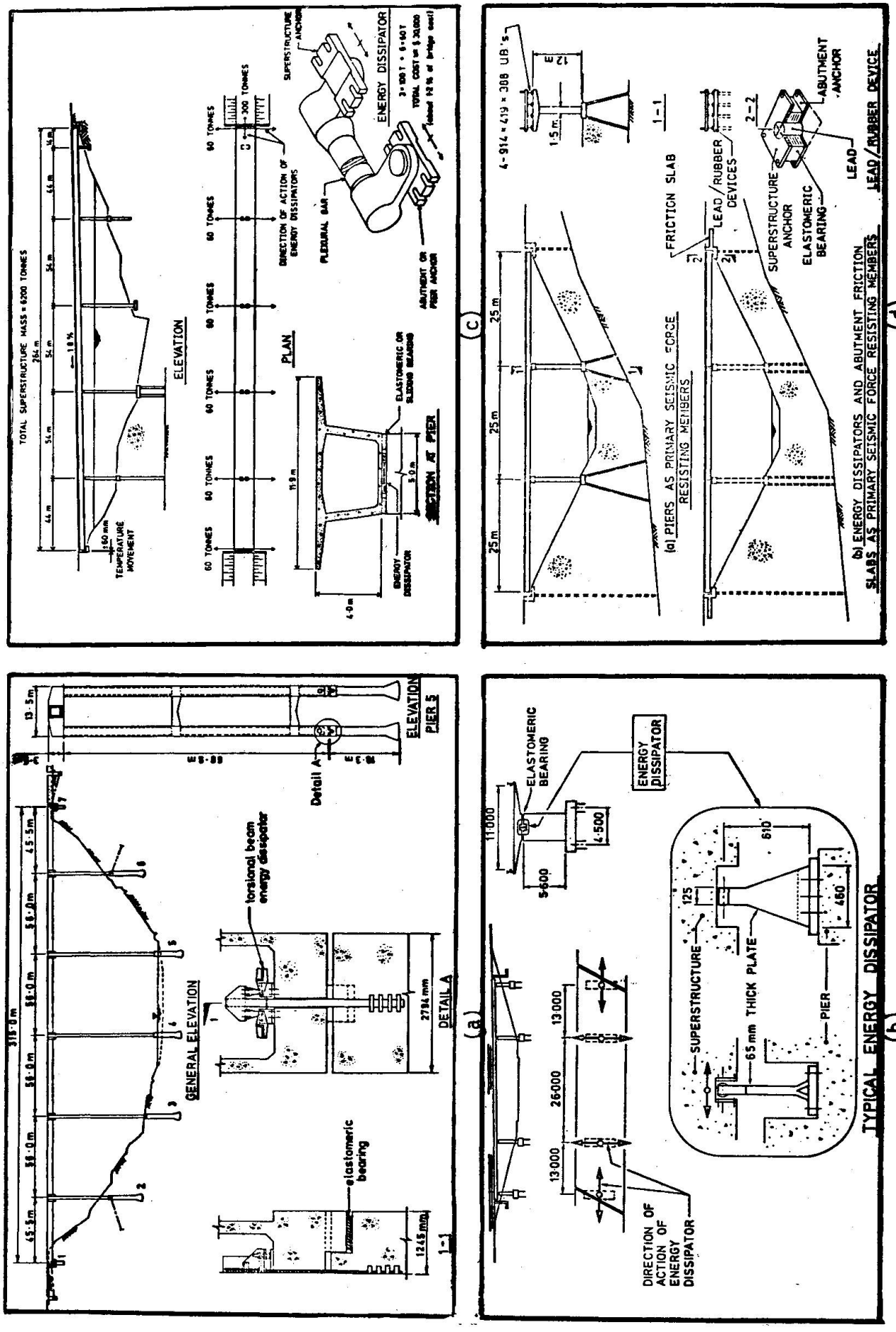

FIG 7: Examples of Application of Mechanical Energy Dissipating Devices.

that under earthquake attack the piers will "step", that is rock transversely to the bridge axis with each leg alternately lifting from the foundations. The lateral displacements are limited to acceptable values by energy dissipation in devices of the 'torsional beam' type at the base of the piers. The cost of the structure with the "stepping" details is comparable to that without, but the benefits lie in protecting the structure from earthquake induced damage and in limiting the axial forces induced in the piers.

(b) A three-span twin overpass with a prestressed concrete hollow cell superstructure and reinforced concrete piers and abutments was designed with uniaxial action energy dissipating devices of the steel "flexural plate" type. Those at the tops of the piers act in the transverse direction of the superstructure and those at the abutment act longitudinally. Provision is made in the latter location for accommodation of lengthening and shortening effects, such as thermal and creep movements, before the devices become effective. The design forces chosen for the structure were similar to those for a conventional design; the benefit was that without any cost penalty the degree of protection against damage was dramatically increased.

(c) A conceptual design of this six-span prestressed concrete box girder bridge on tall reinforced concrete piers incorporated energy dissipating devices of the uniaxial "flexural beam" type. Longitudinal seismic forces are resisted by devices at one rock abutment. Lateral forces are resisted by devices at the tops of the piers. The advantage in this case is that it is economic to design the piers not to yield even under a severe earthquake, and therefore damage may be avoided below the waterline where it is difficult to inspect and repair.

(d) As a result of preliminary studies on this three-span steel universal beam and concrete deck bridge, the seismic design concept was changed from a conventional approach with ductile reinforced concrete piers to a system with energy dissipators and abutment friction slabs as primary seismic force resisting members. The devices adopted were of the "lead/rubber" type, which are simple in application being positioned in the same manner as a normal elastomeric bearing, omnidirectional in action and can creep to accommodate lengthening and shortening effects. The benefits were substantial construction economies for piers and foundations and a large reduction in superstructure movements to be allowed for at the abutments.

3.3 Dynamic Response Analysis Results

Results of extensive numerical integration time-history dynamic analyses in the bridge shown in Fig 7(b) are described more fully elsewhere [8,13]. Fig 8 plots the relationship between maximum force imposed on the substructure of this bridge and period of vibration of the structure. Allowance was made for flexibility of the foundations and a vibrating mass of soil. Damping ratios of 4% and 5% equivalent viscous damping were assumed for modes 1 and 2 respectively. The yield level of the combination of dissipators acting in each principal direction was chosen as 0.05 times the weight of the superstructure. The properties of the elastomeric bearings were chosen after sensitivity analyses. The bearings require sufficient shear stiffness to provide an adequate centring force, but should not be so stiff as to impose excessive forces on the substructure at design earthquake displacements. The structure incorporating energy dissipating devices is compared in Fig 8 with an elastic single mass resonator with 5% equivalent viscous damping responding to three earthquakes, namely El Centro 1940 N-S and the artificial earthquakes B1 and A1. The curves show the dramatic reduction that may be achieved in response forces by the incorporation of energy dissipating devices, particularly for stiff structures. This is accomplished without requiring the structural members to sustain inelastic deformations and damage.

Some results of the time-history of displacement response of the structure shown

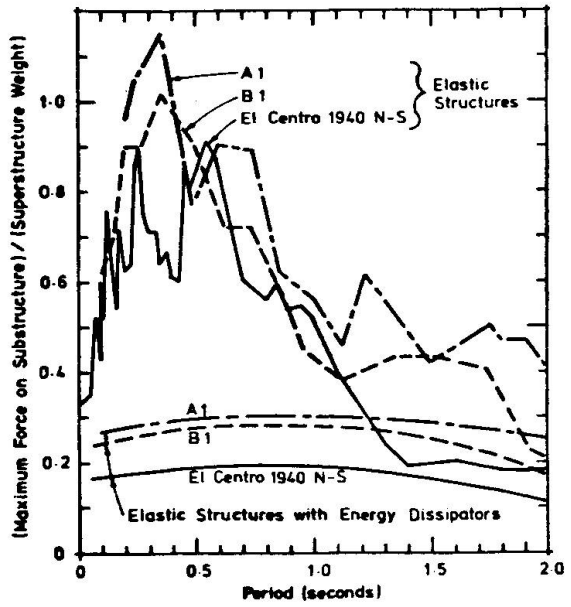

FIG 8: Bridge Substructure Forces for Elastic Structures with and without Dissipators

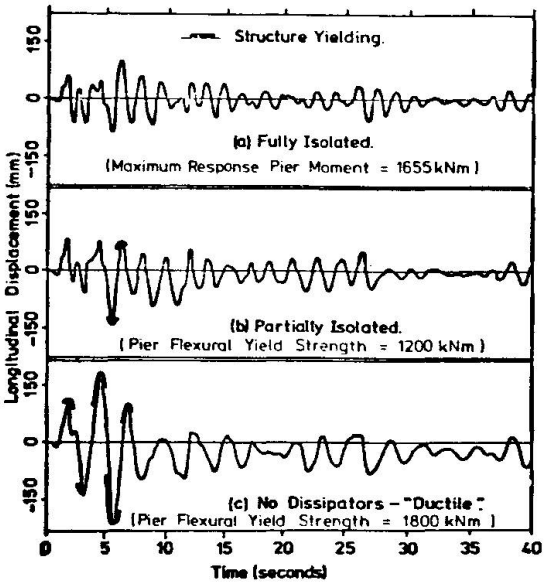

FIG 9: Longitudinal Response of Bridge for Three Structural Alternatives (El Centro 1940 N-S)

in Fig 7(b) to the El Centro 1940 N-S earthquake are shown in Fig 9. Cases (a) and (b) incorporate energy dissipating devices of equivalent characteristics. However, in case (a) the piers have been reinforced so that they would not flexurally yield during an earthquake of this intensity, whereas in case (b) the strength of the piers has been reduced to achieve construction economies. Case (c) corresponds to the conventional ductile design approach without energy dissipators. The intervals of the response during which the piers were yielding is shown. Comparison of (a), (b) and (c) shows that incorporation of energy dissipating devices has the potential for reduction of response displacements, reduction or elimination of damage at the "design" earthquake intensity and construction economies through reduced design forces on structure and foundations.

3.4 Design Philosophy

3.4.1 Advantages

The use of mechanical energy dissipating devices offers a number of advantages for the design of earthquake resisting bridges and other structures such as buildings, nuclear power plants and offshore gravity platforms.

(a) *Conceptual Simplicity:* Earthquake energy dissipation is concentrated in specially developed components which may be readily replaced if necessary. By effectively increasing the structural damping, a desirable seismic response may be achieved.

(b) *Design Simplicity:* The potential for development of standardised solutions for design of bridges incorporating these devices is an advantage relative to the substantial design effort required in the conventional ductile design method.

(c) *Structural Optimisation:* The designer is free to adjust the principal variables, being yield level of the dissipators, yield level of the structural members and intensity of design earthquake, to achieve an optimum solution in terms of construction costs and an acceptable frequency of earthquake induced damage.

(d) *Use of Non-Ductile Forms or Components:* There is new scope for economic or aesthetic advantage through use of non-ductile structural forms or components

with sufficient strength to remain elastic under the expected forces imposed by yielding of the dissipators.

(e) *Superior Performance:* Response displacements may be reduced and structural damage minimised or eliminated at the "design" earthquake intensity.

3.4.2 Philosophy

The following is a suggested philosophy based on varying levels of earthquake attack:

(a) *Moderate Earthquake:* For a moderate earthquake, such as may be expected 2 or 3 times during the life of a structure, energy dissipation should be confined to the devices and there should be no damage to structural members.

(b) *"Design" Earthquake:* For a "design" earthquake, for example one with a return period one or two times the anticipated life of the structure, the designer may adjust the strength levels in the structural members to achieve an optimum solution between construction economies and anticipated frequency of earthquake induced damage, with regard to the client's wishes. However, the degree of protection against yielding of the structural members should be at least as great as that implied in relevant codes relating to the conventional seismic design approach without dissipators.

(c) *Extreme Earthquake:* For an extreme earthquake there should be a suitable hierarchy of failure of the structural and foundation members that will preclude a brittle collapse. This may be achieved by appropriate margins of strength between non-ductile and ductile members and with attention to detail.

Although the above philosophy encompasses three earthquake levels, the design practice need only be based on the "design" earthquake. In the course of that design, the implications of yield levels on response to the "moderate" earthquake would have to be considered, as would also the implications of strength margins and detailing for an "extreme" earthquake.

4. CONCLUSION

There have been recent developments in New Zealand regarding the seismic design of bridges both for the conventional approach, based on ductile flexural yielding of the piers, and an alternative approach using mechanical energy dissipating devices. For the conventional approach, research has given useful information on the ductility demand on reinforced concrete piers, and their ductility capability. Also, a design office procedure has been developed for ready assessment of the ductility capability of a bridge structure. The development of practical, low cost, low maintenance mechanical energy dissipating devices has fostered the alternative approach of isolating the structure from the worst effects of ground shaking. This approach has potential for construction cost savings and a greater degree of protection against damage to structural members, with particular benefits for structures in the more seismically active areas.

5. ACKNOWLEDGEMENTS

The permission of the Commissioner of Works to publish this paper is acknowledged. Grateful acknowledgement is made to members of the Civil Design Office for their assistance.

6. REFERENCES

1. **PRIESTLEY, M.J.N,, R.PARK, B.E.DAVEY and I.R.M.MUNRO:** "Ductility of Reinforced Concrete Bridge Piers", *Proc. 6th World Conference on Earthquake Eng., New Delhi, January, 1977.*

2. _____ "Building Code Requirements for Reinforced Concrete (ACI 318-71)", *American Concrete Institute, Detroit, 1971.*

3. _____ "Highway Bridge Design Brief", *Ministry of Works and Development, Wellington, New Zealand, July 1973.*

4. _____ "Ductility of Bridges with Reinforced Concrete Piers", *Ministry of Works and Development, Civil Division Publication CDP 810/A, Wellington, New Zealand, April 1975, 109 pp.*

5. **SHARPE, R.D:** "The Seismic Response of an Elastic Bridge Structure Taking the Site into Consideration", *Seminar on Bridge Design and Research, TC4 Committee, Road Research Unit of the National Roads Board, Wellington, New Zealand, October 1974.*

6. **SHARPE, R.D:** "The Seismic Response of Inelastic Structures", *Ph.D. Thesis, University of Canterbury, November 1974.*

7. **CAMERON, A.J:** "The Response of Reinforced Concrete Bridge Piers to Seismic Motions", *M.E. Thesis, University of Canterbury, February 1975.*

8. **BLAKELEY, R.W.G. and C.R. STUART:** "Analysis and Design of a Bridge Incorporating Mechanical Energy Dissipating Devices for Earthquake Resistance", *Private Publication, Civil Division, Ministry of Works and Development, Wellington, New Zealand.*

9. **CHAPMAN, H.E:** "Earthquake Resistant Design of Bridges with Ductile Reinforced Concrete Piers". *Submitted for presentation at the 8th Congress of Fédération Internationale de la Précontrainte, London, May 1978.*

10. **PARK, R and T.PAULAY:** "Reinforced Concrete Structures", *John Wiley and Sons, New York, 1975, pp 28,594.*

11. **SKINNER, R.I., J.M.KELLY and A.J.HEINE:** "Hysteretic Dampers for Earthquake-Resistant Structures", *Int. Journal of Earthquake Engineering and Structural Dynamics, Vol. 3, 1975, pp 287-296.*

12. **ROBINSON, W.H. and A.G.TUCKER:** "A Lead-Rubber Shear Damper", *Bull. of N.Z. Nat. Soc. for Earthquake Engineering, Vol. 10, No 3, Sept 1977, pp 151-153.*

13. **BLAKELEY, R.W.G:** "Prestressed Concrete Bridges Incorporating Mechanical Energy Dissipating Devices for Earthquake Resistance", *Technical Contribution to 8th Congress Fédération Internationale de la Précontrainte, London, May, 1978.*

Leere Seite
Blank page
Page vide

ASEISMIC DESIGN OF MULTI-STORY SPACE FRAMES

T. M. S. Raghavan

Graduate Student, Department of Civil Engineering
Indian Institute of Technology, Kanpur, India

and

N. C. Nigam

Professor in Aeronautical Engineering
Indian Institute of Technology, Kanpur, India

SUMMARY

The inelastic behavior of a six-story space frame is investigated under the simultaneous action of the two horizontal components of El-Centro-1940 earthquake. The response is compared with elastic and inelastic behavior of constituent plane frames subjected to individual components. The results indicate that inelastic interaction has a significant effect on the response.

1. INTRODUCTION

The inelastic behavior of structures under dynamic loads has received considerable attention during the last two decades. In the design of structures subjected to occasional loads, such as the dynamic loads due to strong motion earthquakes and blasts, it is now generally accepted that the excursion of structural material into inelastic range must be permitted to achieve economical and safe design. This realization has led to extensive research in the inelastic behavior of structures for such loads. Early investigations in this area were based on the considerations of energy input, the elastic energy capacity and the energy dissipated through inelastic deformations, without obtaining a detailed response of the structure [1,2,3]. The availability of high speed digital computers, permitting step-by-step integration of large systems, stimulated detailed studies by several investigators [4,5,6,7,8,9,10]. In these and other similar investigations, the inelastic response of framed structures is obtained under the following simplifying assumptions:

(i) A three-dimensional framed structure is treated as an assemblage of plane frames along each of its principal directions.

(ii) The yield behavior at a section is assumed to depend only on flexure, neglecting the effect of axial and shear forces.

(iii) The response is obtained on the basis of a preassumed moment-rotation (or curvature) relationship of either general yielding [9,10], bilinear [7,8] or elastic-perfectly-plastic type [4].

Since the behavior of a structure during inelastic excursions is nonlinear, the principle of superposition is not applicable, and a response analysis treating a space frame as an assemblage of plane frames subjected to in-plane ground motion is not valid. It is necessary to model a framed structure as a space frame subjected to simultaneous action of ground motion components. A general theory, incorporating the effects of inelastic interactions on the dynamic response of space frames, was developed and applied to a simple space frame in 1967 [11,12]. Since then, several investigators have studied inelastic response of space frames, including the effects of work-hardening [13,14,15,16,17]. The work has also been extended to R/C frames [18].

In this paper, the behavior of a six-story building frame is investigated under the simultaneous action of two horizontal components of El. Centro, 1940 earthquake. The response is compared with the elastic and inelastic behavior of constituent plane frames subjected to individual components investigated by PENZIEN [4]. The results indicate that inelastic interaction has a significant effect on the response.

2. THEORY OF INELASTIC INTERACTION

A framed structure consists of an assemblage of discrete one-dimensional elements interconnected at their ends. Consider a

section of such an element and assume that:

(i) Stress-strain relation is elastic-perfectly-plastic.

(ii) The yield behavior at the section is described by an yield surface [11]:

$$\Phi(\bar{Q}) = 1$$

such that
the section is elastic if $\Phi(\bar{Q}) < 1$ (1)

or if $\Phi(\bar{Q}) = 1$ and $\dot{W}^p < 0$ (2)

the section is yielding if $\Phi(\bar{Q}) = 1$ and $\dot{W}^p \geq 0$ (3)

where $\bar{Q}$ is the generalised force vector at the section, $\bar{q}$ is the generalised displacement vector at the section, and

$$\dot{W}^p = \langle \bar{Q}, \dot{\bar{q}}^p \rangle \quad (4)$$

representing the rate of plastic work.

Under above assumptions it can be shown that at a regular point on the yield surface [11]

$$\bar{Q} = [K](\bar{q} - \bar{q}_o) \quad (5)$$

if the section is elastic, and

$$\dot{\bar{Q}} = [K]\left(\dot{\bar{q}} - \frac{\langle K\dot{\bar{q}}, \frac{\partial \Phi}{\partial \bar{Q}} \rangle}{\langle K \frac{\partial \Phi}{\partial \bar{Q}}, \frac{\partial \Phi}{\partial \bar{Q}} \rangle} \frac{\partial \Phi}{\partial \bar{Q}}\right) \quad (6)$$

if the section is yielding.

$\bar{q}_o$ denotes the current position of equilibrium and K is the stiffness matrix.

The force-displacement relations for elastic and yielding behaviors of a one dimensional element can be derived on the basis of equations (5) and (6) [12]. If the effects of inelastic interaction are neglected, Equation (6) reduces to

$$\dot{Q}_i = 0 \quad \text{if} \quad |Q_i| = Q_{yi} \text{ and } \dot{W}_i^p \geq 0 \quad (7)$$

where Q_{yi} is the yield level of Q_i.

3. SIX-STORY SPACE FRAME

Consider a six-story space frame shown in Figure 1. The frame is identical in directions 1-1 and 2-2. The floors are assumed to rigid and remain parallel during lateral deformation. The elastic stiffness is such that the fundamental mode of vibration of the plane frames is triangular in shape. The damping is assumed to be viscous and proportional to story stiffness. The entire mass of the structure is concentrated equally at each floor level and the story heights are equal. The yield strength of each plane-frame is specified by a parameter, θ, defined as the ratio of the

yield value of the base shear to the total weight of the structure based on idealised elastoplastic behavior shown in Figure 2(b). The yield value of the story shear, $(Q_i)y$, is assumed to be proportional to story stiffness k_i. Table 1 gives the stiffness, damping and yield strength characteristics of the frame.

Under the simplifying assumptions stated above, yielding in a story occurs at the top and bottom sections of the columns simultaneously. The forces acting at these sections are the axial force and bending moments and shear forces in directions 1-1 and 2-2. The yield behavior is governed by the interaction between these forces. If the effect of the axial force and shear forces is neglected, the yield behavior at a section is governed by the interaction between M_{i1} and M_{i2}, the bending moments in the directions 1-1 and 2-2. Since the story shear

$$Q_{ij} = \frac{8M_{ij}}{h_i} \qquad \begin{matrix} i = 1,2,\ldots 6 \\ j = 1,2 \end{matrix} \qquad (8)$$

the yield behavior of a story is identical to the yield behavior at the end sections and may be expressed in terms of the story shears Q_{i1} and Q_{i2}. Figure 2(a) shows the yield surface in the two dimensional force space. If the effects of interaction are neglected, the yield behavior reduces to idealised elasto-plastic behavior as shown in Figure 2(b).

3.1 Equations of Motion

The equations of motion of the space frame due to base excitation during an earthquake can be written in terms of story shear, Q_{ij}, and lateral displacement, u_{ij}, using Equations (5), (6) and (7). For the ith mass the equations of motion are:

$$m_i \ddot{u}_{1i} + c_i (\dot{u}_{1i} - \dot{u}_{1i-1}) - c_{i+1} (\dot{u}_{1i+1} - \dot{u}_{1i}) + (Q_{1i} - Q_{1i+1}) = m_i \ddot{Z}_1(t)$$

$$m_i \ddot{u}_{2i} + c_i (\dot{u}_{2i} - \dot{u}_{2i-1}) - c_{i+1} (\dot{u}_{2i+1} - \dot{u}_{2i}) + (Q_{2i} - Q_{2i+1}) = m_i \ddot{Z}_2(t) \qquad (9)$$

where subscripts 1 and 2 denote directions 1-1 and 2-2 and i denotes the story as shown in Figure 1. Further

m_i - ith mass;

c_i - inter floor viscous damping coefficient in the ith story;

u_{1i}, u_{2i} - the lateral displacements of mass m_i relative to the base;

Q_{1i}, Q_{2i} - story shears in the ith story;

$\ddot{Z}_1, \ddot{Z}_2$ - horizontal components of the ground acceleration during an earthquake.

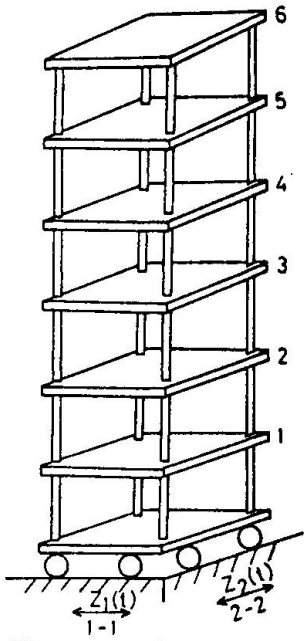

Fig.1 Space Frame

Story	$\frac{K_i}{K_1}$	$\frac{C_i}{C_1}$	$\frac{(Q_i)_y}{(Q_1)_y}$
6	6/21	6/21	6/21
5	11/21	11/21	11/21
4	15/21	15/21	15/21
3	18/21	18/21	18/21
2	20/21	20/21	20/21
1	1	1	1

$M = \sum_{i=1}^{6} mi$

$K_1 = \frac{14\pi^2 M}{T^2}$

$C_1 = \frac{14\pi M \zeta}{T}$

$(Q_1)_y = \theta Mg$

Table.1 Structural Properties of Space Frame

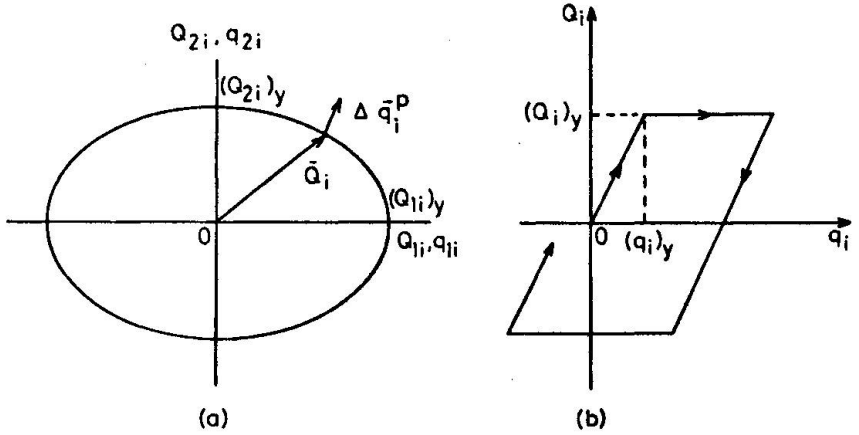

Fig.2 Yield Surface for i th Story (a) With Interaction (b) Without Interaction

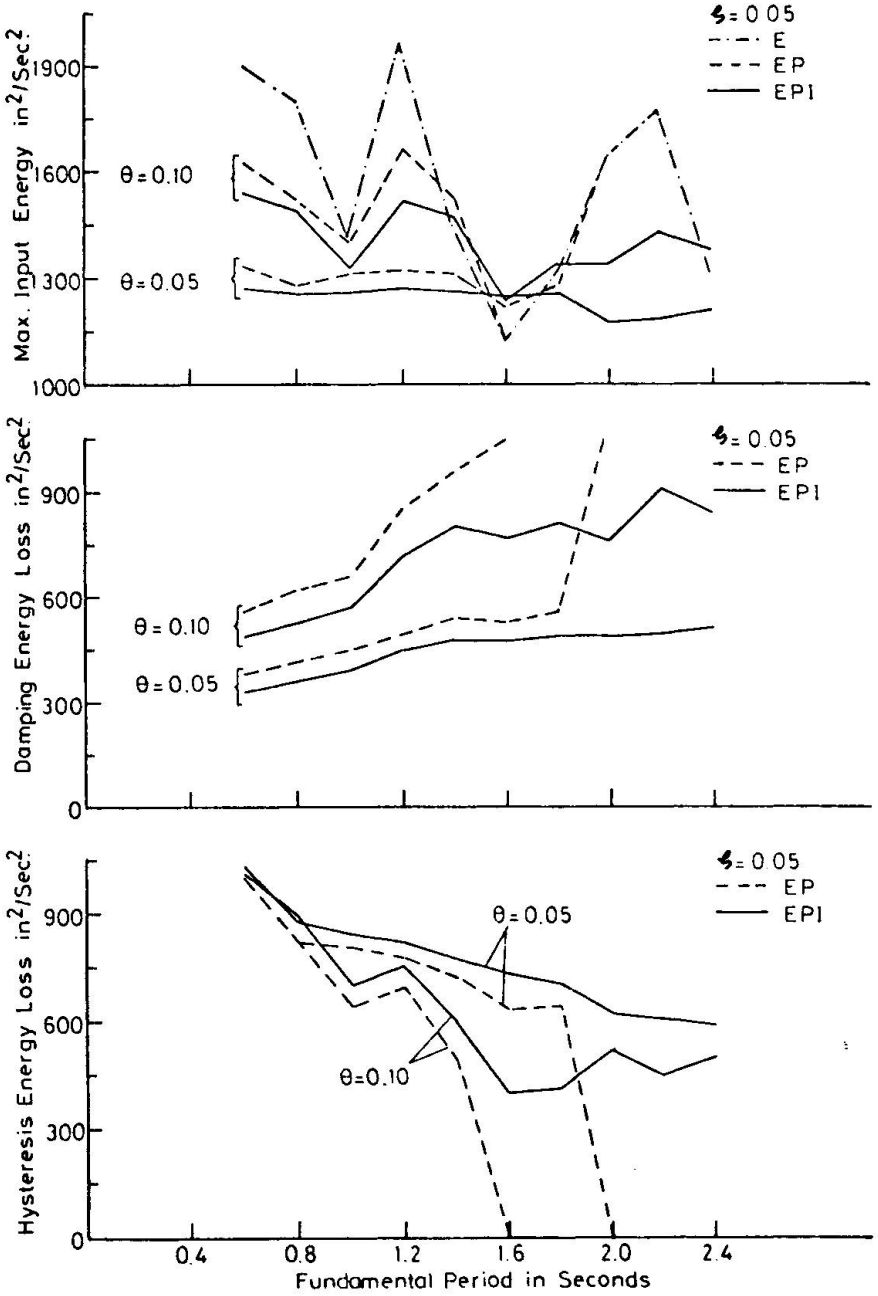

Fig.3 Energy Input and Dissipation.

The relationship between story shears and story displacements depends upon whether the story is elastic or yielding. Further during yielding it depends upon whether the effects of inelastic interaction are included or ignored. For each of these three cases, the story shear-displacement relations can be derived using Equations (5), (6) and (7) as under:

Elastic Behavior (E)

$$\begin{aligned} Q_{1i} &= k_i\, q_{1i} \\ Q_{2i} &= k_i\, q_{2i} \end{aligned} \tag{10}$$

where

$$\begin{aligned} q_{1i} &= (u_{1i} - u_{1i-1}) \\ q_{2i} &= (u_{2i} - u_{2i-1}) \end{aligned}$$

Elasto-Plastic Behaviour Without Interaction (EP)

$$\begin{aligned} Q_{1i} &= k_i\,[q_{1i} - (q_{1i})_o] \quad \text{if } |Q_{1i}| < (Q_{1i})_y \\ &\qquad \text{or if } |Q_{1i}| = (Q_{1i})_y \text{ and } \dot{W}^p_{1i} < 0 \\ |Q_{1i}| &= (Q_{1i})_y \quad \text{if } \dot{W}^p_{1i} \geq 0 \\ Q_{2i} &= k_i\,[q_{2i} - (q_{2i})_o] \quad \text{if } |Q_{2i}| < (Q_{2i})_y \\ &\qquad \text{or if } |Q_{2i}| = (Q_{2i})_y \text{ and } \dot{W}^p_{2i} < 0 \\ |Q_{2i}| &= (Q_{2i})_y \quad \text{if } \dot{W}^p_{2i} \geq 0 \end{aligned} \tag{11}$$

Elasto-Plastic Behavior with Interaction (EPI)

$$\begin{aligned} Q_{1i} &= k_i\,[q_{1i} - (q_{1i})_o] \\ Q_{2i} &= k_i\,[q_{2i} - (q_{2i})_o] \end{aligned}$$

$$\text{if} \quad \phi\,(Q_{1i}, Q_{2i}) < 1, \quad \text{or if } \phi\,(Q_{1i}, Q_{2i}) = 1 \quad \text{and} \quad \dot{W}^p_i < 0 \tag{12}$$

and

$$\dot{Q}_{1i} = \frac{k_i\left[\left(\frac{\partial \phi}{\partial Q_{2i}}\right)^2 \dot{q}_{1i} - \frac{\partial \phi}{\partial Q_{1i}} \frac{\partial \phi}{\partial Q_{2i}} \dot{q}_{2i}\right]}{\left[\left(\frac{\partial \phi}{\partial Q_{1i}}\right)^2 + \left(\frac{\partial \phi}{\partial Q_{2i}}\right)^2\right]}$$

$$\dot{Q}_{2i} = \frac{k_i\left[-\frac{\partial \phi}{\partial Q_{1i}} \frac{\partial \phi}{\partial Q_{2i}} \dot{q}_{1i} + \left(\frac{\partial \phi}{\partial Q_{1i}}\right)^2 \dot{q}_{2i}\right]}{\left[\left(\frac{\partial \phi}{\partial Q_{1i}}\right)^2 + \left(\frac{\partial \phi}{\partial Q_{2i}}\right)^2\right]}$$

$$\text{if} \quad \Phi(Q_{1i}, Q_{2i}) = 1 \quad \text{and} \quad \dot{W}_i^p \geq 0 \qquad (13)$$

It may be noted that for elastic (E) and elasto-plastic behavior (EP), the equations of motion are uncoupled in the directions 1-1 and 2-2 and can be integrated independently. For elasto-plastic behavior with interaction (EPI), the equations of motion are coupled.

3.2 Response Computation

The equations of motion of the space frame for elastic, elasto-plastic and elasto-plastic behavior with interaction are integrated using the fourth order Runge-Kutta method of step-by-step integration. First 30 seconds of the E-W and N-S components of El-Centro-1940 earthquake record are used as ground acceleration $\ddot{Z}_1$ and $\ddot{Z}_2$ respectively. The interval of integration $\Delta t = T/50$, where T is the fundamental natural period of the frame. The response is computed for yield strength parameter $\theta = 0.05, 0.1, 0.2$; damping ratio $\zeta = 0.05$ and fundamental period T varying from 0.6 to 2.4 secs. For elasto-plastic behavior with interaction, the yield surface is expressed by

$$\left[\frac{Q_{1i}}{(Q_i)_y}\right]^2 + \left[\frac{Q_{2i}}{(Q_i)_y}\right]^2 = 1 \qquad (14)$$

The response parameters computed are the energy input and energy dissipated due to damping and hysteresis during yielding; absolute displacements and ductility ratios; permanent set and number of inelastic excursions and plastic energy ratio for each story.

4. RESULTS AND DISCUSSION

Figure 3 shows the maximum energy input per unit mass to the space frame during the earthquake and the energy loss due to damping and hysteresis during yielding for elastic, and elasto-plastic behavior with and without interaction. The curves show that, in general, inelastic deformations reduce the energy input and interaction reduces it further, the reduction depending significantly on the yield strength parameter θ. The inelastic deformations reduce the energy dissipation due to damping and interaction reduces it further. This fact is significant in modern high-rise buildings with low damping as it implies less dependence on damping to limit the response. It is further seen that if the interaction is ignored, elasto-plastic analysis would indicate that the space frame remains elastic for ($T > 1.6$, $\theta = 0.1$) and ($T > 2.0$; $\theta = 0.05$), whereas, the frame will actually yield due to interaction.

Figure 4 shows the absolute displacements of the space frame in the two directions for the fundamental periods $T = 0.6$ and 1.2. It is seen from the curves that for $T = 0.6$, interaction causes a large increase in displacement over elastic and elasto-plastic behavior in both directions. For $T = 1.2$, there is a large increase in the direction 1-1 due to interaction, but the dis-

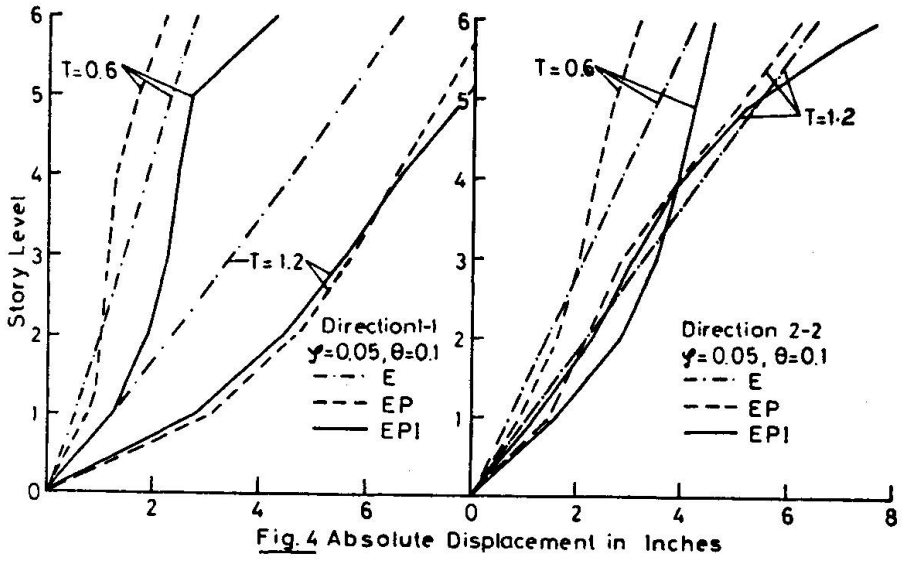

Fig. 4 Absolute Displacement in Inches

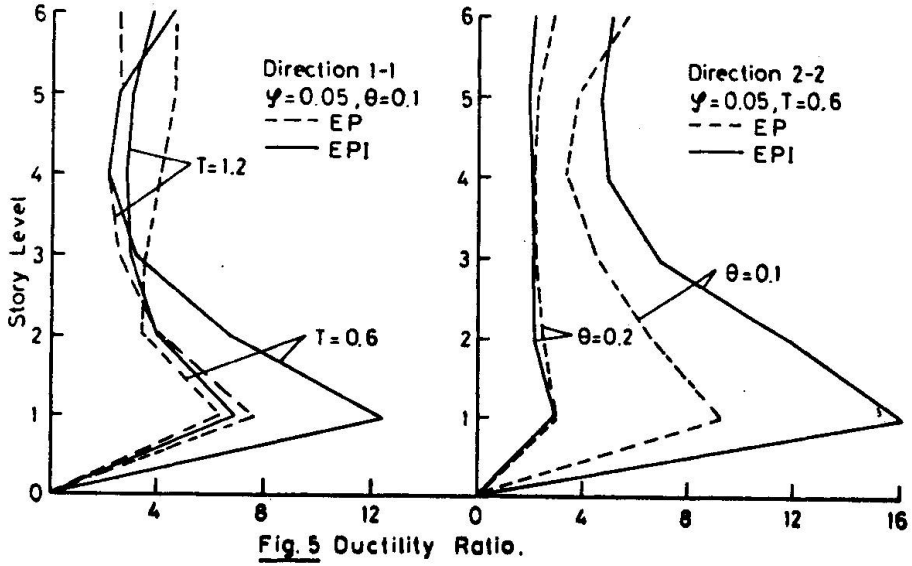

Fig. 5 Ductility Ratio.

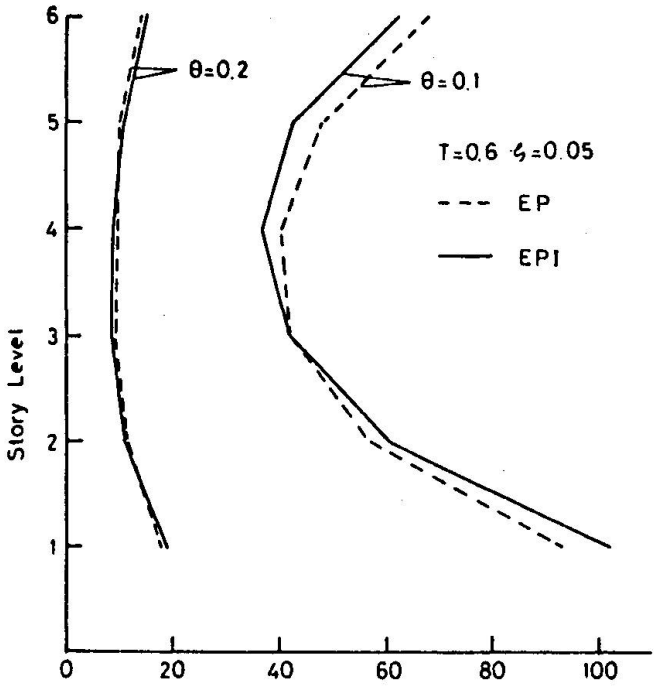

Fig. 6 Story Plastic Energy Ratio

Story	Permanent Set (ins)		No. of inelastic excursion	
	E - P 1 - 1	E P I	E P 1-1	E P I
1	0.036	0.656	30	55
2	0.03	0.280	29	50
3	0.0033	0.0403	27	48
4	-0.0426	-0.0198	29	47
5	0.00248	-0.112	34	50
6	0.099	-0.329	39	59

Table 2: Permanent Set and Number of Inelastic Excursions. θ = 0.1, T = 0.6.

placements are nearly same in the direction 2-2. Large interfloor displacements occur in the top and bottom storys due to inelastic behavior and interaction causes further increase suggesting the need to strengthen these storys. If the interaction effects are ignored, as in conventional plane frame elasto-plastic analysis, displacements may be grossly under estimated.

Figure 5 shows the ductility ratio in each story for T = 0.6, 1.2 and θ = 0.1 in direction 1-1 and T = 0.6 and θ = 0.1 and 0.2 in direction 2-2. It is seen that for T = 0.6 and θ = 0.1, the ductility requirement is large in the top and bottom storys. For T = 0.6 and θ = 0.2, the ductility requirement is significantly reduced and interaction effects are insignificant. Comparison of curves for θ = 0.1 and 0.2 also indicates, what may happen to a structure designed for θ = 0.1, if it is subjected to an earthquake of twice the intensity of the design earthquake. For T=1.2 sec and θ = 0.1, the ductility requirement is low and interaction effects are significant only in the top story. On the basis of idealised elasto-plastic analysis of plane frames, PENZIEN [4] recommended optimum values of θ = 0.3, 0.2 and 0.1 for T = 0.3, 0.6, 0.9 and more, respectively. Due to large computer time required, it has not been possible to study the response for several values of θ. However, on the basis of limited results and the fact that the general nature of response for elasto-plastic behavior, with and without interaction, is same, it appears that the above recommendations shall also apply to space frames. The large ductility requirements in top and bottom storys suggest strengthening of these storys to remain within acceptable limits for safe aseismic design.

Plastic energy ratio has been suggested as a criterion for inelastic design [11,12]. Figure 5 shows the plastic energy ratio in each story for T = 0.6 and θ = 0.1 and 0.2. It is seen that unlike ductility ratio the effect of interaction on plastic energy ratio is small. Increase in θ from 0.1 to 0.2 decreases the ductility requirement significantly and makes it nearly uniform over the entire frame.

Table 2 gives the number of excursions in the inelastic range and the permanent set at the end of the earthquake in the direction 1-1. The behavior in direction 2-2 is similar. It is seen that elasto-plastic analysis without interaction grossly under estimates the number of excursions. This result is important because strength degradation during repeated yielding increases with the number of excursions in the inelastic range. The interaction significantly increases the permanent set in the top and bottom storys, which may determine the serviceability of the structure after an earthquake.

The inelastic behavior of the space frame has been analysed in terms of parameters governing inelastic design, such as, energy input and energy dissipated, lateral displacement, ductility ratio, plastic energy ratio, number of excursions into the inelastic range and permanent set. The overall behavior is consistent with the general findings of the earlier investigations based on simple space frames [11,13]. The results clearly show that the conventional elasto-plastic analysis, treating a space frame as an assemblage of plane frames, may significantly underestimate the ductility requirements in the low period range for

small values of yield strength. The inelastic behavior is sensitive to the yield strength parameter, θ, which must be chosen carefully. Several codes specify stiffness distribution to give a triangular first mode. The results indicate the need to strengthen the top and bottom storys of such frames. The investigation did not take into account the P-Δ effect and the effect of work-hardening which may alter some of the conclusions.

REFERENCES

1. HOUSNER, G.W.: Limit Design of Structures. Proceedings of the First World Conference on Earthquake Engineering, San Francisco, June 1956, pp.5:1-5:11.

2. HOUSNER, G.W.: Behavior of Structures During Earthquakes. Proceedings ASCE, Vol. 85, Oct. 1959, pp. 109-129.

3. BLUME, J.A.: A Reserve Energy Technique for Earthquake Design and Rating of Structures in the Inelastic Range. Proceedings of the Second World Conference on Earthquake Engineering, Vol. II, Tokyo and Kyoto, Japan, 1960, pp.1061-1084.

4. PENZIEN, J.: Elasto-Plastic Response of Idealised Multi-Story Structures Subjected to a Strong Motion Earthquake. ibid, pp.739-760.

5. HOUSNER, G.W.: The Plastic Failure of Frames During Earthquakes. ibid, pp. 997-1012.

6. CLOUGH, R.W., et al: Inelastic Earthquake Response of Tall Buildings. Proceedings of the Third World Conference on Earthquake Engineering, Vol. II, Auckland and Wellinton, New Zealand, Jan. 1965, pp.68-89.

7. SAUL, W.E. et al: Dynamic Analysis of Bilinear Inelastic Multiple Story Shear Buildings. ibid, pp.533-551.

8. GIBERSON, M.F.: The Response of Nonlinear Multi-Story Structures Subjected to Earthquake Excitation. Ph.D. Thesis, California Institute of Technology, 1967.

9. JENNINGS, D.C.: Response of Simple Yielding Structures to Earthquake Excitation. Ph.D. Thesis, California Institute of Technology, 1963.

10. GOEL, S.C.: Inelastic Behavior of Multi-Story Building Frames Subjected to Earthquake Motion. Ph.D. Thesis, The University of Michigan, 1967.

11. NIGAM, N.C.: Inelastic Interactions in the Dynamic Response of Structures. Ph.D. Thesis, California Institute of Technology, 1967.

12. NIGAM, N.C.: Yielding in Framed Structures Under Dynamic Loads. J. Engg. Mech. Divn., ASCE, EM5, Oct. 1970, pp.687-709.

13. WEN, R.K. and FARHOOMAND, F.: Dynamic Analysis of Inelastic Space Frames. J. of Engg. Mech. Divn., ASCE, EM5, Oct. 1970, pp. 667-686.

14. NIGAM, N.C.: Aseismic Design of Structures in the Inelastic Range. Proceedings of the Fourth Symposium on Earthquake Engineering, University of Roorkee, India, Nov. 1970, pp. 262-265.

15. PORTER, F.L. and POWELL, G.H.: Static and Dynamic Analysis of Inelastic Frame Structures. Earthquake Engineering Research Centre, University of California, Berkeley, Report No. EERC 71-3, June, 1971.

16. KOBORI, T. et al: Earthquake Response of Frame Structures Composed of Inelastic Members. Proceedings of the Fifth World Conference on Earthquake Engineering, Vol. II, Rome, 1974, pp.1772-1781.

17. PADILLA-MORA, R. and SCHNOBRICH, W.C.: Non-linear Response of Framed Structures to Two-dimensional Earthquake Motion. Department of Civil Engineering, University of Illinois. Report No. YILU-ENG-74-2015, July 1974.

18. TAKIZAWA, H. and AOYAMA, H.: Biaxial Effects in Modelling Earthquake Response of R/C Structures. Earthquake Engineering and Structural Dynamics, Vol.4, No.6, Oct.-Dec. 1976, pp. 523-552.

Leere Seite
Blank page
Page vide

DYNAMIC RESPONSE OF BUILDING WITH ISOLATION ON RUBBER CUSHIONS

by

Jakim PETROVSKI, Professor and Director
Dimitar JURUKOVSKI, Associate Professor

Institute of Earthquake Engineering and Engineering Seismology, University of Skopje, Yugoslavia

Vladimir SIMOVSKI, Assistant Professor

Civil Engineering Faculty,
University of Skopje, Yugoslavia

SUMMARY

Dynamic response of the three-story reinforced concrete school building with foundation isolation constructed in Skopje is presented and discussed. The idea of foundation isolation has been achieved by applying rubber cushions between the strip foundation and the ground floor slab of the supper-structure.

Full-scale studies were carried out in order to determine dynamic properties of the building,and the response of the building with foundation isolation effect is analysed.

1. INTRODUCTION

Foundation isolation is one of the oldest attempts to isolate the structures from the influence of the ground earthquake motions. In the past few years new ideas in modern construction have been theoretically and experimentally investigated and developed by engineers and scientists (4,6), for practical application.

The results presented in this paper concern the dynamic response of three-story reinforced concrete school building, constructed in Skopje in 1969. The building was designed and developed by Swiss engineers (6). The main idea of foundation isolation has been achieved by applying rubber cushions between the strip foundation and the first floor slab of the supper-structure. The building is constructed as reinforced concrete walled structure in both orthogonal directions.

Ambient vibration tests were carried out in order to determine dynamic properties of the building. Simple cantilever beam model with interactive stiffness parameters has been used to model building-foundation system. Using experimental results the formulation of the mathematical model has been performed. A good correlation between the experimental and analytical results for both rezonance frequencies and the mode shapes have been obtained and typical results are presented.

2. DESCRIPTION OF THE BUILDING

The building of the classroom wing of the "H.Pestalozzi" school is designed and built as monolithic walled structure with base isolation applying rubber cushion elements over the strip foundation. The "H.Pestalozzi" school was designed by Swiss engineers (6) and built with the funds provided by the Swiss people and authorities in organization of the Swiss Group of the Inter-parliamentary Union, as a contribution in the gigantic programme of rehabilitation and reconstruction of Skopje after the catastrophic earthquake of July 26, 1963.

The supper structure of the classroom wing is monolithic three story reinforce concrete walled structure with thickness of the walls of 20-33 cm, and 20 cm depth of the monolithic reinforce concrete floor slabs. Typical floor plan and cross section of the wing are shown in Figs 1 and 2.

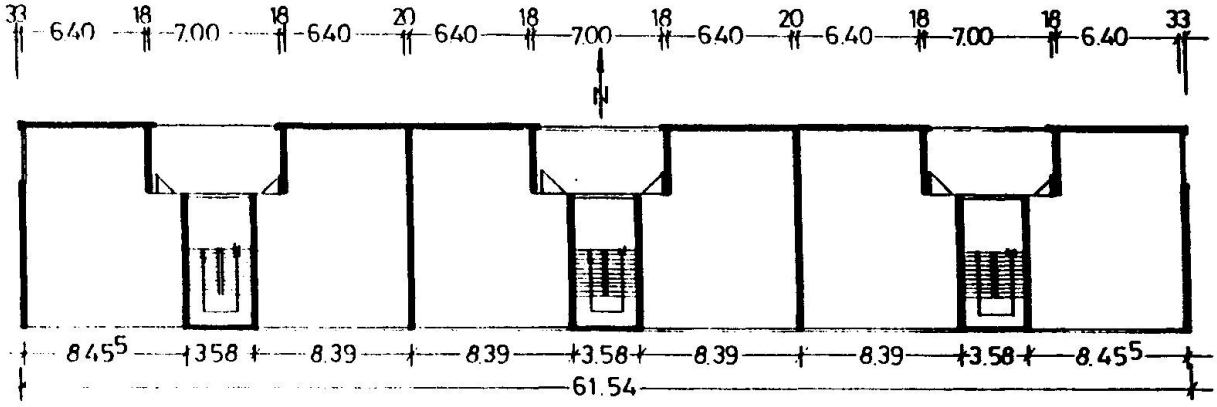

Fig. 1 Plan of a typical floor of the building

The strip reinforced concrete foundation is placed in a dence graved, and special housing for the rubber cushion elements was provided within strip foundations. The total number of the rubber cushion elements in which the supper structure of the building is placed is 54 (Fig. 3).

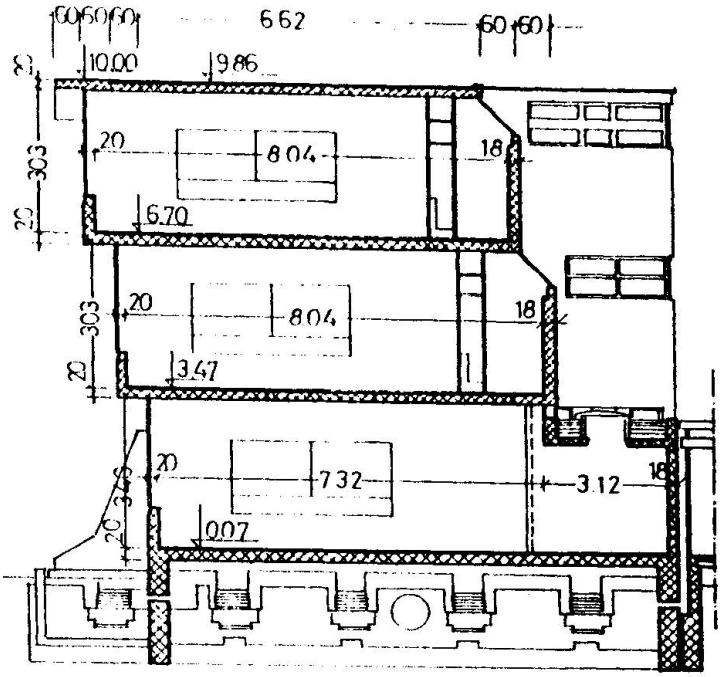

Fig. 2 Cross-section of the building

These elements are designed, developed and tested (6) in cooperation of the designers of the building, engineers of Swiss rubber factory and the E.M.P.A (Swiss Federal Research and Testing Laboratories for Buildings Materials). The dimensions of each rubber cushion are 70/70/35 cm. made of the vulcanized India rubber in order to achieve maximal isolation effect for the frequency range of 5 to 30 cps with high damping effects. Fig. 3 (a),(b),(c). The supper structure was built on a reinforce concrete gride and continuous slab at the ground floor. After completion of the supper structure rubber elements were inserted in their position and fixed. Then each of the rubber elements was put under prestabilized pressure lifting their bearing beam to the determined level. With two groups of hydraulic presses in the corresponding sequence the rubber elements were put under stress constituting them as bearing supports of the supper structure.

3. AMBIENT VIBRATION TESTS

The objective of performing the ambient vibration study was to obtain dynamic properties of the building and then to compare them with those obtained from the analyses of the mathematical model response. The ambient vibration method of testing full-scale structures is based on wind and microtremor-induced vibrations. It is a fast and relatively simple method of field measurements without interference in the normal building function. Although this method of dynamic testing of full-scale structures is based on small levels of exitation, compared to strong earthquake ground motion, the derived dynamic properties of the structural systems are invaluable since they offer a sound basis for rational improvements of the formulation of the mathematical models in the elastic range of behaviour of the structural systems (5,7). In this specific case of the classroom building of the school in Skopje, the response of the building is practically controlled by the rubber cushion elements, thus the application of this method is quite efficient.

The microtremor-induced vibrations were measured using Kinemetrics Ranger Seismometers, Model SS-1. Single Conditioner, Model SC-1 was used to amplify and control simultaneously four seismometer signals. The amplified analogue signals were recorded on a four-channel HP magnetic tape recorder and converted into a digital form using LPS (Lab periferial system) of the PDP 11/45 computer system.

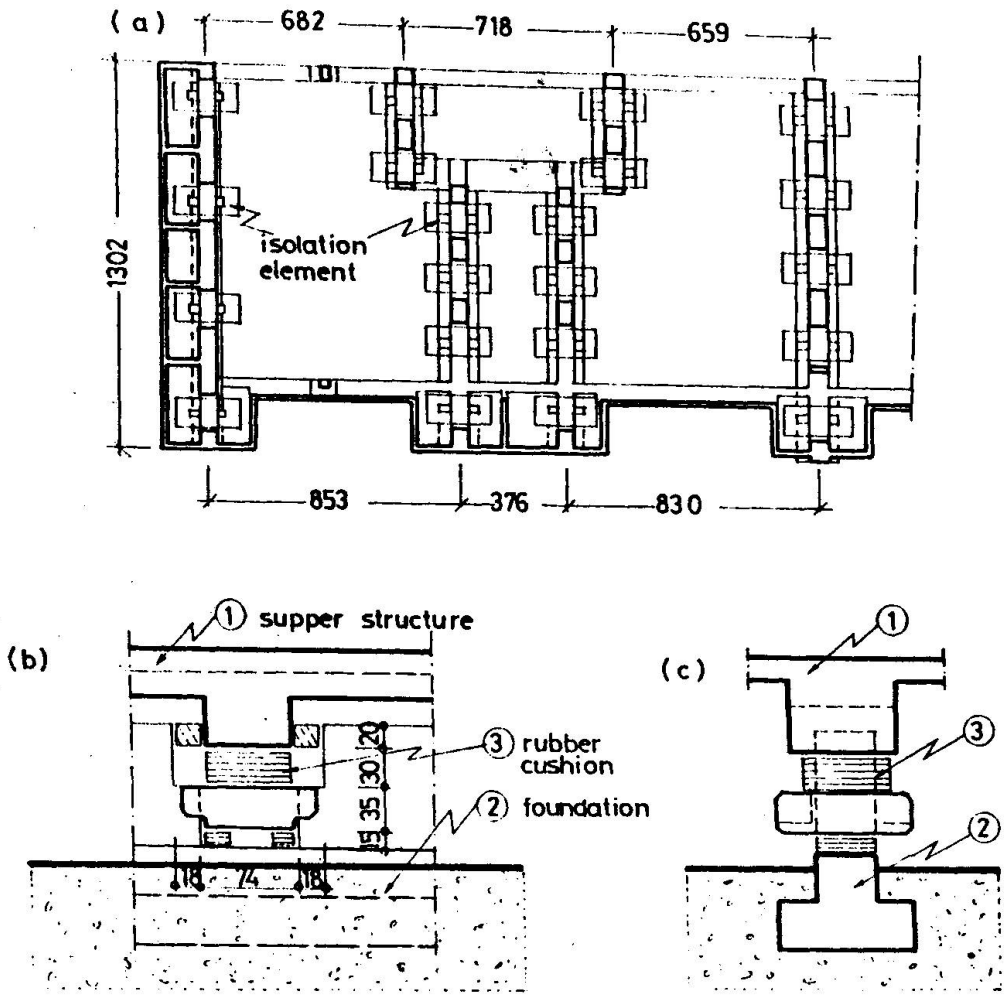

Fig. 3 (a) Partial foundation plan with position of rubber cushions

(b) Detail of rubber cushions position in the foundation structure

(c) Cross-section of the foundation with isolation elements

The effective rate of the recorded data from the horizontal vibrations was 60 sec. The signal before recording had passed through a low pass filter set at 40 Hz. Twenty seconds of data from each channel were used in the calculations of the Fourier amplitude spectra. The standard Fourier amplitude spectrum was smoothed by 1/4, 1/2, 1/4 weights.

In the experimental study of building vibration which is based on the linear model, it is assumed that the resulting motions can be expressed as the superposition of models associated with the discrete frequencies. This approach then requires a simultaneous measurement of motion in a given direction for at least two different floors to obtain their relative amplitude and phase, the two quantities required to determine mode shapes. For that reason the first field measurement was a calibration run at the ground floor. All four seismometers were placed at the centre of the ground floor identically oriented. To obtain translational mode frequencies two pairs of seismometers were located at the ground floor centre, oriented in south and west direction, respectively. For this location were carried out several tests. The smoothed Fourier amplitude spectrum for the ground floor is shown in Fig. 4.

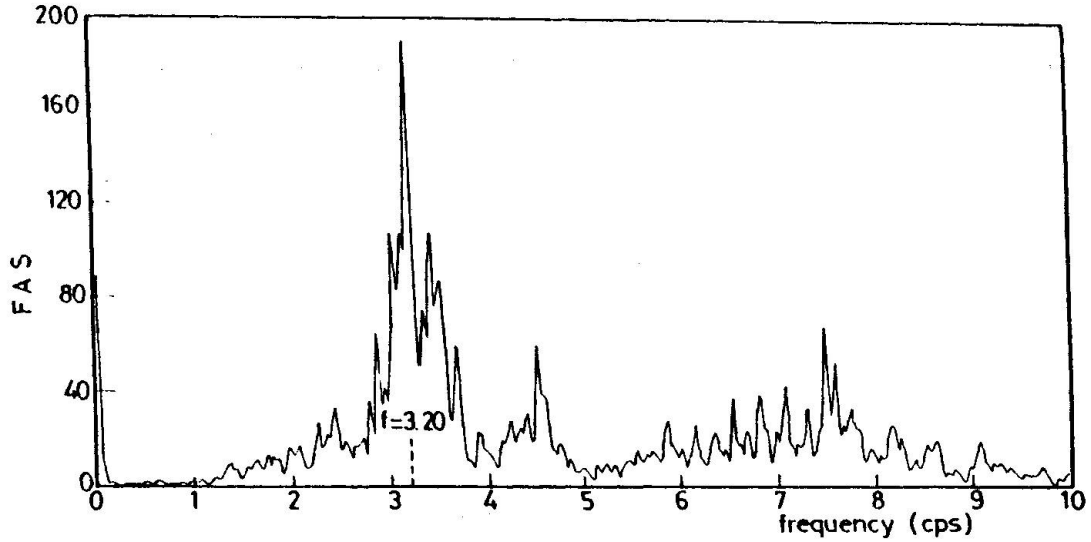

Fig. 4 Fourier amplitude spectra on the ground floor

Similar measurements were carried out at the foundation level of the building under the rubber cushions and the Fourier amplitude spectrum for this level is shown in Fig. 5.

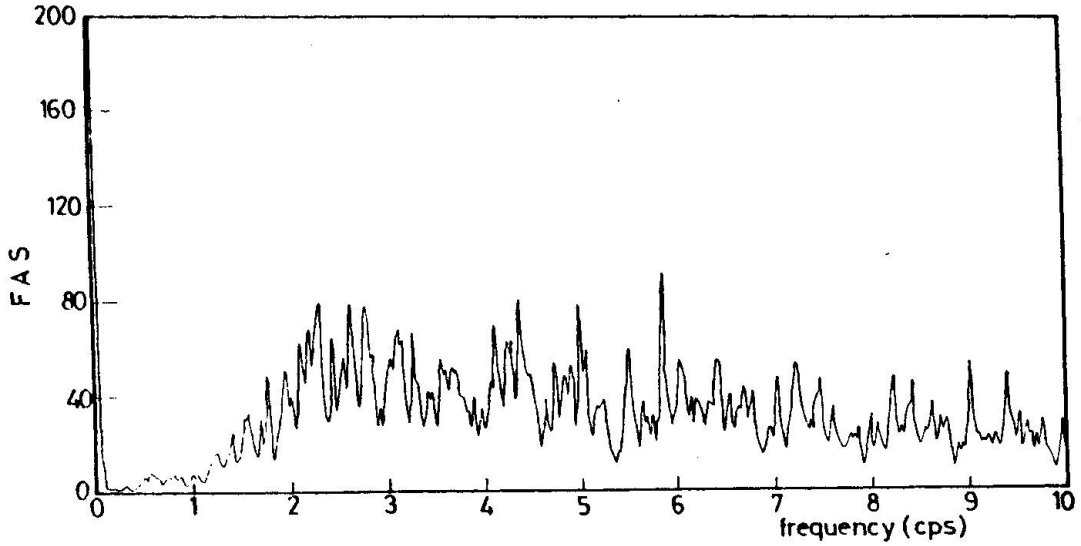

Fig. 5 Fourier amplitude spectra on the foundation under rubber cushion

For measurement of the translational mode shapes two seismometers were placed in the centre of the ground floor and oriented south and west, repsectively. The other two seismometers were relocated for each test in the centres of the first and second floor. The measured vertical mode shape is shown on Fig. 6

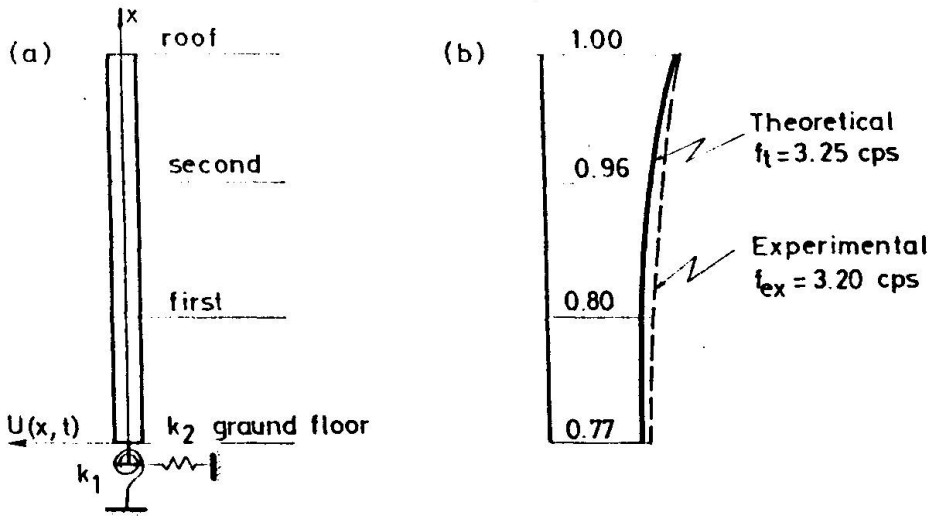

Fig. 6 (a) Cantilever beam model with interactive parameters

(b) Comparison of the theoretical and experimental mode shape

4. FORMULATION OF THE MATHEMATICAL MODEL

Simple Euler cantilever beam model was chosen to model the behaviour of the building-foundation system. In Fig. 5(a) schematic presentation of the cantilever beam model, with the interactive parameters representing flexibility of the rubber elements is given.

The partial differential equation of the motion for this case of the beam model may be written

$$\frac{\partial^2}{\partial x^2}\,(EI)\,\frac{\partial^2 U}{\partial x^2} + \bar{m}\,\frac{\partial^2 U}{\partial t^2} = 0 \qquad \ldots (1)$$

This equation neglects the influence of the deformations due to shear forces and the inertial resistance to rotational acceleration of the beam cross section. In equation (1), E is the modulus of elasticity; I is the moment of inertia of the beam; $\bar{m}$ is the mass per unit length of the beam; and L is the length of the beam.

The methods used for solution of this equation is separation of variables which leads to the well known characteristic function:

$$\Phi(x) = A_1 \sin ax + A_2 \cos ax + A_3 \sin h\, ax + A_4 \cos h\, ax \qquad \ldots(2)$$

where

$$a^4 = \frac{\omega^2 \bar{m}}{EI} \qquad \ldots (3)$$

Four constants A_n in the equation (2) define the shape and amplitude of the beam vibration and they are evaluated by consideration of the boundary conditions at the ends of the beam segment. Substituting the shape-function expression or its derivatives into these boundary conditions leads to the following matrix form:

$$\begin{bmatrix} EIa^3 & -K_1 & -EIa^3 & -K_1 \\ -K_2 & EIa & -K_2 & EIa \\ -\sin(aL) & -\cos(aL) & \sinh(aL) & \cosh(aL) \\ -\cos(aL) & \sin(aL) & \cosh(aL) & \sinh(aL) \end{bmatrix} \begin{Bmatrix} A_1 \\ A_2 \\ A_3 \\ A_4 \end{Bmatrix} = 0 \qquad \ldots(4)$$

Setting the determinant of the square matrix equal zero provides frequency equation from which a could be obtained. After the modal value of a is obtained from frequency equation it is substituded into the shape-function expression to obtain the corresponding mode shape.

The aim of this analytical presentation is to construct a model of the building in N-S direction that would closely match the dynamic characteristics measured by ambient vibration tests. For this analysis it was assumed that the supper structure is very rigid. Values of the interactive parameters k_1 and k_2 were determined from the geometrical and mechanical properties of the rubber cushions. A slight adjustement in the initial value of k_1 was required.

The experimental and theoretical mode shapes for the translational direction (N-S) of the building at the first resonant frequency of 3.20 cps are compared in Fig. 6(b). A comparison of the experimental and analytical results for the resonant frequencies and the mode shapes show very good agreement and approves the consistency of the formulated mathematical model.

5. DISCUSSION OF THE RESULTS

From the Fourier amplitude spectra at the foundation level under the rubber cushion (Fig. 5) it could be seen that the spectra is of about the same amplitude content for the wide frequency range. The Fourier amplitude spectra at the ground floor (Fig. 4) for the same conditions of microtremor-induced vibrations shows dominant peaks at frequencies 3.20, 4.50 and 7.50 cps. It is evident that at these frequancies are possible resonances of the considered building. The shape difference between two amplitude spectra at the ground floor and foundation level is evident, and it could be concluded that the vibration amplitudes for the frequencies larger than 3.20 cps are significantly damped.

In order to predict the dynamic propeeties of the building a simple mathematical model was formulated. The super structure is taken as relatively rigid with dominant bending deformations.

Most important part in the mathematical model formulation is determination of the interactive parameters. Experimental results are showing that for this system the dominant effect is of the horizontal deformations of the rubber cushions. Based on the mode shape evaluation for the resonant frequency at 3.25 cps the translational spring (k_2) controlles about 80% of the total amplitude of vibration. The rest 20% of the amplitude of vibration are controlled by the rotational stiffness of the rubber cushions and the super structure flexibility.

6. CONCLUSIONS

The dynamic properties of the building with base isolation on rubber elements as obtained from ambient vibration tests and as predicted from analytical model are in good correlation. The effectivness of base isolation is evident in the wide range of frequencies before and after 3.20 cps. More detailed investigations of

the building are needed by performing forced-vibration tests for several different levels of excitation. The building is instrumented with four strong-motion accelerographs, two at the foundation level under rubber cushions and two at the ground floor level, respectively. Expected strong-motion records will give data for final verification of the isolation effect of the system.

REFERENCES

1. Bouwkamp, J.G. and Rea, D., "Dynamic Testing and Formulation of Mathematical Models", Chapter VIII in Earthquake Engineering, editor Wiegel, R. L., Prentice Hall, 1970.

2. Clough, R.W. and Penzien, J., Dynamics of Structures, Mc Graw Hill, 1975

3. Cooley, J.W. and Tukey, J.W., "An Algorithm for the machine calculation of complex Fourier series", Math. of Comp. 19, p. 297-301 (1965)

4. Derham, C.J., at all "Natural rubber foundation bearings for earthquake protection - experimental results", NR Technology, Vol. 8, Part 3, 1977

5. Petrovski, J., Stephen, R.M., Gartenbaum, E. and Bouwkamp, J.G., "Dynamic Behaviour of a Multistory Triangular-shaped Building", Rep. No. EERC 76-3, University of California, Berkeley, 1976

6. Roth, A., Hubacher, C., Staudacher, E., Sigenthaler, R., Haldimann, W. and Held, F., "Erdbebensicherung im Banen - Das Schulhaus Heinrich Pestalozzi in Skopje, Jugoslavien", Separatbruch ans der Neken Zurcher Zectung, Beilage Twchnik, vom. 9, Februar 1970

7. Trifunac, M.D., "Comparisons Between Ambient and Forced Vibration Experiments" Earthquake Engineering and Structural Dynamics, 1, 1972, p. 133-150.